UNCLASSIFIED

AD NUMBER
ADC013177
CLASSIFICATION CHANGES
TO: unclassified
FROM: confidential
LIMITATION CHANGES
TO: Approved for public release, distribution unlimited
FROM: Distribution limited to U.S. Gov't. agencies and their Contractors; Specific authority; Oct 77. Other requests must be referred to Commanding Officer, Naval Research Lab., Washington, DC 20375.
AUTHORITY
OCA; IAW markings on document, 31 Dec 83; NRL ltr dtd 27 Nov 95

THIS PAGE IS UNCLASSIFIED

ADC013177

DDC
MAR 6 1978
A

CONFIDENTIAL

UNCLASSIFIED
SECURITY CLASSIFICATION OF THIS PAGE (When Data Entered)

REPORT DOCUMENTATION PAGE

READ INSTRUCTIONS BEFORE COMPLETING FORM

1. REPORT NUMBER: NRL Report 8163
2. GOVT ACCESSION NO.
3. RECIPIENT'S CATALOG NUMBER
4. TITLE (and Subtitle): RADAR CROSS SECTIONS OF THE AC-130H AT 1300, 2800, 5500, AND 9225 MHz [Unclassified Title]
5. TYPE OF REPORT & PERIOD COVERED: Final report on an NRL Problem
6. PERFORMING ORG. REPORT NUMBER
7. AUTHOR(s): F. D. Queen, E. E. Maine, Jr., and H. A. Brown
8. CONTRACT OR GRANT NUMBER(s)
9. PERFORMING ORGANIZATION NAME AND ADDRESS: Naval Research Laboratory, Washington, D. C. 20375
10. PROGRAM ELEMENT, PROJECT, TASK AREA & WORK UNIT NUMBERS: NRL Problem R12-45; ~~Project~~ Order ASD6-1375P
11. CONTROLLING OFFICE NAME AND ADDRESS: Aeronautical Systems Division, Air Force Systems Command, Wright-Patterson AFB, OH 45433
12. REPORT DATE: October 28, 1977
13. NUMBER OF PAGES: 66
14. MONITORING AGENCY NAME & ADDRESS (if different from Controlling Office)
15. SECURITY CLASS. (of this report): CONFIDENTIAL
15a. DECLASSIFICATION/DOWNGRADING SCHEDULE: GDS-[redacted]/1983

16. DISTRIBUTION STATEMENT (of this Report)

Distribution limited to U.S. Government Agencies only; test and evaluation; October 1977. Other requests for this document must be referred to the Commanding Officer, Naval Research Laboratory, Washington, D. C. 20375.

17. DISTRIBUTION STATEMENT (of the abstract entered in Block 20, if different from Report)

18. SUPPLEMENTARY NOTES

DDC
RECEIVED
MAR 6 1978
A

19. KEY WORDS (Continue on reverse side if necessary and identify by block number)

AC-130H
Radar cross section
Echoing area

20. ABSTRACT (Continue on reverse side if necessary and identify by block number)

(U) Radar cross sections of the AC-130H were determined at frequencies of 1300, 2800, 5500, and 9225 MHz using the NRL area-measurement facility. The 20, 50, and 80 percentiles of the radar cross-section distribution function are given for azimuth aspect angles from 20 to 160 for a -10-degree elevation aspect and for elevation aspects from 0 to 56 degrees for nose-on and tail-on views. Polar plots show the results obtained from orbits flown at a variety of altitudes, bank angles, and offset ranges from the radar. Vertical and horizontal polarizations were used for the orbits. The differences

(Continued)

DD FORM 1 JAN 73 1473 EDITION OF 1 NOV 65 IS OBSOLETE
S/N 0102-LF-014-6601

UNCLASSIFIED
SECURITY CLASSIFICATION OF THIS PAGE (When Data Entered)

(This page is unclassified CONFIDENTIAL

20. ABSTRACT (Continued)

in cross sections between the starboard side of this aircraft and those previously determined for a C-130 are discussed.

Subject to GDS
Declassify: 31 Dec. 1983

CONTENTS

INTRODUCTION 1

DATA ACQUISITION 1

DATA REDUCTION 1

RESULTS 4

SUMMARY OF RESULTS 4

ACKNOWLEDGMENT 4

APPENDIX A — Radar System 57

APPENDIX B — Data Reduction 61

ACCESSION for
NTIS White Section
DDC Buff Section
UNANNOUNCED
JUSTIFICATION
BY
DISTRIBUTION/AVAILABILITY CODES
Dist. AVAIL. and/or SPECIAL
B

"NATIONAL SECURITY INFORMATION"

"Unauthorized Disclosure Subject to Criminal Sanctions"

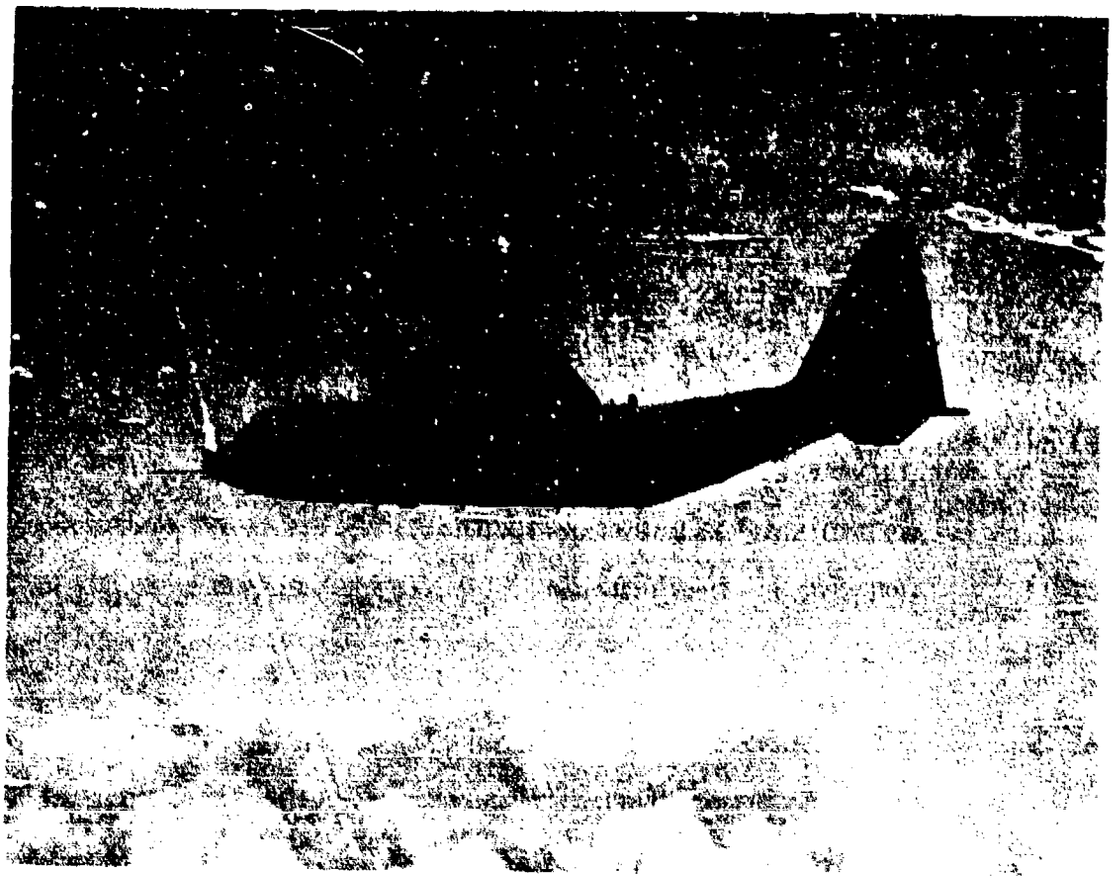

Fig. 1 — The AC-130H gunship

RADAR CROSS SECTIONS OF THE AC-130H AT 1300, 2800, 5500, and 9225 MHz
[Unclassified Title]

INTRODUCTION

(U) Radar cross sections were determined for the AC-130H using the NRL area-measurement facility (Appendix A). Data were taken with the aircraft flying both straight courses and typical gunship orbits. Horizontal polarization was used for the straight courses, and both vertical and horizontal polarizations were used for the orbits. The orbits were flown at a variety of altitudes, bank angles, and ranges which provided data for aspect angles in elevation from +20 to -80 degrees for 360 degrees in azimuth aspect. The data from the orbits are presented in the form of polar plots of radar cross section (RCS) in dB above 1 m^2 versus azimuth aspect angle for 5-degree increments. The 20, 50, and 80 percentile values of the RCS distribution function are given. The data are intended to demonstrate the variation in RCS with the aircraft in a specified bank angle centered at a designated range.

DATA ACQUISITION

(U) Data were acquired in the orbits with both left- and right-hand turns. Table 1 lists the data run number of the RCS measurement system and the aircraft altitude and position data.

(U) The straight-line courses provided data for comparison of the RCS of this aircraft (Fig. 1) with RCS values of a standard C-130.* The courses provided azimuth aspect angle coverage form 20 to 160 on both the port and starboard sides of the aircraft for an average 10-degree elevation aspect (±5 degrees centered at 10 degrees radar elevation). In addition, radial courses were flown to obtain elevation profiles of the aircraft for nose-on (0-degree) and tail-on (180-degree) aspects.

DATA REDUCTION

(U) The data reduction is described in Appendix B. Briefly, the azimuth and elevation aspects are determined as a function of time during the data run, and a pulse-by-pulse tape of the RCS is segmented according to aspect angle to form a distribution function from which the percentiles can be read. For the data contained herein, the elevation angles for the orbits are not presented. Fine-grain analysis of the NRL data tapes for the orbits was the responsibility of Georgia Institute of Technology on a separate U.S. Air Force contract.

---

*F. D. Queen and E. E. Maine, Jr., "A Compendium of Radar Cross Sections of U.S. Aircraft," NRL Report 7190, (Confidential), Nov. 1970.

Manuscript submitted August 24, 1977.

(U) Table 1 – Aircraft Altitude and Position for the RCS Data Runs

Run Number	Bank Angle (deg)	Pitch Angle (deg)	True Airspeed (knots)	Altitude		Direction of Turn	Radar Range to Center of Orbit (n.mi.)
				km	kft		
Horizontal Polarization							
1227	40	10	180	2.7	9	L	1.81
1228	20	10	180	3.0	10	L	2.55
1229	20	10	180	3.0	10	L	3.13
1230	20	10	180	3.0	10	L	3.95
1231	20	8	165	2.6	7.5	L	3.95
1232	20	6.5	165	1.5	5	L	3.95
1233	20	8	155	0.3	1	L	4.11
1235	20	7	160	0.3	1	L	2.14
1236	40	8	180	3.0	10	R	1.81
1237	20	8	180	3.0	10	R	2.55
1238	20	8	180	3.0	10	R	3.13
1239	20	8	180	3.0	10	R	3.95
1241	20	8	165	2.6	7.5	R	3.95
1242	20	8	165	1.5	5	R	3.95
1243	20	8	155	0.3	1	R	4.11
1244	10	8	155	0.3	1	R	4.11
1245	20	8	155	0.3	1	R	2.14
1246*	20	8	155	0.3	1	L	2.14
1247*	10	8	155	0.3	1	L	4.11
1248*	20	8	155	0.3	1	L	4.11
Vertical Polarization							
1262	20	8	155	0.3	1	L	2.14
1263	10	8	155	0.3	1	L	4.11
1264	20	8	155	0.3	1	L	4.11
1265	20	9.5	160	1.5	5	L	3.95
1266	20	8	160	2.6	7.5	L	3.95
1267	20	5	160	1.5	5	L	1.73
1268	30	5	160	1.5	5	L	1.48
1269	20	5	160	1.5	5	L	1.97
1270	20	8	160	1.5	5	L	2.3
1271	30	8	160	1.5	5	R	1.48
1272	20	8	160	1.5	5	R	1.73
1273	30	8	160	1.5	5	R	0.9
1274	20	8	160	1.5	5	R	1.97
1275	20	7	160	1.5	5	R	2.3
1276	20	7	160	1.5	5	R	2.69
1277	20	7	160	1.5	5	R	3.95
1278	20	6	160	0.3	1	R	4.11
1279	10	6	160	0.3	1	R	4.11
1280	20	6	160	0.3	1	R	2.14
1281†	20	7	160	0.3	1	L	2.14
1282†	10	7	160	0.3	1	L	4.11
1283†	20	7	160	0.3	1	L	4.11
1284†	20	7	160	1.5	5	L	3.95
1285†	20	7	160	1.5	5	L	2.69
1286†	20	7	160	1.5	5	L	2.3
1287†	20	7	160	1.5	5	L	1.97
1288†	20	7	160	1.5	5	L	1.73
1290†	30	7	160	1.5	5	L	0.9

*Vertical polarization transmitted and received at 5500 and 9225 MHz.
†Run with the rear door of the aircraft open.

(U) The pulse-by-pulse tape of calibrated RCS values is generated by processing each received pulse in accordance with

$$\sigma = \sigma_s \left(\frac{R_m}{R_s}\right)^4 \left(\frac{\alpha_m}{\alpha_s}\right)\left(\frac{E_m}{E_s}\right)^2 ,$$

where

σ is the aircraft RCS,

σ_s is the RCS of the calibration sphere,

E_s is the voltage produced by the sphere,

R_s is the range to the sphere,

α_s is the attenuation in the receiver for the sphere measurement,

E_m is the voltage produced by the target,

R_m is the range to the target, and

α_m is the attentuation in the receiver during the target measurement.

(U) Due to the unavailability of the onboard recording of time versus heading, the radar-mount pointing coordinates and range versus time had to be used to synthetically generate the onboard recording to be used in subsequent RCS processing. The mount azimuth and elevation, the WWV time, and the target range sampled at 4 per second provided the input data. The bearing and elevation data were smoothed by passing them through the filter

$$y_i = 0.25y_{i-1} + 0.5x_i + 0.25x_{i+1}$$

20 times, and the range data were smoothed by passing them through 40 times. These low-pass filters have 3-dB points of less than 0.4 Hz. The target aspects angle α was then computed from

$$\tan \alpha = \frac{\sin \delta}{\frac{R_1}{R_2} - \cos \delta} ,$$

where δ is the angle between ground ranges R_1 and R_2 at times t and $t + 0.25$ s. The WWV time code and angle α converted to magnetic heading sampled at 4 per second then provided the synthetic onboard tape.

RESULTS

(U) The results of the measurements are contained in Figs. 2 through 53. The 20, 50, and 80 percentiles of the RCS distribution function are plotted in dB above 1 m^2. For the straight-line courses linear plots are used. The plotted RCS percentiles are derived using all data contained in a 10-degree aspect cell centered at the designated aspect for the azimuth profiles. For the elevation profiles of the nose and tail views a 2-degree cell size is used. In addition the profiles of the tail view contain RCS values for the aircraft with the rear door open for elevation angles from 0 to -6 degrees (6 degrees below the aircraft).

(U) The captions for the polar plots, Figs. 6 through 53, identify the frequency, polarization, system run number, and direction of the turn. The first letter of the designations LHH, SHH, CHH, and XHH indicate L band (1300 MHz), S band (2800 MHz), C band (5500 MHz) and X band (9225 MHz) respectively. The HH and VV designations indicate either horizontal or vertical polarization was transmitted and received. The aircraft bank angle and position with respect to the measurement radar for each plot can be found in Table 1. CCW or CW indicates either a left- or right-hand turn for the orbit. Port broadside on the plot is denoted by 90 degrees, and starboard broadside is 270 degrees.

SUMMARY OF RESULTS

(C) The data from the azimuth profiles (linear plots) for the port and starboard sides shows a higher portside RCS between 120 to 160 degrees at all bands. At 9225 MHz the portside median RCS values are as much as 5 dB higher than the starboard-side RCS. At aspects from 0 to 90 degrees the portside RCS values are never greater that 2 dB above the starboard-side values.

(C) The median RCS values from this measurement for the starboard side of the aircraft were compared to previous NRL measurements on a rescue version of the C-130. The significant difference at the X-band frequency occurs at 180 degrees, where the AC-130 RCS is 6 dB higher. At other aspects the values are generally in agreement. The S-band values differ by 3 dB at angles of 110 and 160 degrees and by 2.5 dB at 50 degrees. Agreement is good at the remaining aspects. The L-band values are within 2 dB except at aspects of 70 and 100 degrees, where a difference of 3.5 dB exists. A detailed study of the differences between the two aircraft would be required to account for the differences in RCS.

ACKNOWLEDGMENT

The assistance of A. E. March in the data processing phase of the problem is gratefully acknowledged.

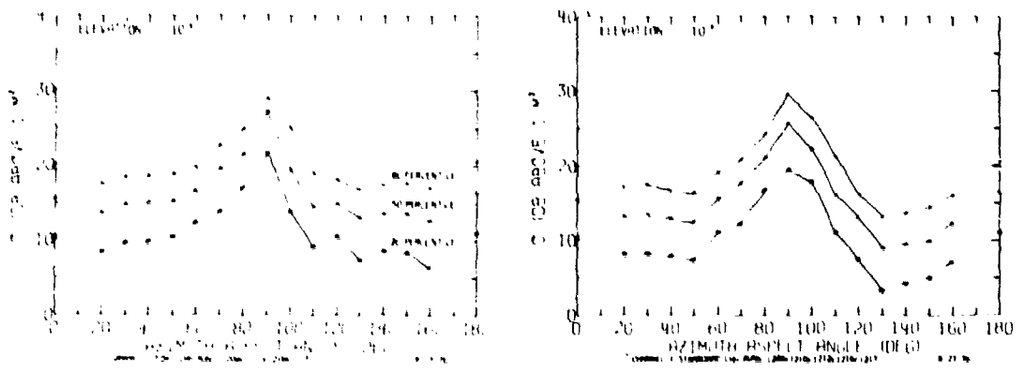

(a) Port side (b) Starboard side

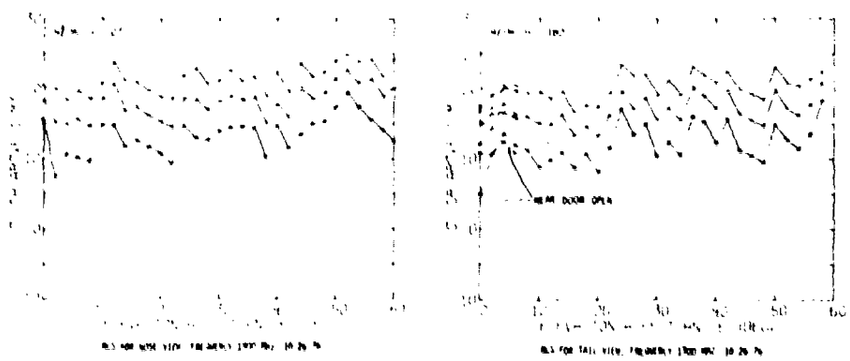

(c) Nose-on aspect (d) Tail-on aspect

(C) Fig. 2 — RCS values for horizontal polarization at 1300 MHz

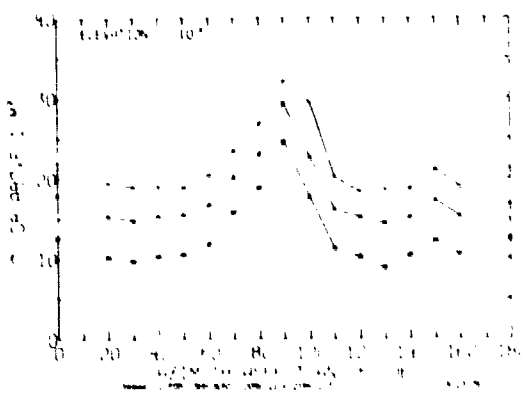

(a) Port side

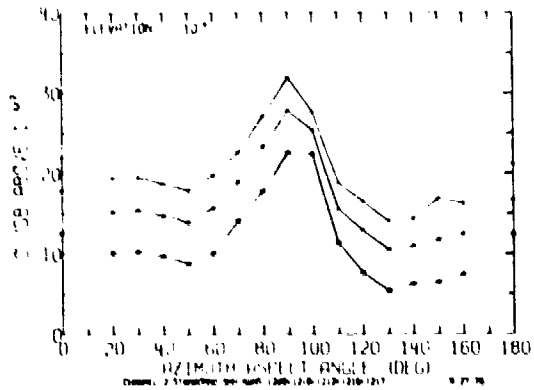

(b) Starboard side

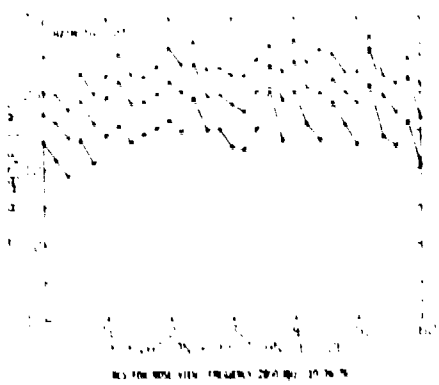

(c) Nose-on aspect

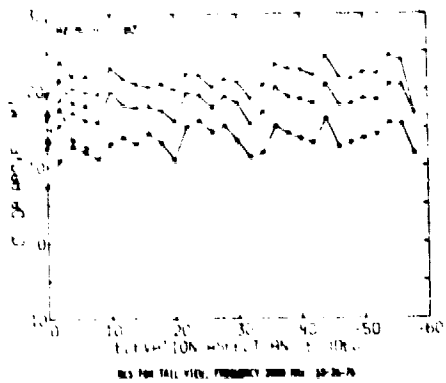

(d) Tail-on aspect

(C) Fig. 3 — RCS values for horizontal polarization at 2800 MHz

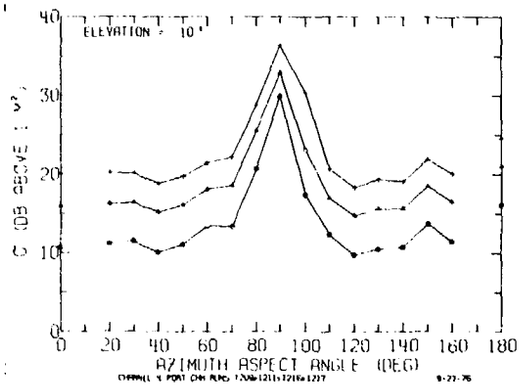

(a) Port side

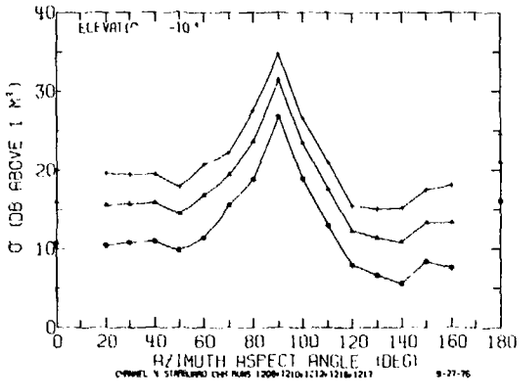

(b) Starboard side

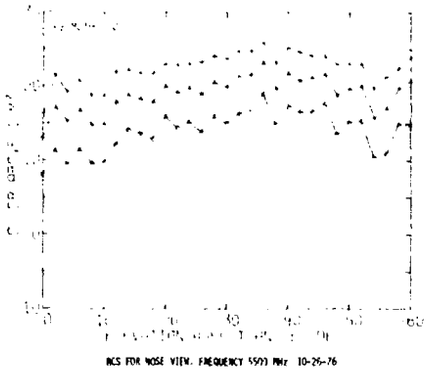

(c) Nose-on aspect

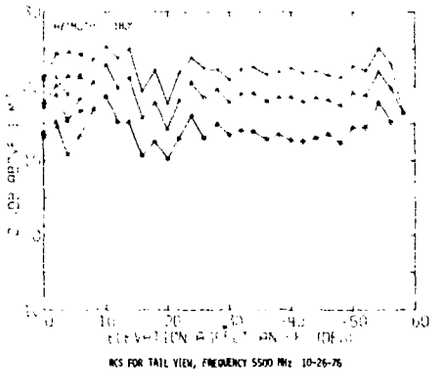

(d) Tail-on aspect

(C) Fig. 4 — RCS values for horizontal polarization at 5500 MHz

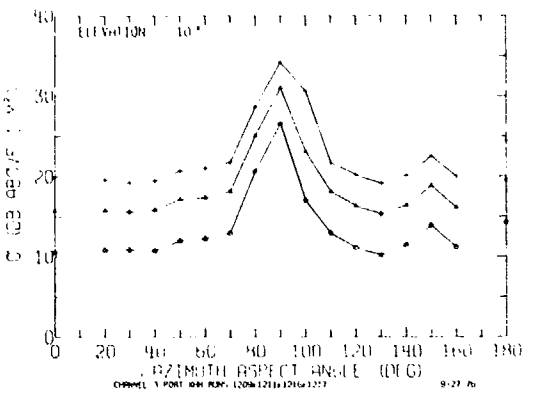

(a) Port side

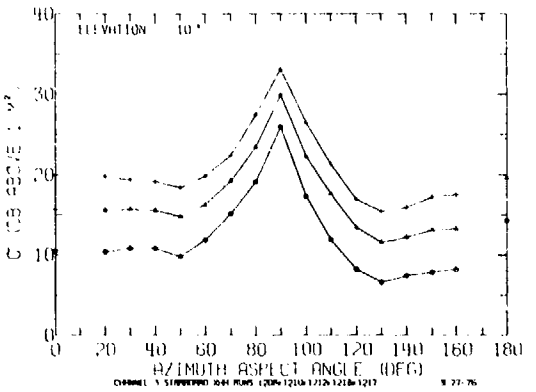

(b) Starboard side

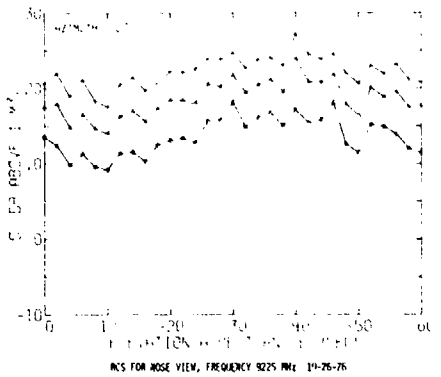

(c) Nose-on aspect

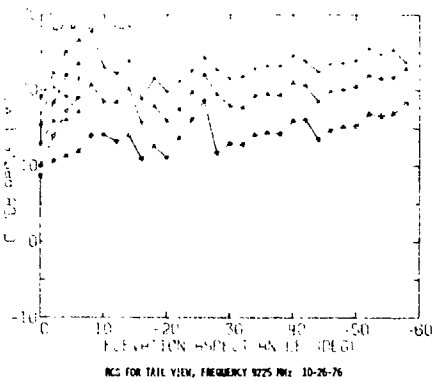

(d) Tail-on aspect

(C) Fig. 5 — RCS values for horizontal polarization at 9225 MHz

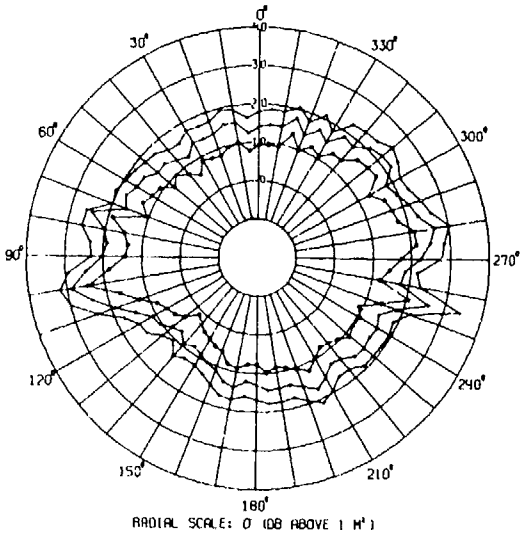

(C) Fig. 6a — Channel 1 LHH RUN 1227 CCW

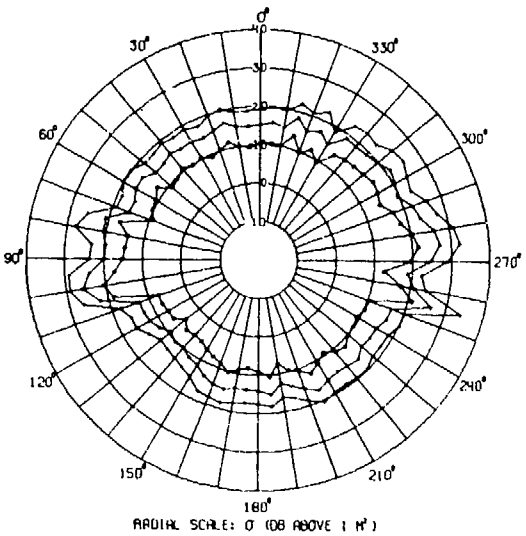

(C) Fig. 6b — Channel 2 SHH RUN 1227 CCW

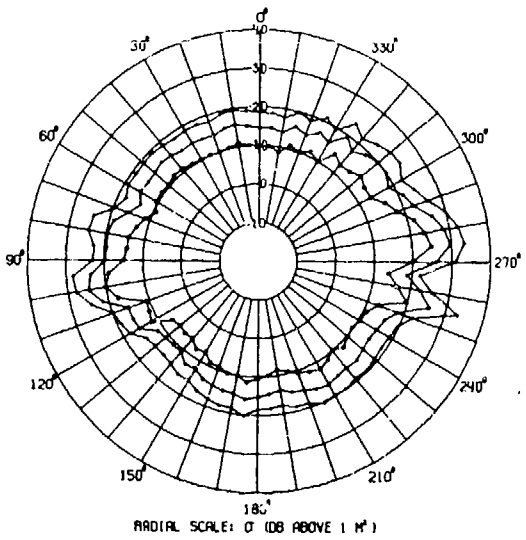

(C) Fig. 6c — Channel 3 XHH RUN 1227 CCW

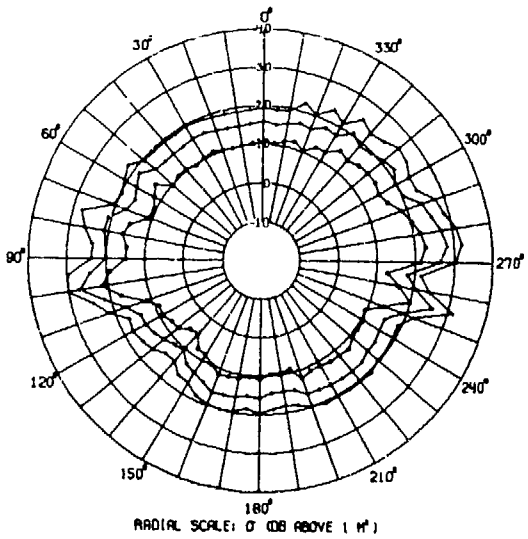

(C) Fig. 6d — Channel 4 CHH RUN 1227 CCW

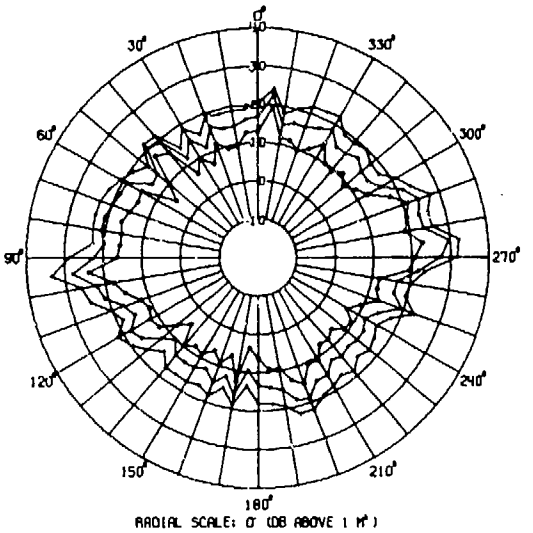

(C) Fig. 7a — Channel 1 LHH RUN 1228 CCW

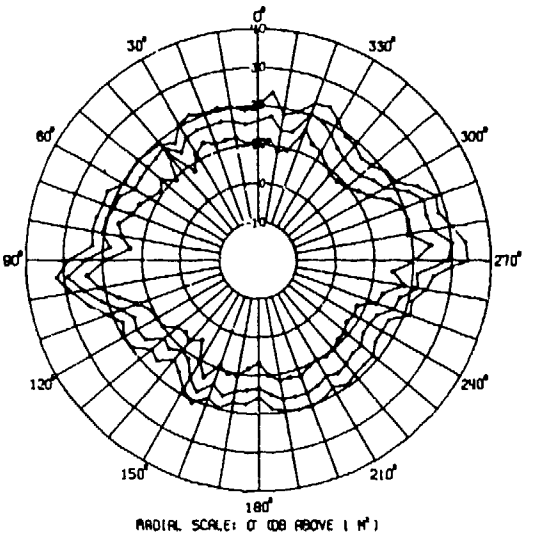

(C) Fig. 7b — Channel 2 SHH RUN 1228 CCW

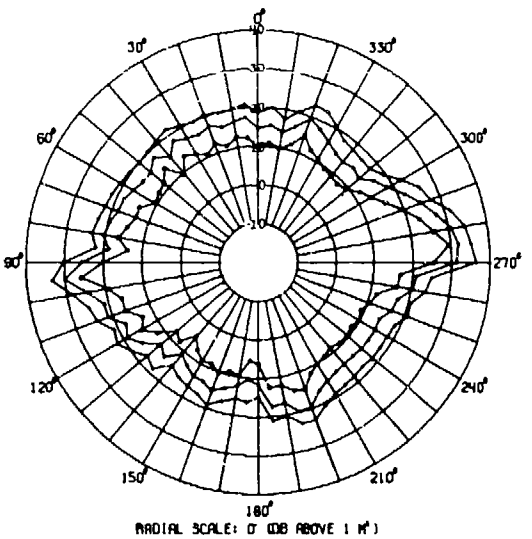

(C) Fig. 7c — Channel 3 XHH RUN 1228 CCW

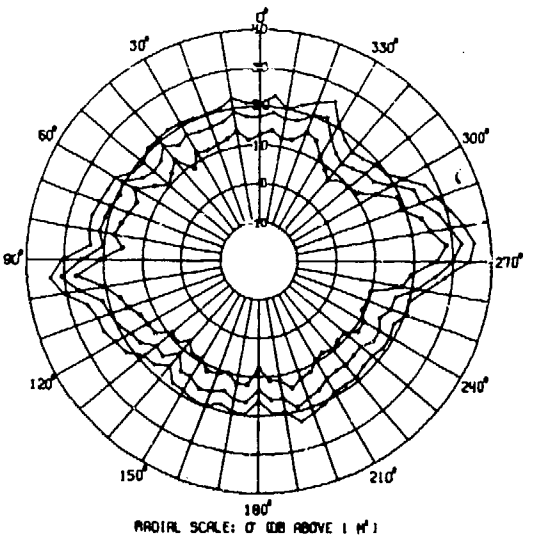

(C) Fig. 7d — Channel 4 CHH RUN 1228 CCW

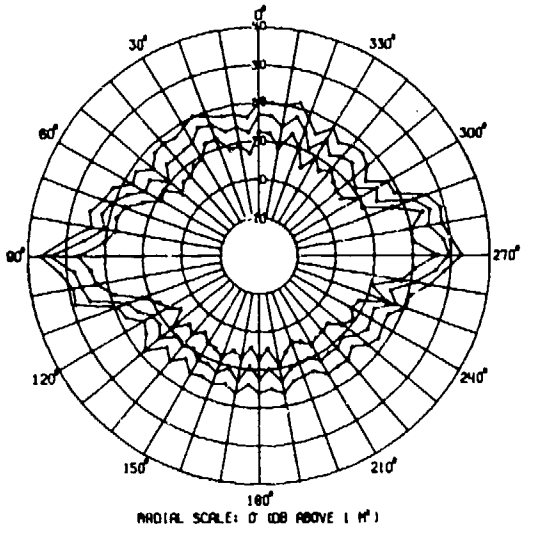

(C) Fig. 8a — Channel 1 LHH RUN 1229 CCW

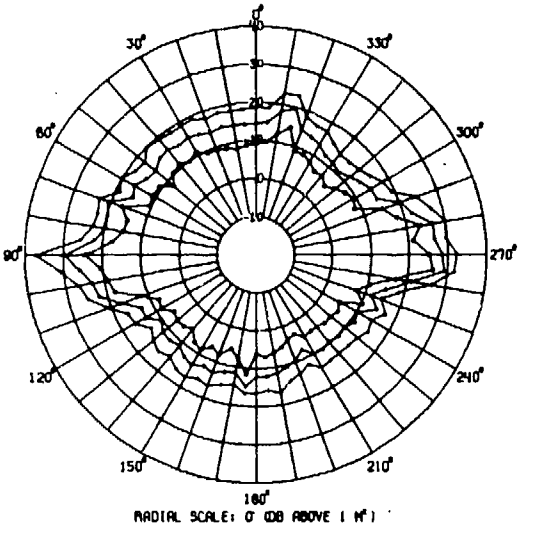

(C) Fig. 8b — Channel 2 SHH RUN 1229 CCW

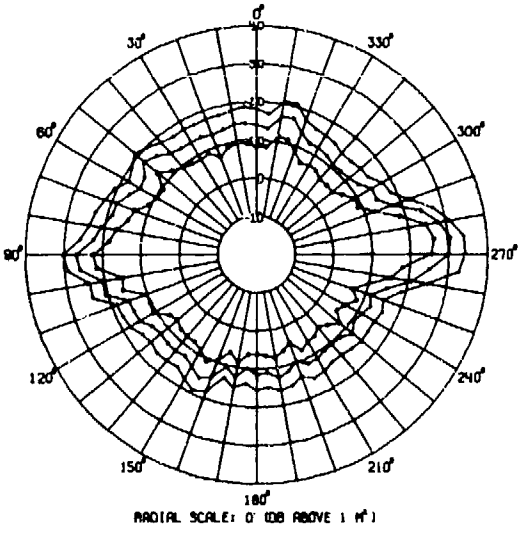

(C) Fig. 8c — Channel 3 XHH RUN 1229 CCW

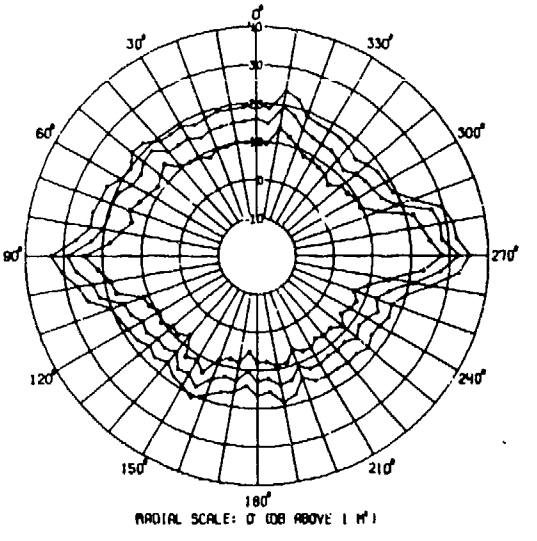

(C) Fig. 8d — Channel 4 CHH RUN 1229 CCW

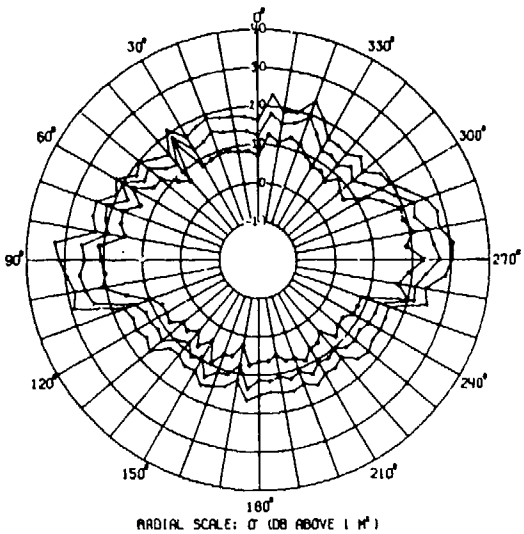

(C) Fig. 9a — Channel 1 LHH RUN 1230 CCW

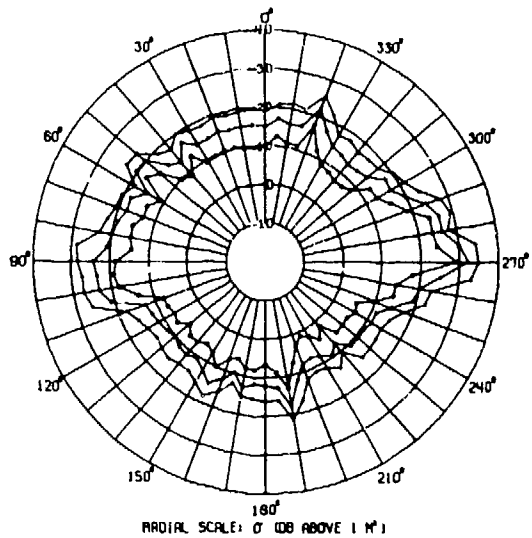

(C) Fig. 9b — Channel 2 SHH RUN 1230 CCW

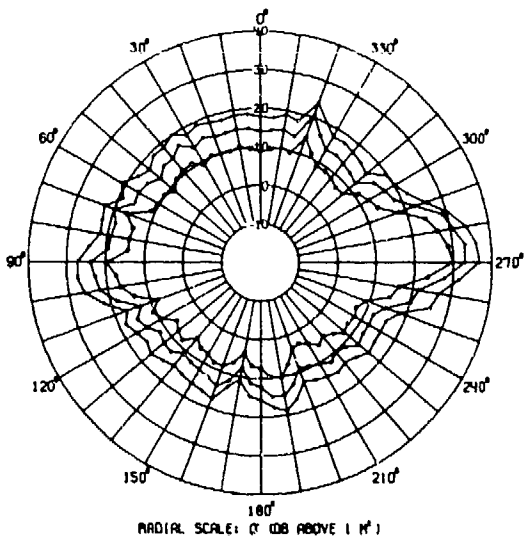

(C) Fig. 9c — Channel 3 XHH RUN 1230 CCW

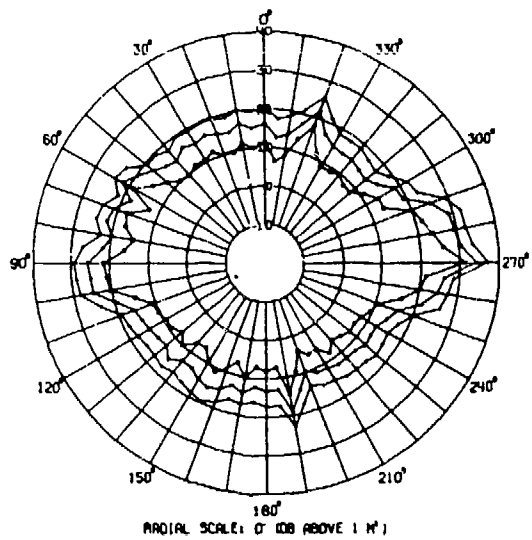

(C) Fig. 9d — Channel 4 CHH RUN 1230 CCW

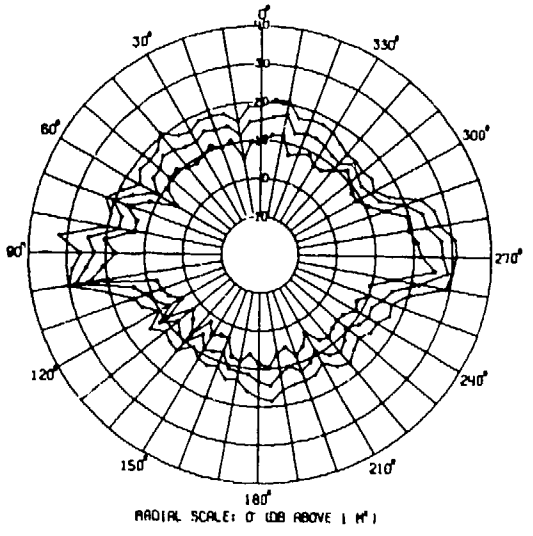

(C) Fig. 10a — Channel 1 LHH RUN 1231 CCW

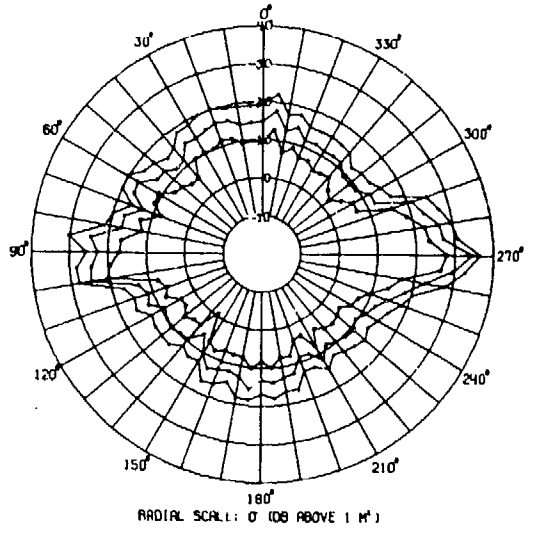

(C) Fig. 10b — Channel 2 SHH RUN 1231 CCW

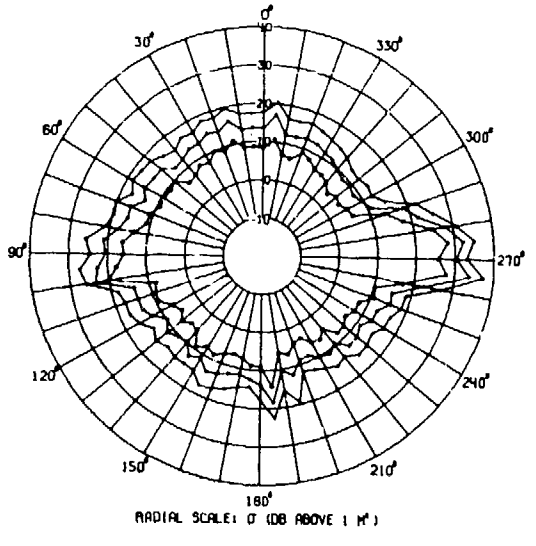

(C) Fig. 10c — Channel 3 XHH RUN 1231 CCW

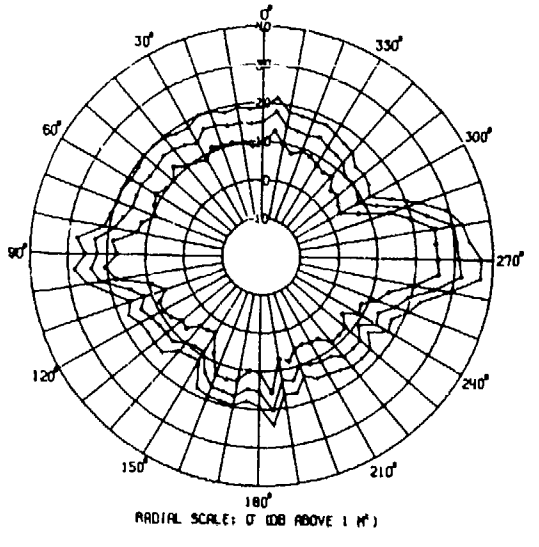

(C) Fig. 10d — Channel 4 CHH RUN 1231 CCW

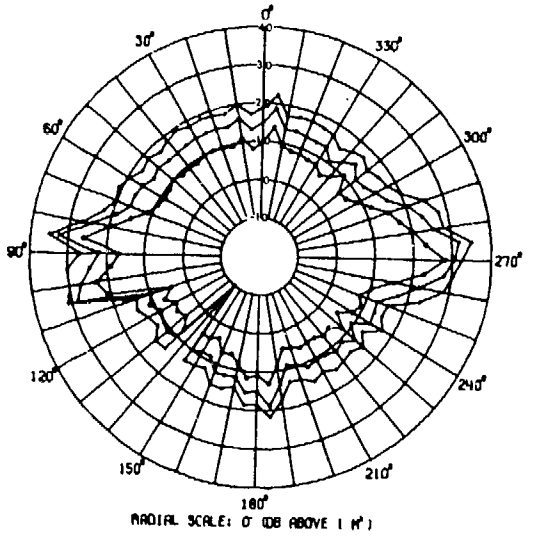

(C) Fig. 11a — Channel 1 LHH RUN 1232 CCW

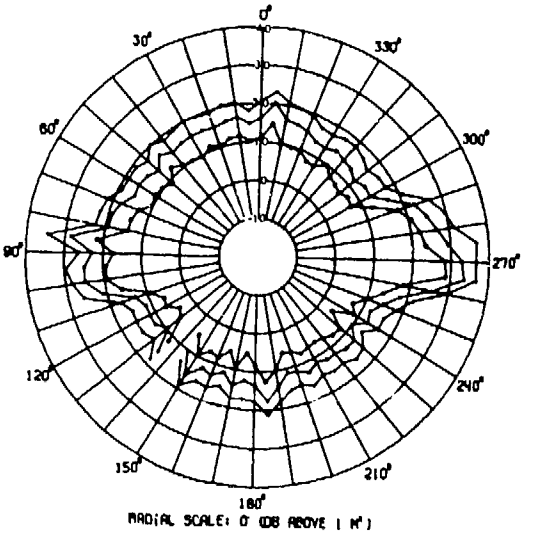

(C) Fig. 11b — Channel 2 SHH RUN 1232 CCW

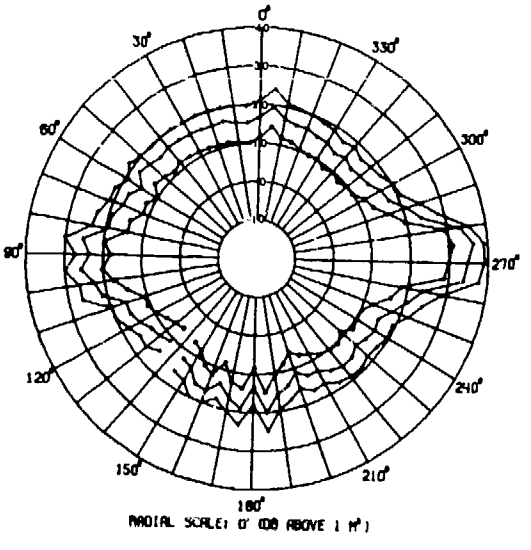

(C) Fig. 11c — Channel 3 XHH RUN 1232 CCW

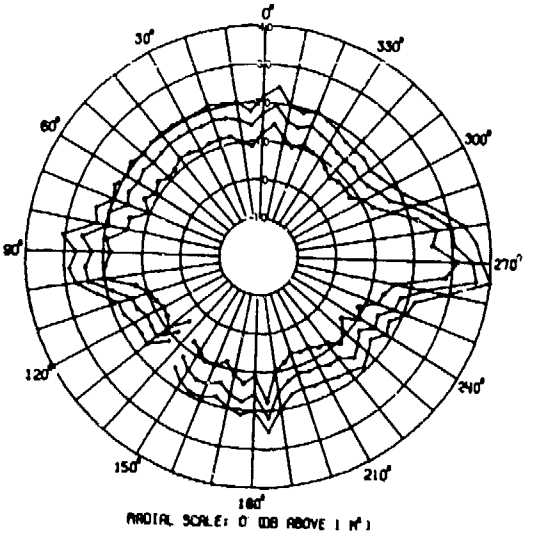

(C) Fig. 11d — Channel 4 CHH RUN 1232 CCW

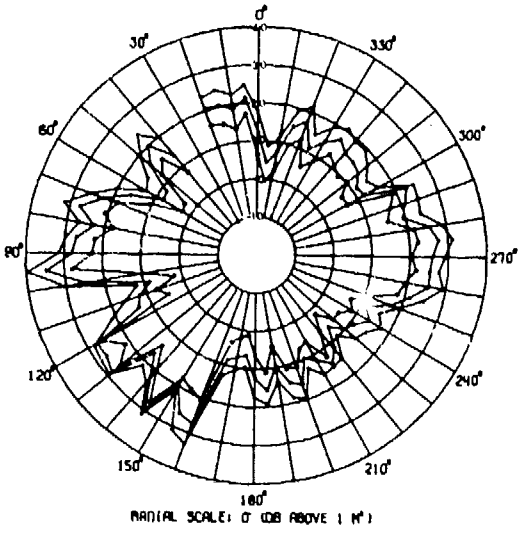

(C) Fig. 12a — Channel 1 LHH RUN 1233 CCW

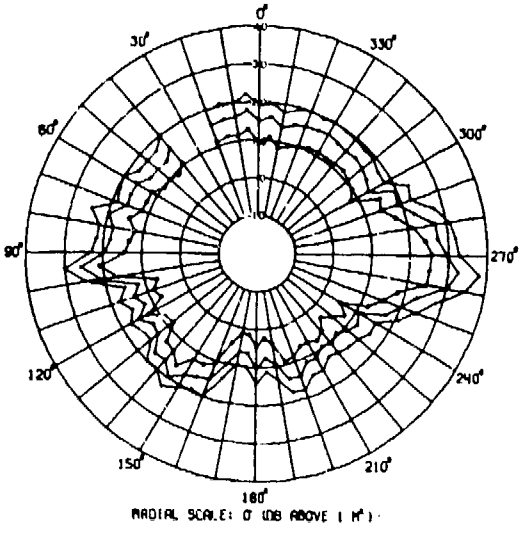

(C) Fig. 12b — Channel 2 SHH RUN 1233 CCW

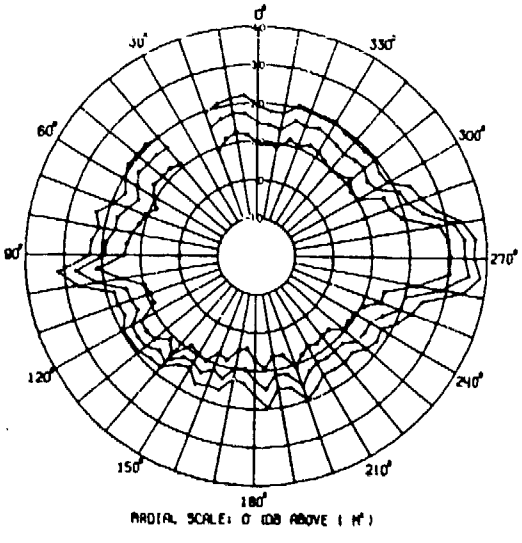

(C) Fig. 12c — Channel 3 XHH RUN 1233 CCW

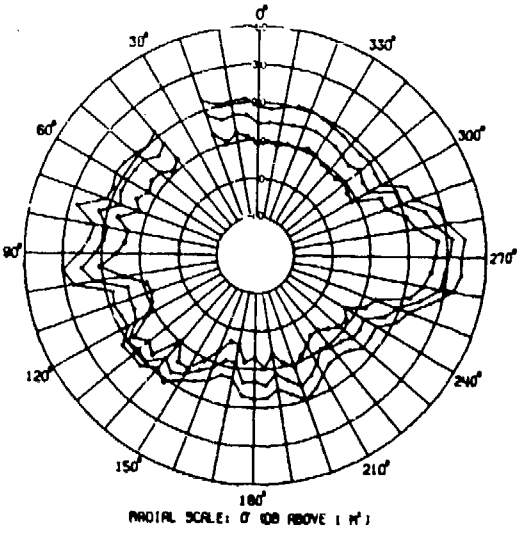

(C) Fig. 12d — Channel 4 CHH RUN 1233 CCW

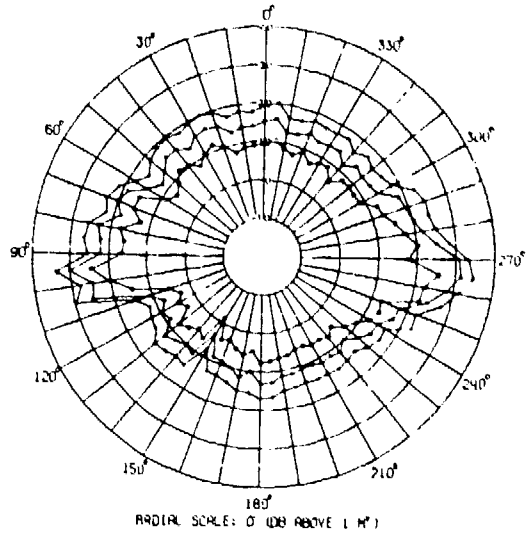

(C) Fig. 13a — Channel 1 LHH RUN 1235 CCW

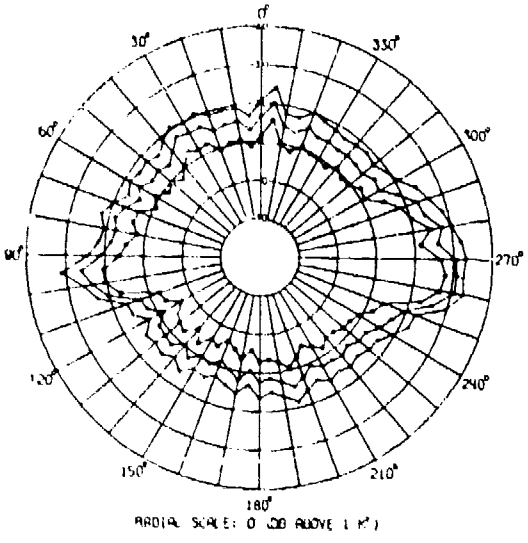

(C) Fig. 13b — Channel 2 SHH RUN 1235 CCW

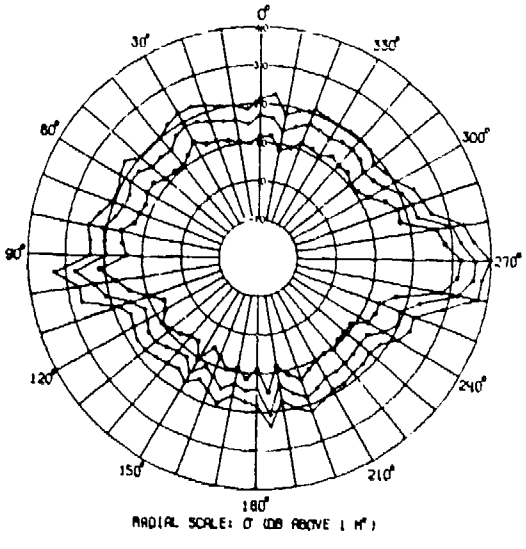

(C) Fig. 13c — Channel 3 XHH RUN 1235 CCW

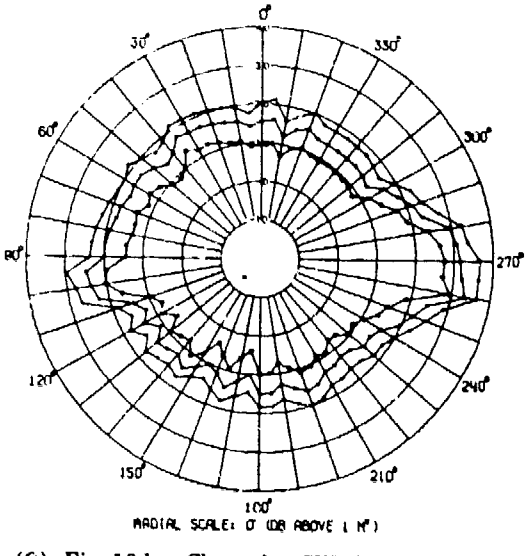

(C) Fig. 13d — Channel 4 CHH RUN 1235 CCW

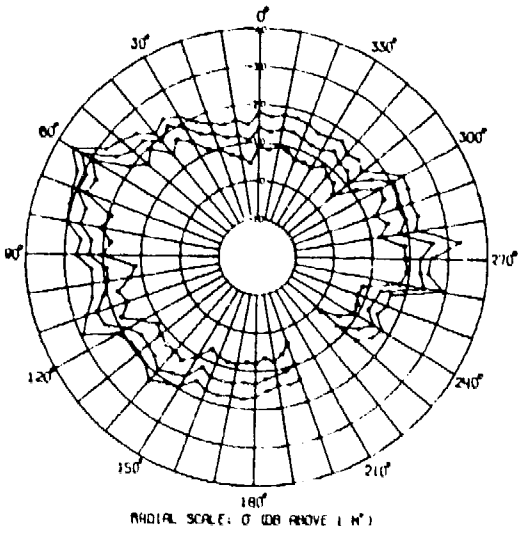

(C) Fig. 14a — Channel 1 LHH RUN 1236 CW

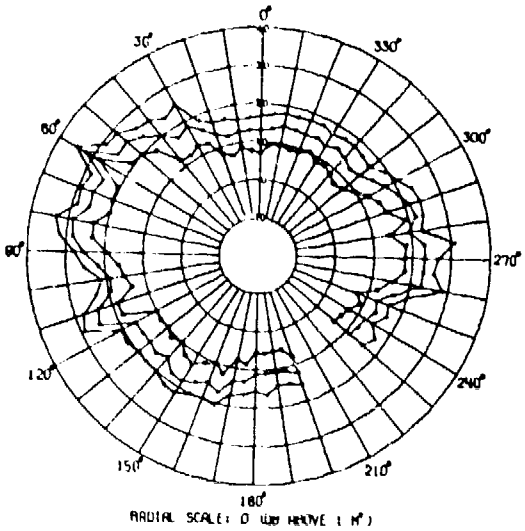

(C) Fig. 14b — Channel 2 SHH RUN 1236 CW

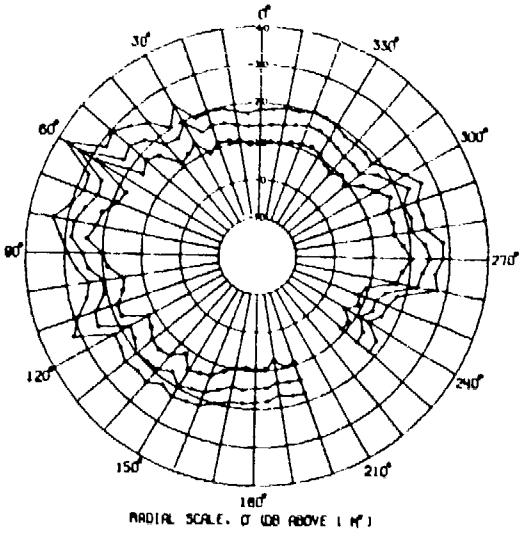

(C) Fig. 14c — Channel 3 XHH RUN 1236 CW

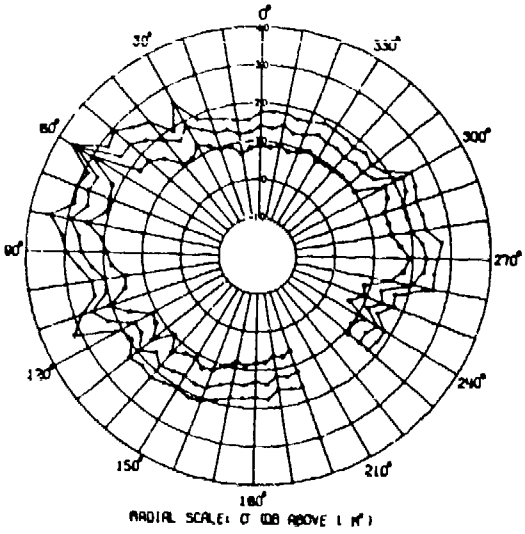

(C) Fig. 14d — Channel 4 CHH RUN 1236 CW

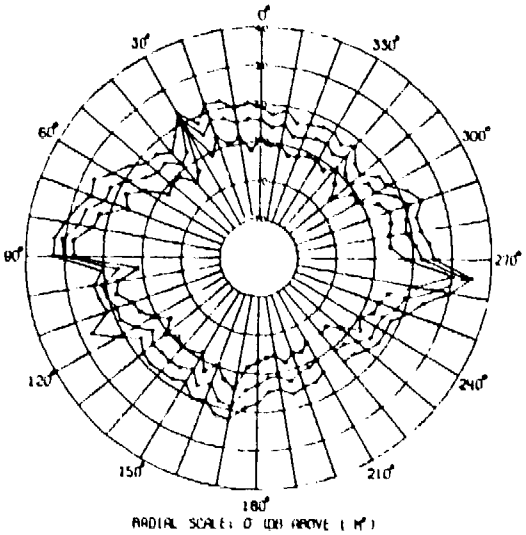

(C) Fig. 15a — Channel 1 LHH RUN 1237 CW

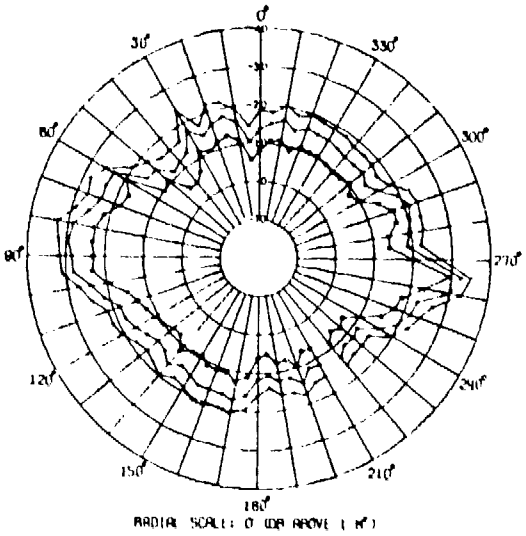

(C) Fig. 15b — Channel 2 SHH RUN 1237 CW

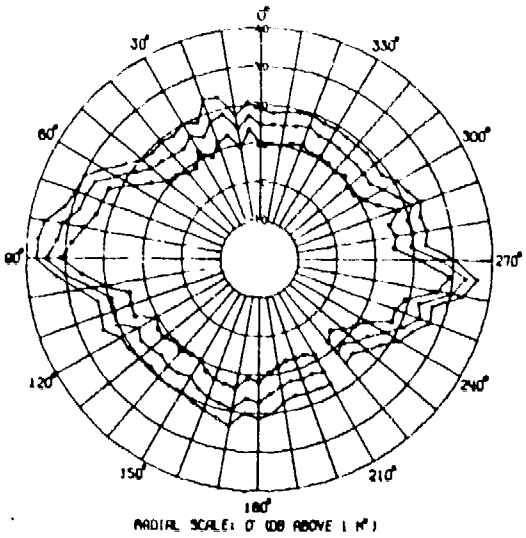

(C) Fig. 15c — Channel 3 XHH RUN 1237 CW

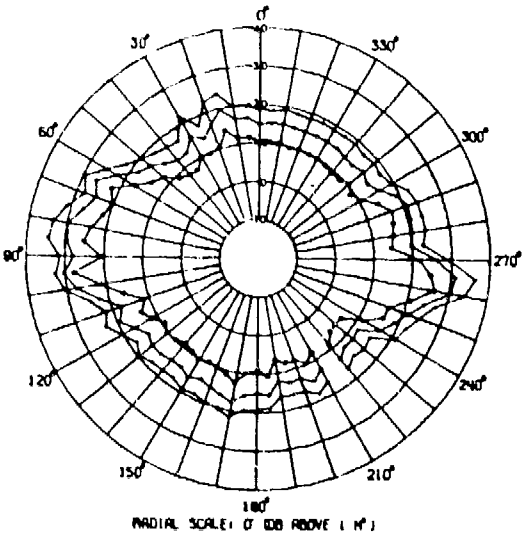

(C) Fig. 15d — Channel 4 CHH RUN 1237 CW

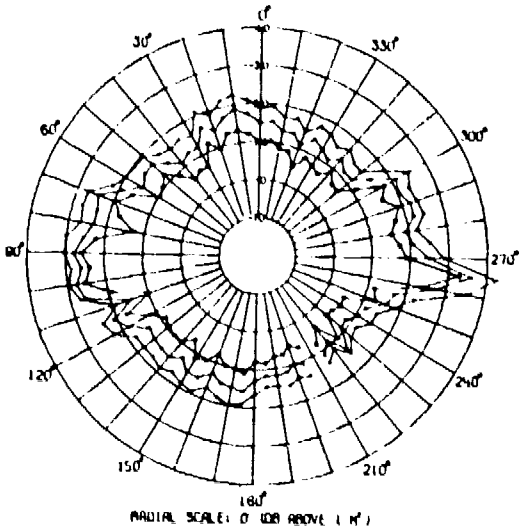

(C) Fig. 16a — Channel 1 LHH RUN 1238 CW

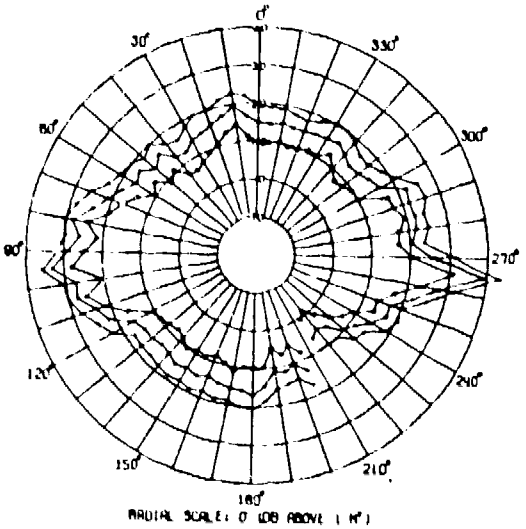

(C) Fig. 16b — Channel 2 SHH RUN 1238 CW

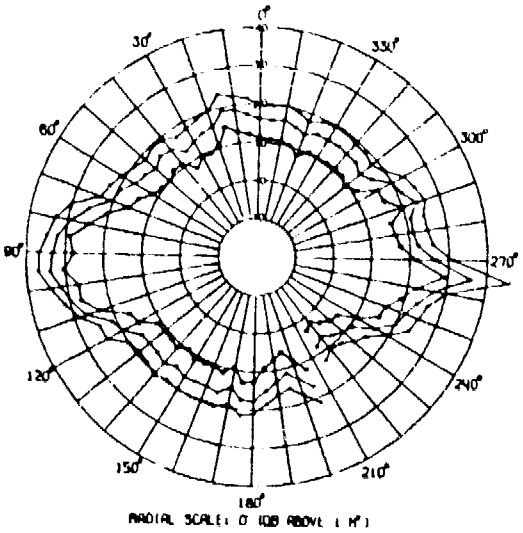

(C) Fig. 16c — Channel 3 XHH RUN 1238 CW

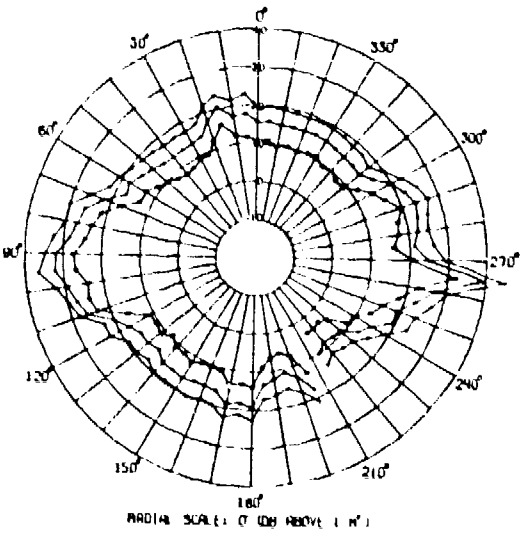

(C) Fig. 16d — Channel 4 CHH RUN 1238 CW

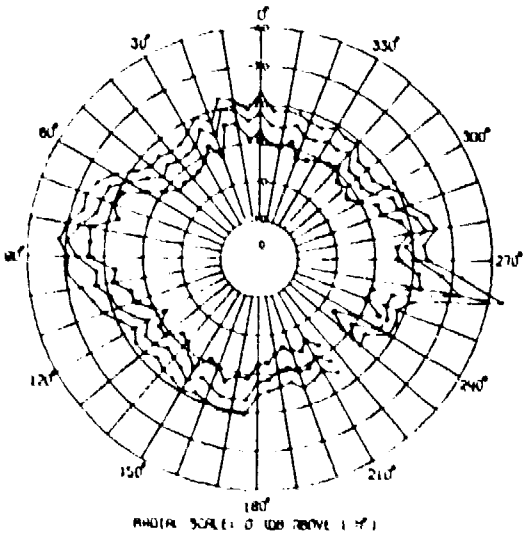

(C) Fig. 17a — Channel 1 LHH RUN 1239 CW

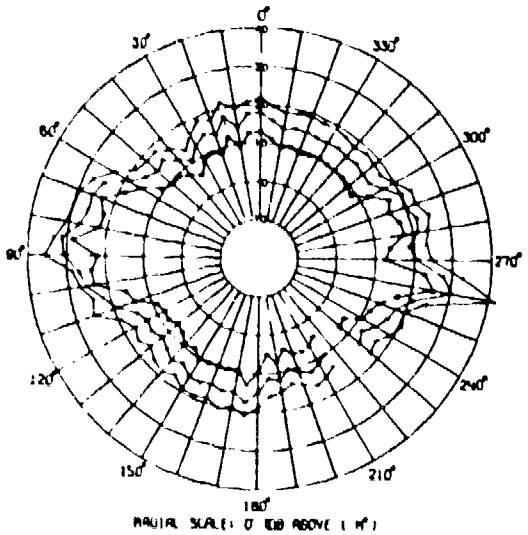

(C) Fig. 17b — Channel 2 SHH RUN 1239 CW

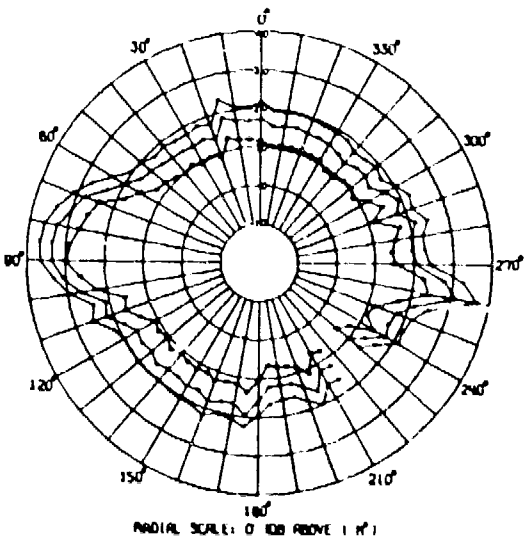

(C) Fig. 17c — Channel 3 XHH RUN 1239 CW

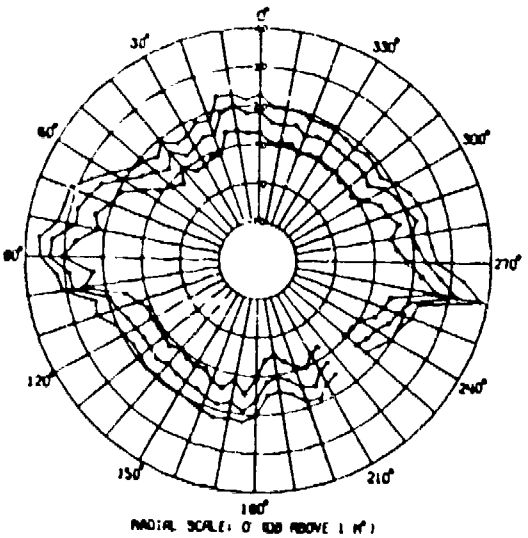

(C) Fig. 17d — Channel 4 CHH RUN 1239 CW

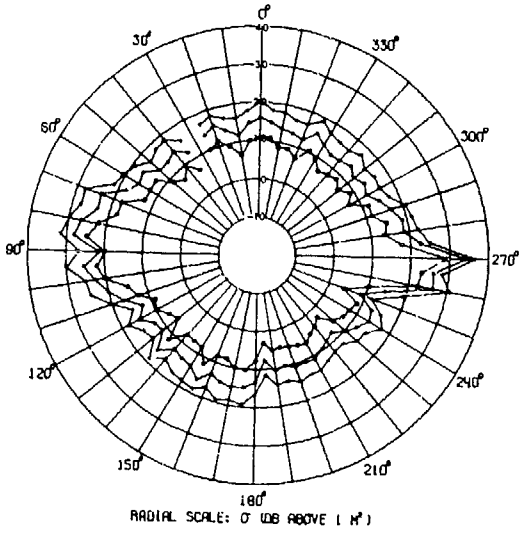

(C) Fig. 18a — Channel 1 LHH RUN 1241 CW

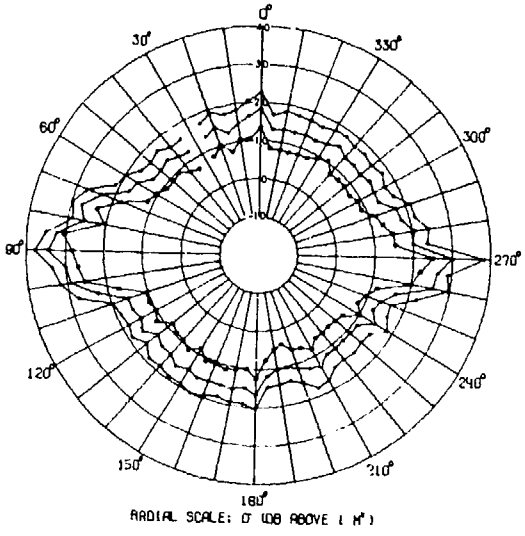

(C) Fig. 18b — Channel 2 SHH RUN 1241 CW

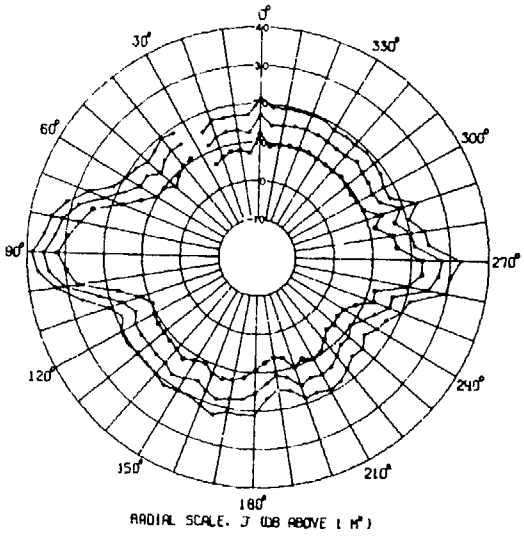

(C) Fig. 18c — Channel 3 XHH RUN 1241 CW

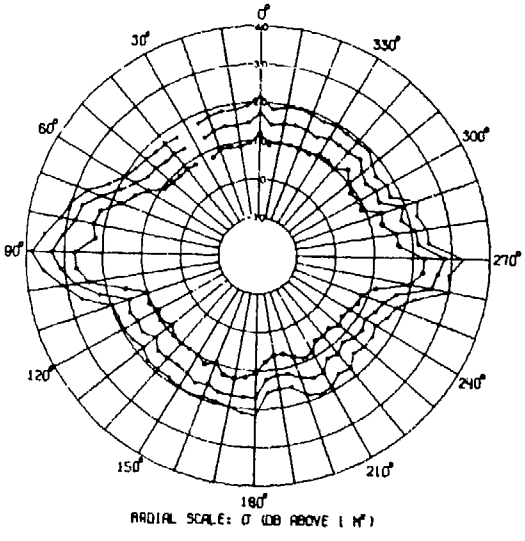

(C) Fig. 18d — Channel 4 CHH RUN 1241 CW

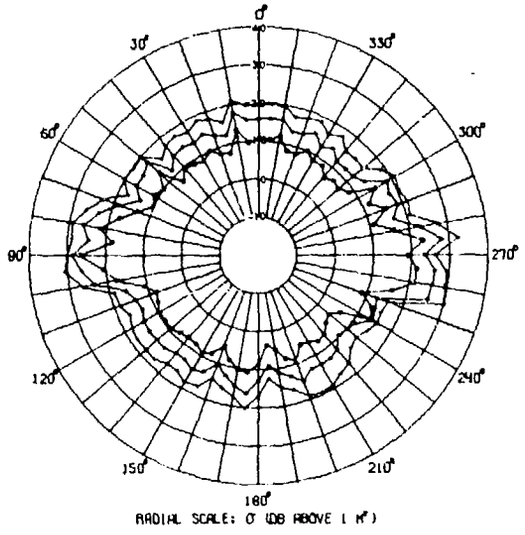

(C) Fig. 19a — Channel 1 LHH RUN 1242 CW

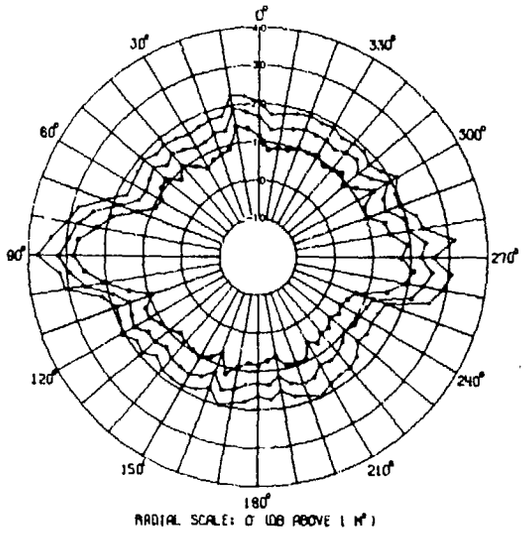

(C) Fig. 19b — Channel 2 SHH RUN 1242 CW

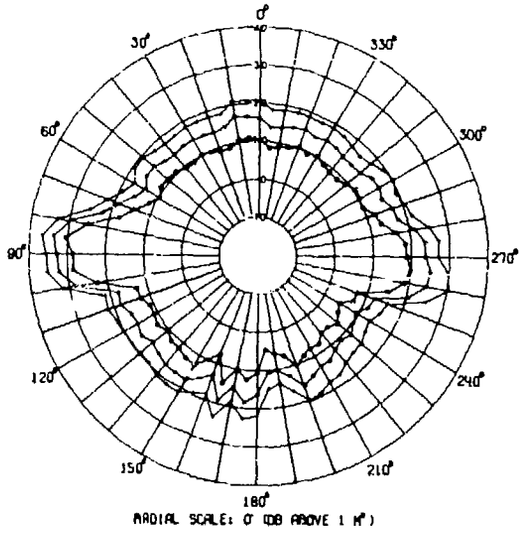

(C) Fig. 19c — Channel 3 XHH RUN 1242 CW

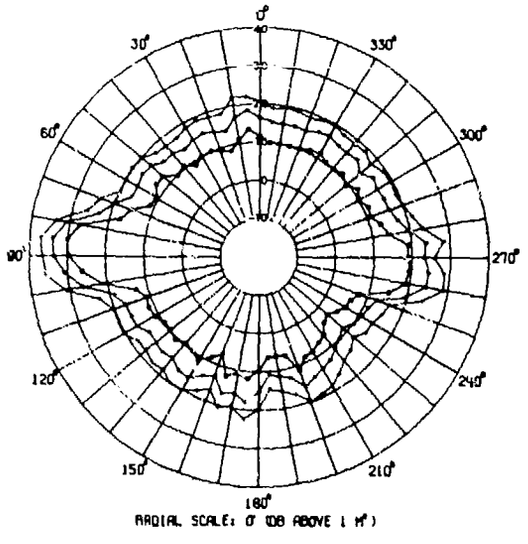

(C) Fig. 19d — Channel 4 CHH RUN 1242 CW

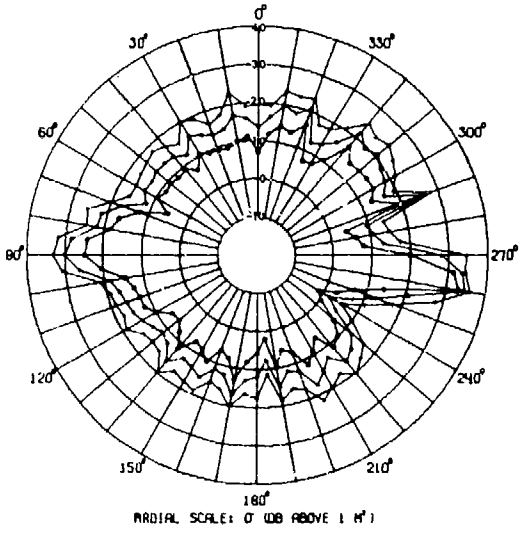

(C) Fig. 20a — Channel 1 LHH RUN 1243 CW

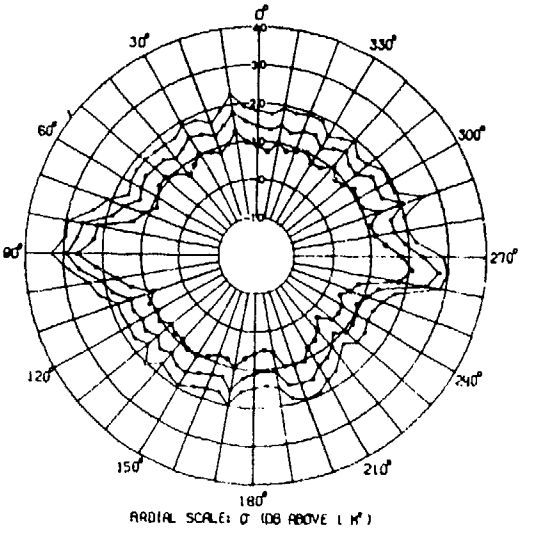

(C) Fig. 20b — Channel 2 SHH RUN 1243 CW

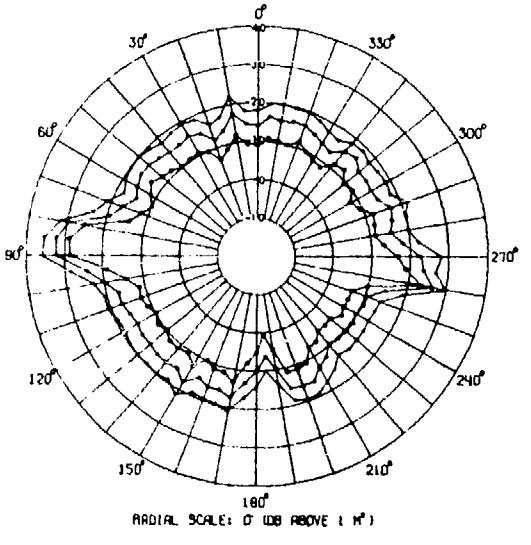

(C) Fig. 20c — Channel 3 XHH RUN 1243 CW

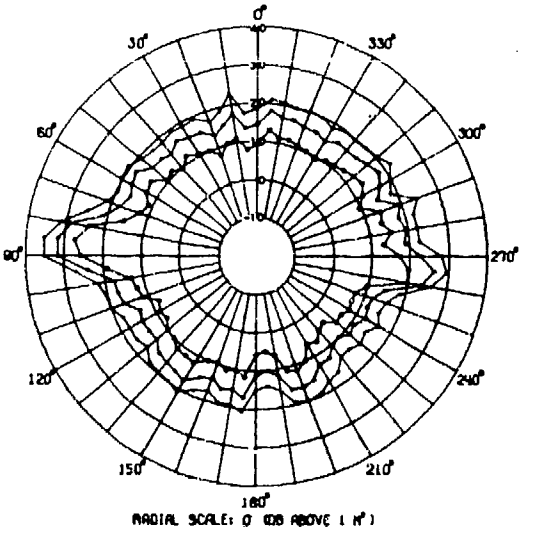

(C) Fig. 20d — Channel 4 CHH RUN 1243 CW

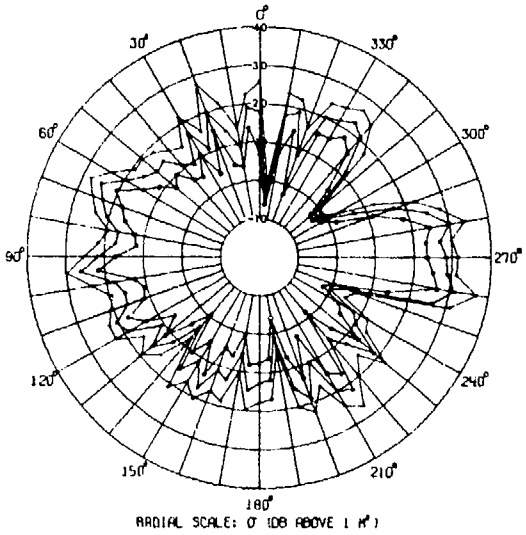

(C) Fig. 21a — Channel 1 LHH RUN 1244 CW

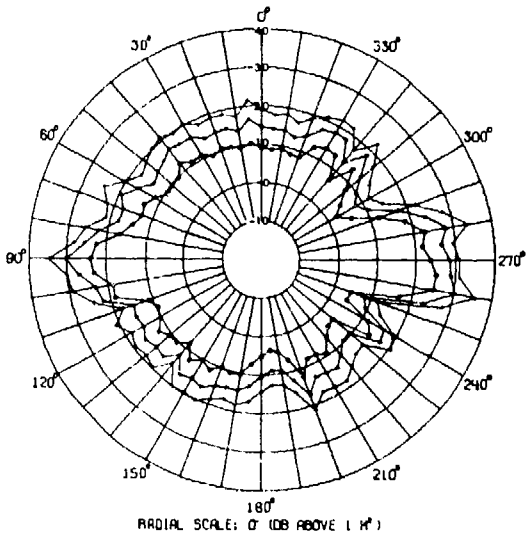

(C) Fig. 21b — Channel 2 SHH RUN 1244 CW

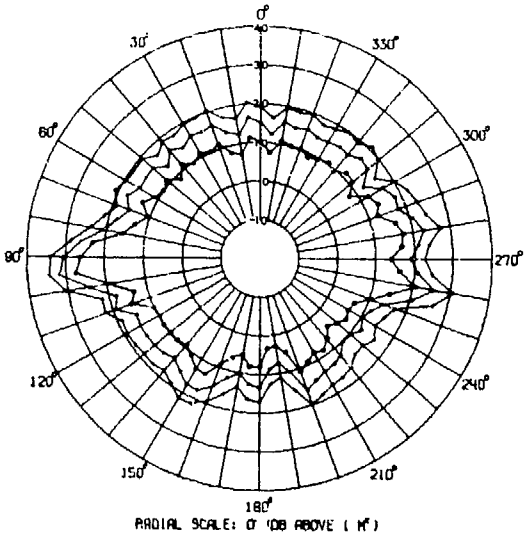

(C) Fig. 21c — Channel 3 XHH RUN 1244 CW

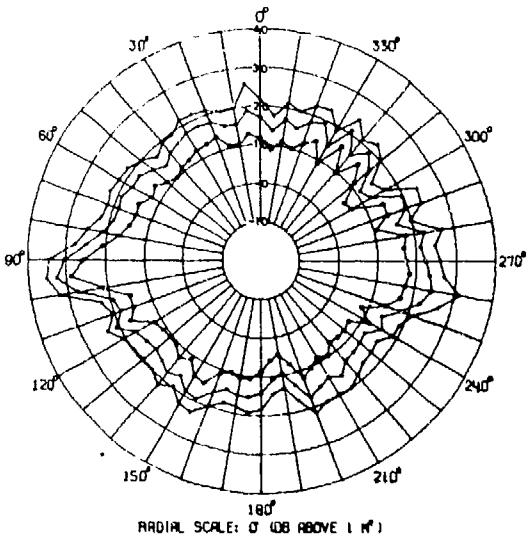

(C) Fig. 21d — Channel 4 CHH RUN 1244 CW

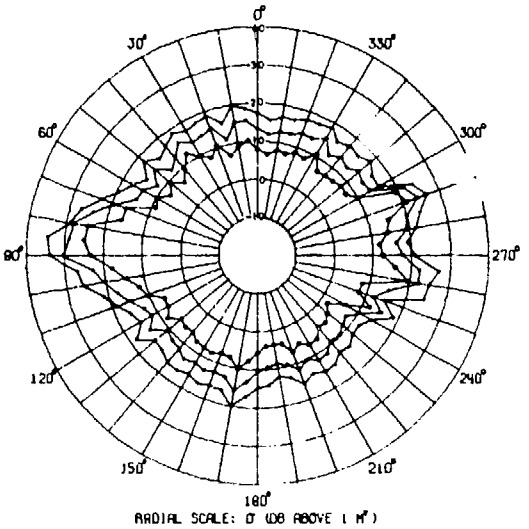

(C) Fig. 22a — Channel 1 LHH RUN 1245 CW

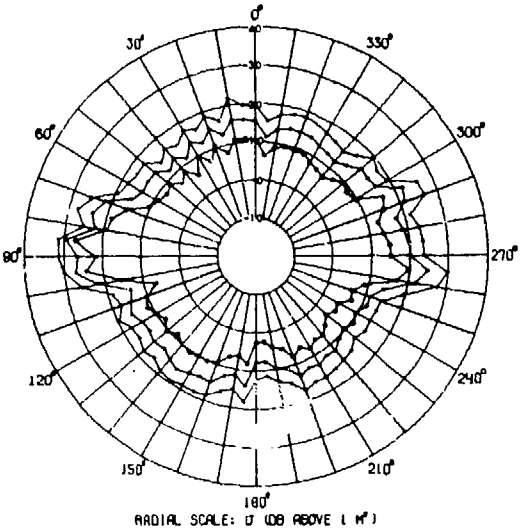

(C) Fig. 22b — Channel 2 SHH RUN 1245 CW

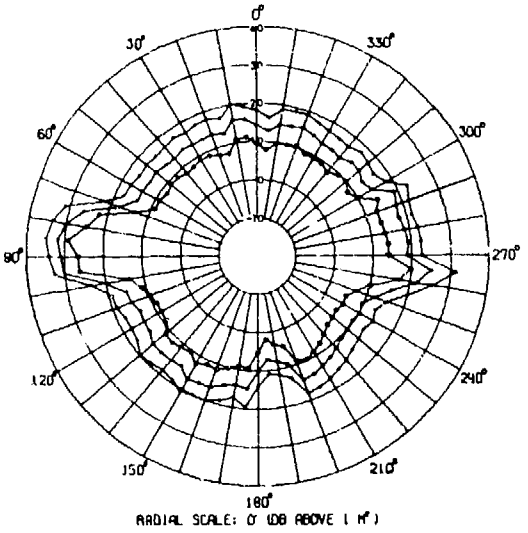

(C) Fig. 22c — Channel 3 XHH RUN 1245 CW

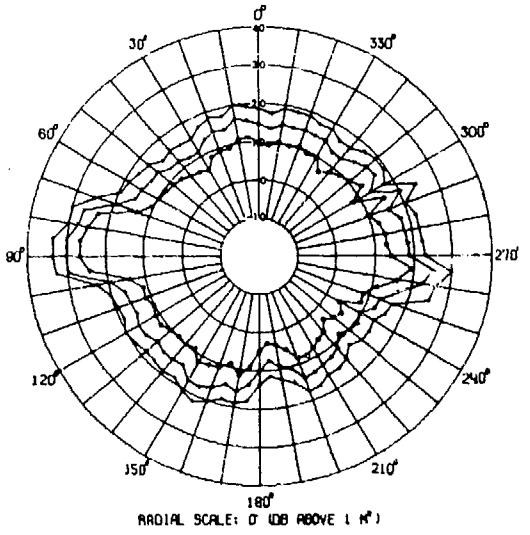

(C) Fig. 22d — Channel 4 CHH RUN 1245 CW

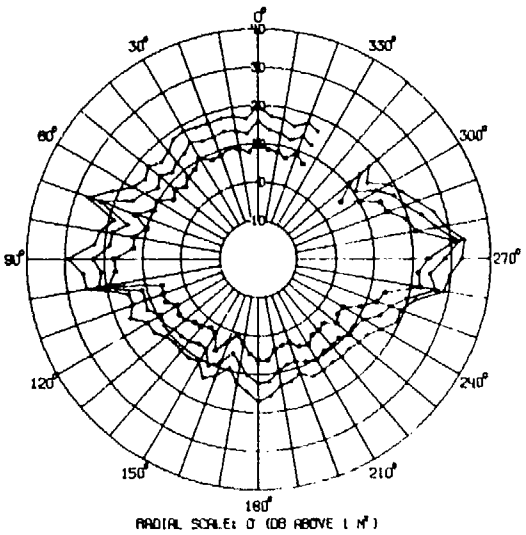

(C) Fig. 23a — Channel 1 LHH RUN 1246 CCW

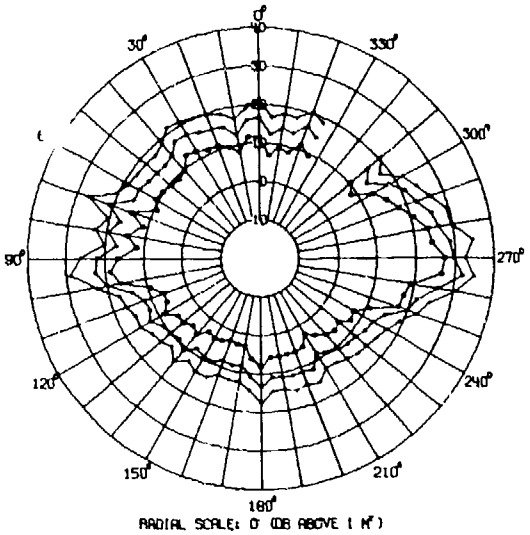

(C) Fig. 23b — Channel 2 SHH RUN 1246 CCW

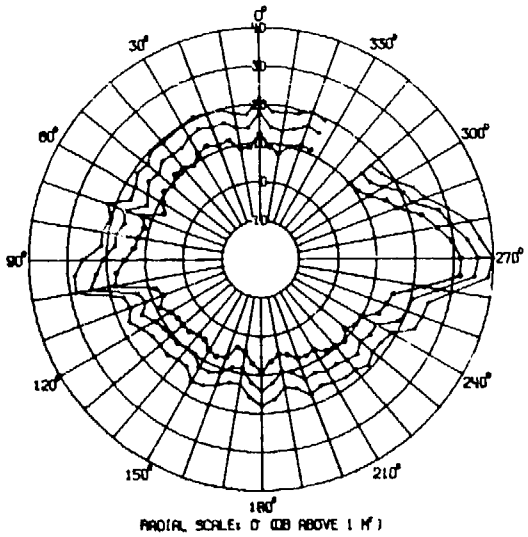

(C) Fig. 23c — Channel 3 XVV RUN 1246 CCW

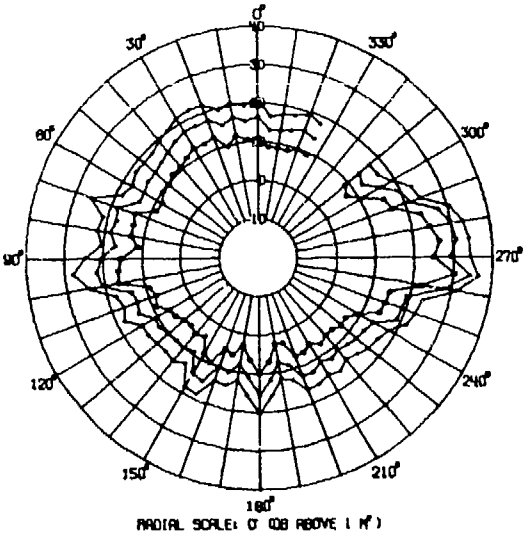

(C) Fig. 23d — Channel 4 CVV RUN 1246 CCW

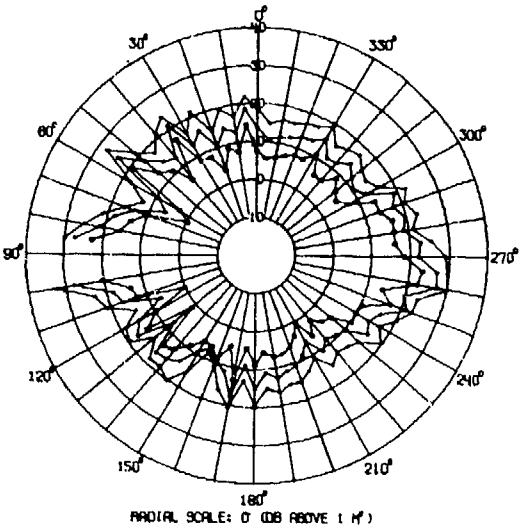

(C) Fig. 24a — Channel 1 LHH RUN 1247 CCW

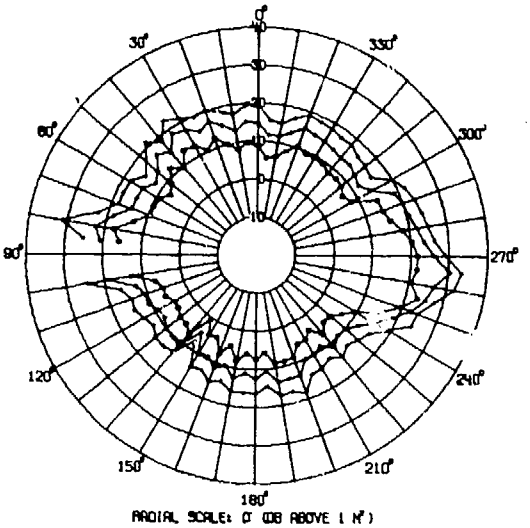

(C) Fig. 24b — Channel 2 SHH RUN 1247 CCW

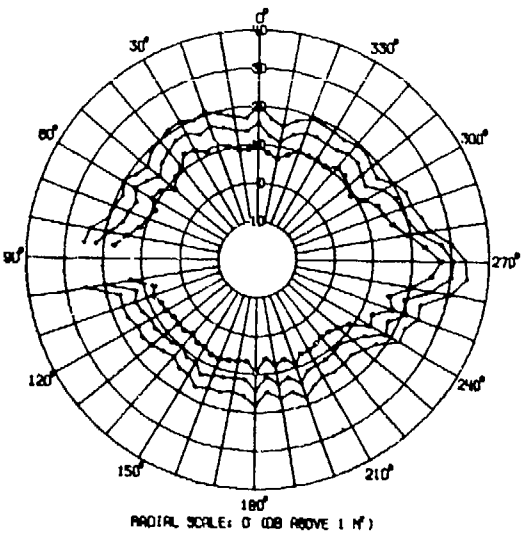

(C) Fig. 24c — Channel 3 XVV RUN 1247 CCW

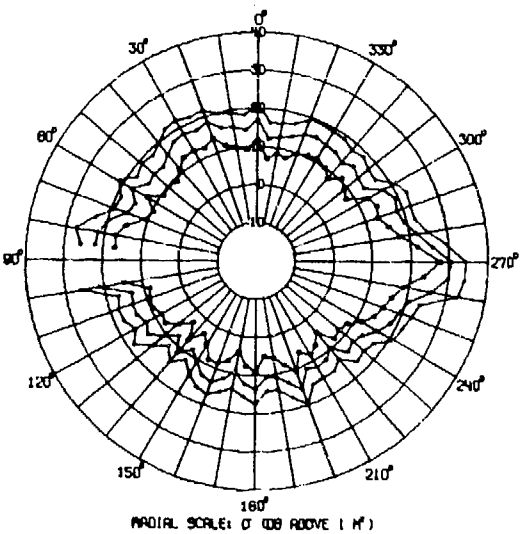

(C) Fig. 24d — Channel 4 CVV RUN 1247 CCW

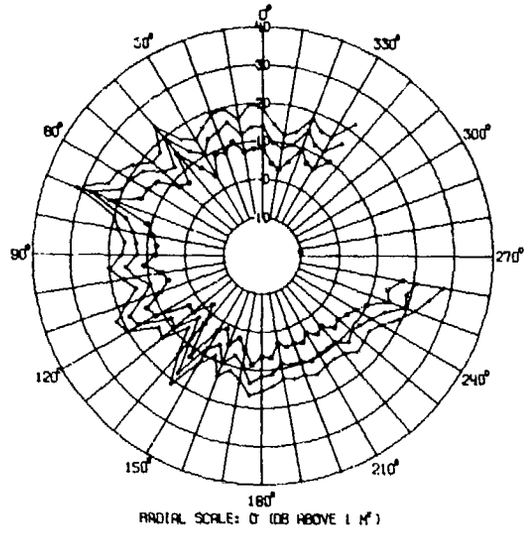

(C) Fig. 25a — Channel 1 LHH RUN 1248 CCW

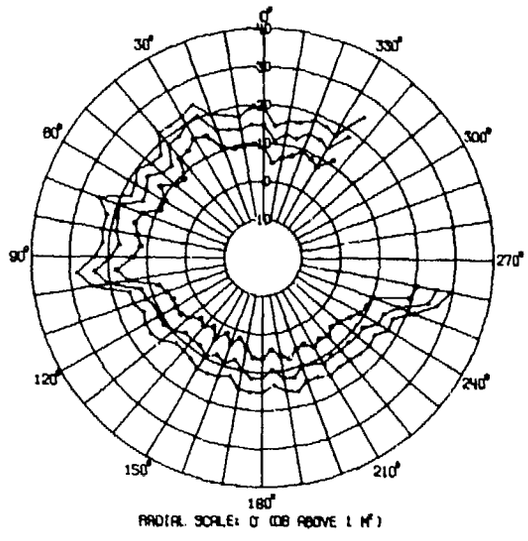

(C) Fig. 25b — Channel 2 SHH RUN 1248 CCW

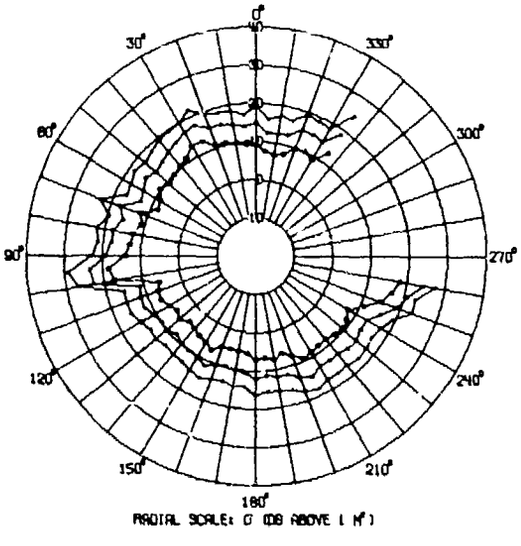

(C) Fig. 25c — Channel 3 XVV RUN 1248 CCW

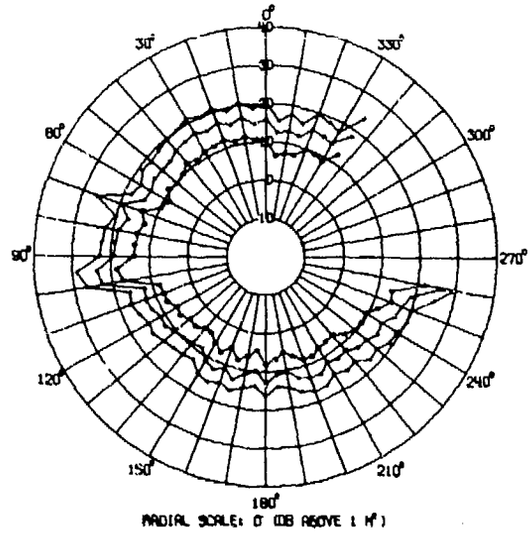

(C) Fig. 25d — Channel 4 CVV RUN 1248 CCW

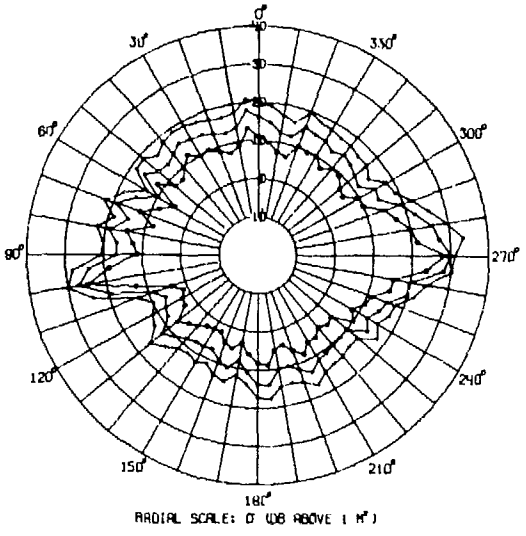

(C) Fig. 26a — Channel 1 LVV RUN 1262 CCW

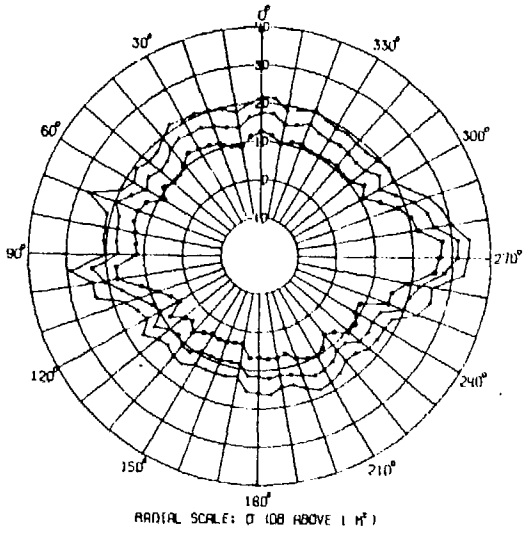

(C) Fig. 26b — Channel 2 SVV RUN 1262 CCW

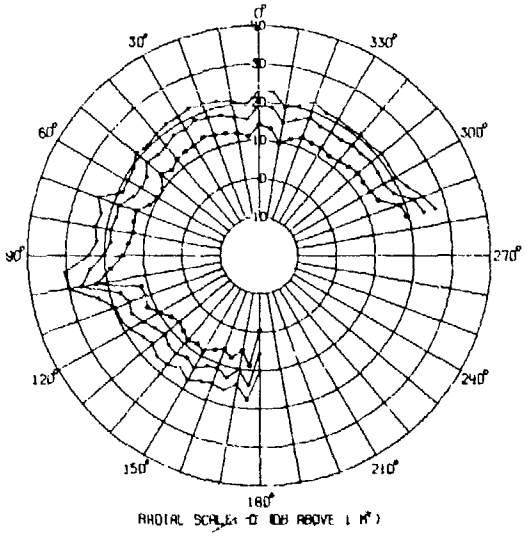

(C) Fig. 26c — Channel 3 XVV RUN 1262 CCW

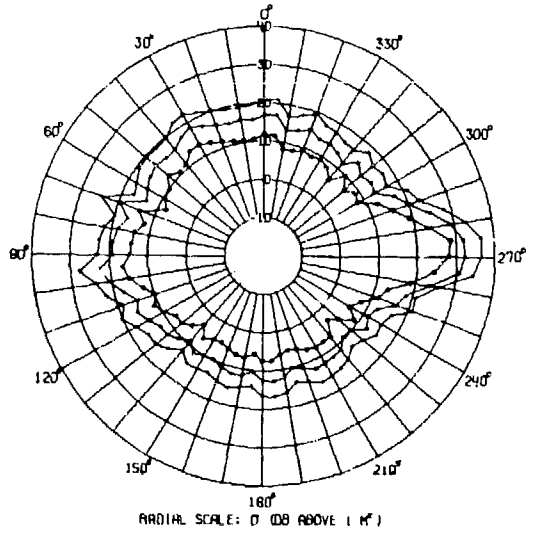

(C) Fig. 26d — Channel 4 CVV RUN 1262 CCW

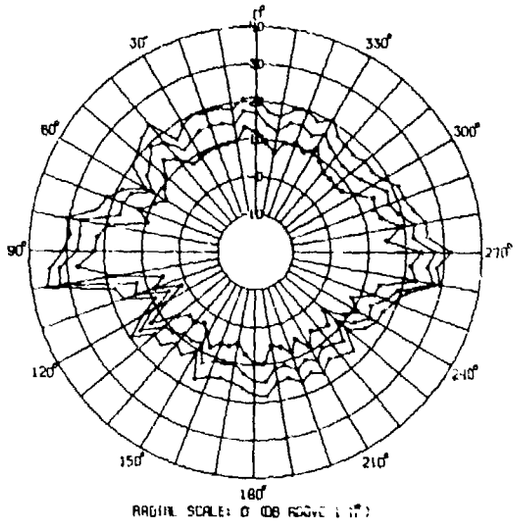

(C) Fig. 27a — Channel 1 LVV RUN 1263 CCW

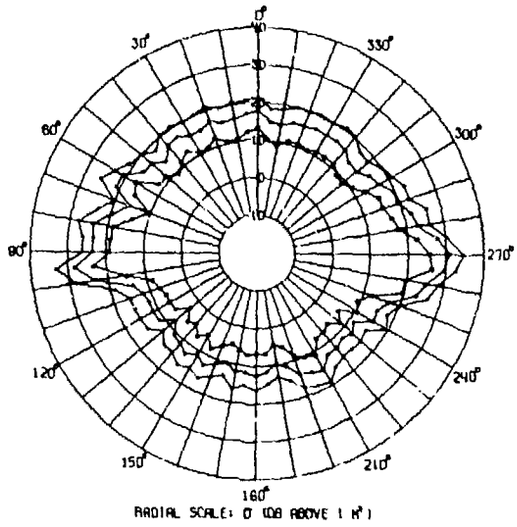

(C) Fig. 27b — Channel 2 SVV RUN 1263 CCW

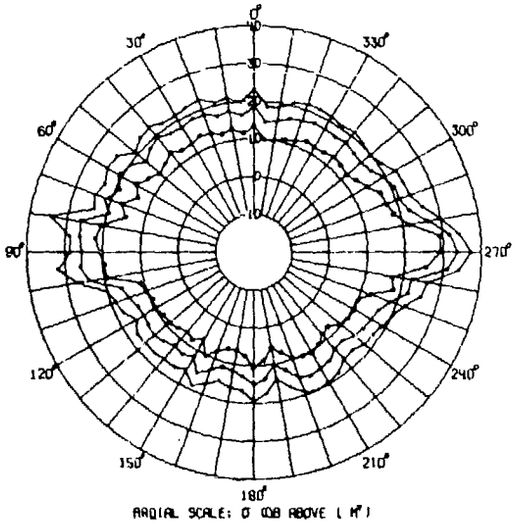

(C) Fig. 27c — Channel 3 XVV RUN 1263 CCW

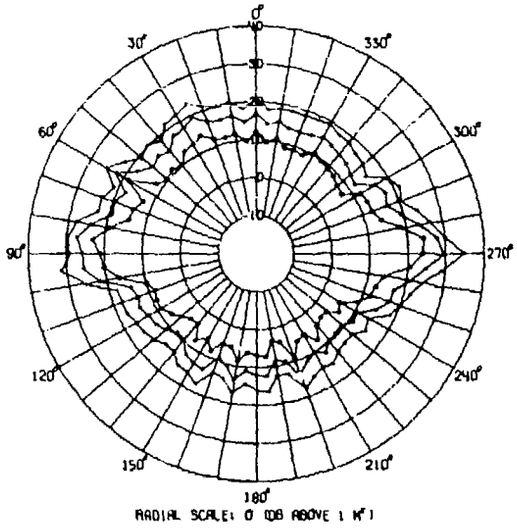

(C) Fig. 27d — Channel 4 CVV RUN 1263 CCW

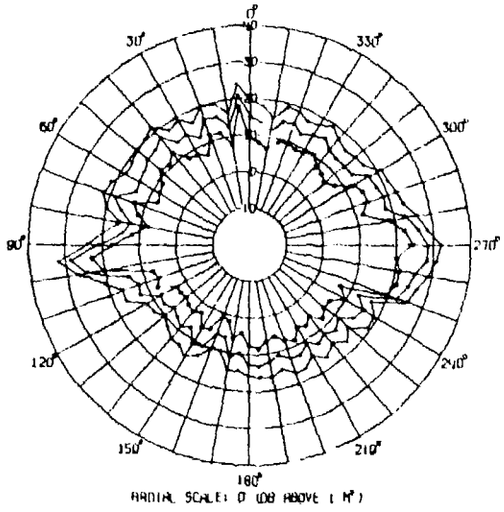

(C) Fig. 28a — Channel 1 LVV RUN 1264 CCW

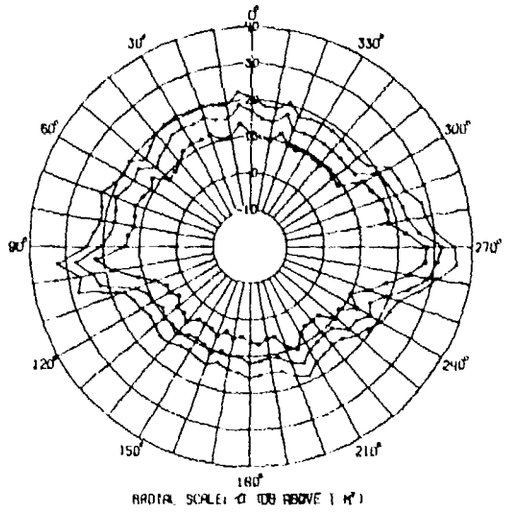

(C) Fig. 28b — Channel 2 SVV RUN 1264 CCW

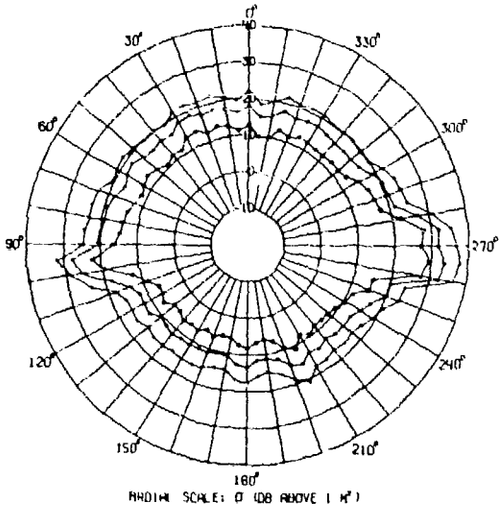

(C) Fig. 28c — Channel 3 XVV RUN 1264 CCW

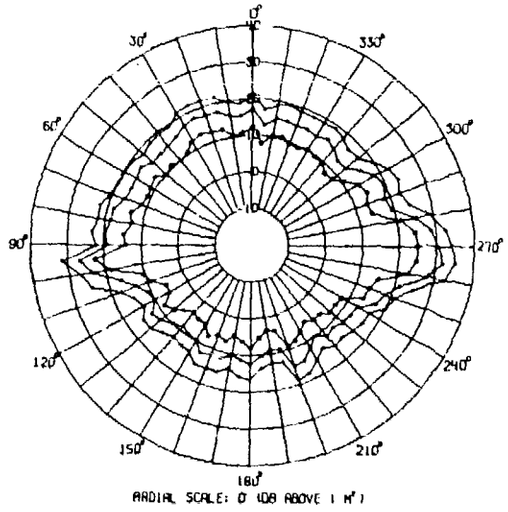

(C) Fig. 28d — Channel 4 CVV RUN 1264 CCW

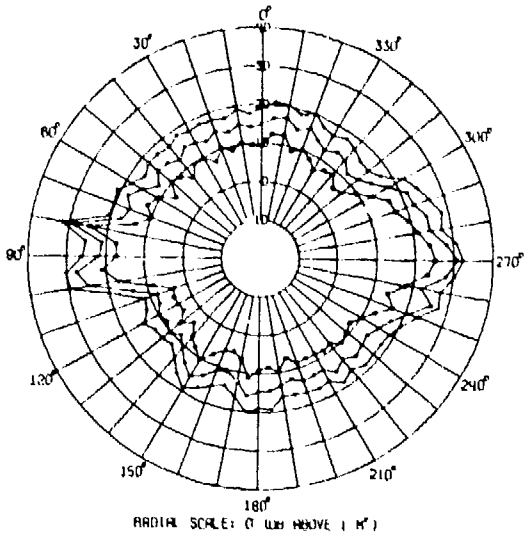

(C) Fig. 29a — Channel 1 LVV RUN 1265 CCW

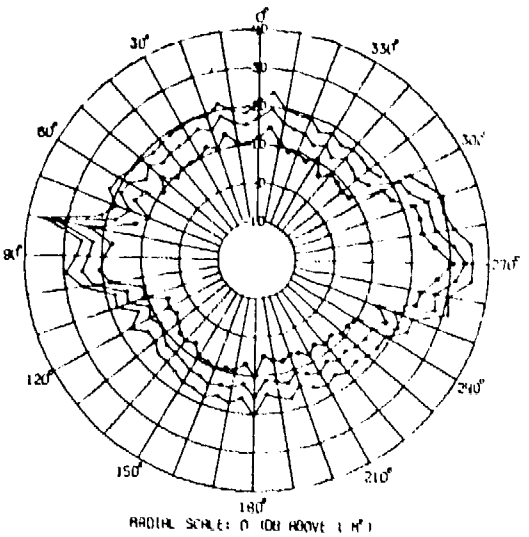

(C) Fig. 29b — Channel 2 SVV RUN 1265 CCW

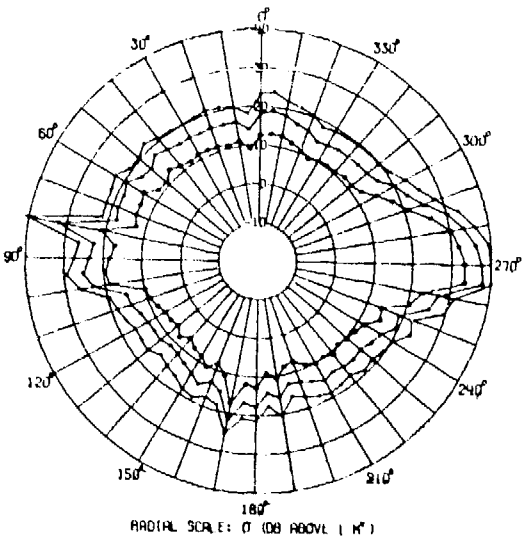

(C) Fig. 29c — Channel 3 XVV RUN 1265 CCW

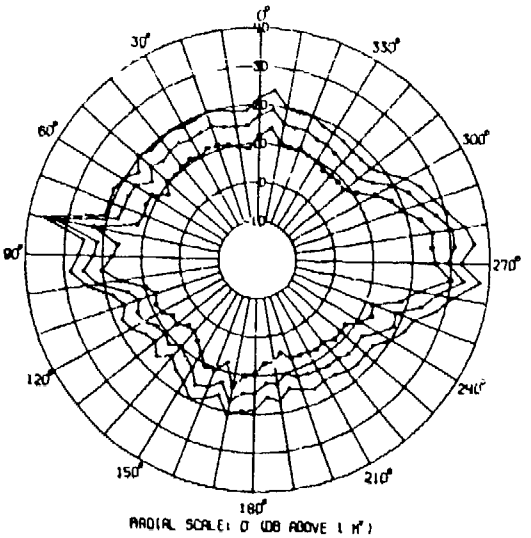

(C) Fig. 29d — Channel 4 CVV RUN 1265 CCW

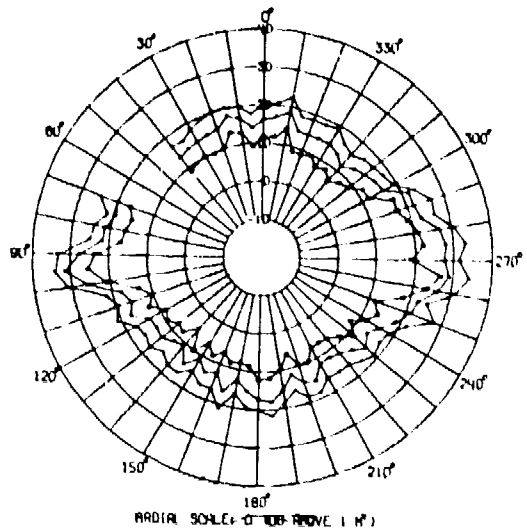

(C) Fig. 30a — Channel 1 LVV RUN 1266 CCW

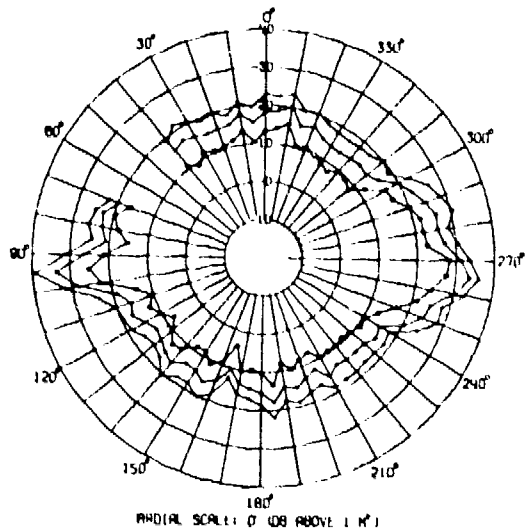

(C) Fig. 30b — Channel 2 SVV RUN 1266 CCW

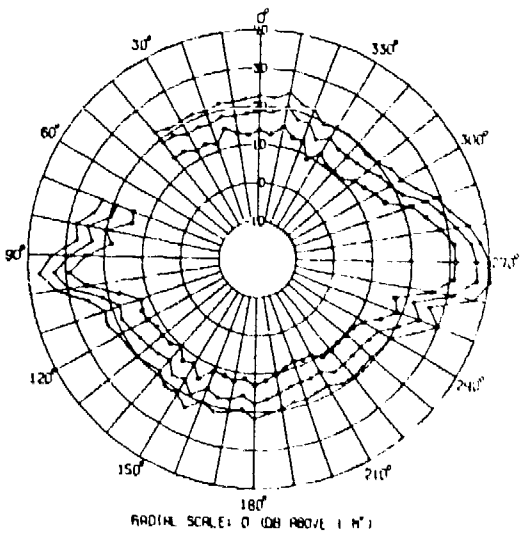

(C) Fig. 30c — Channel 3 XVV RUN 1266 CCW

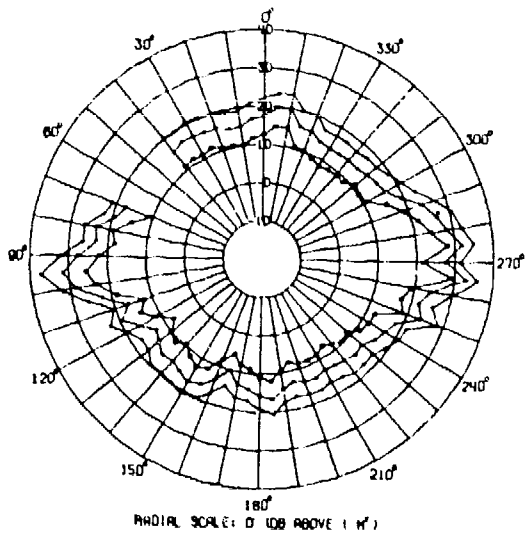

(C) Fig. 30d — Channel 4 CVV RUN 1266 CCW

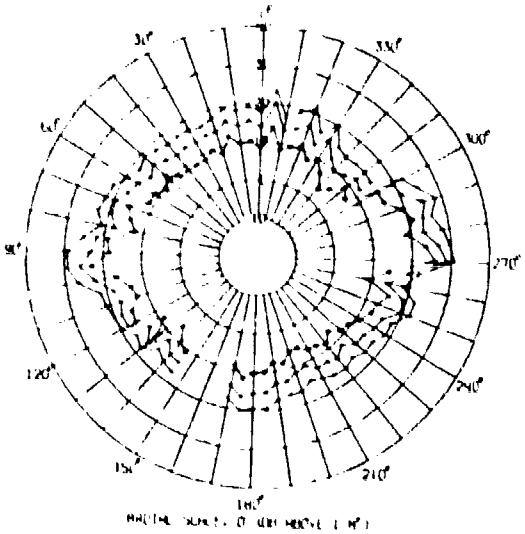

(C) Fig. 31a — Channel 1 LVV RUN 1267 CCW

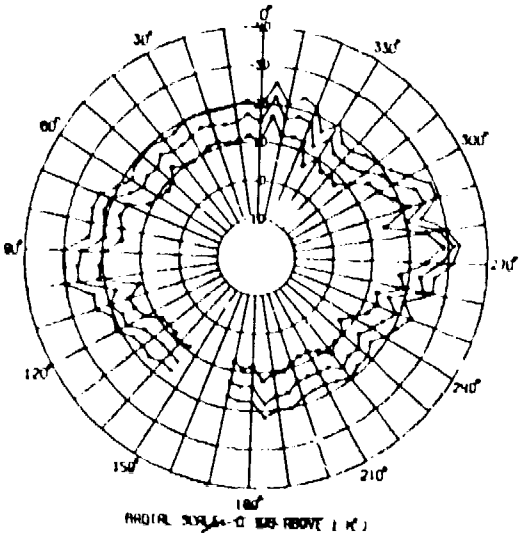

(C) Fig. 31b — Channel 2 SVV RUN 1267 CCW

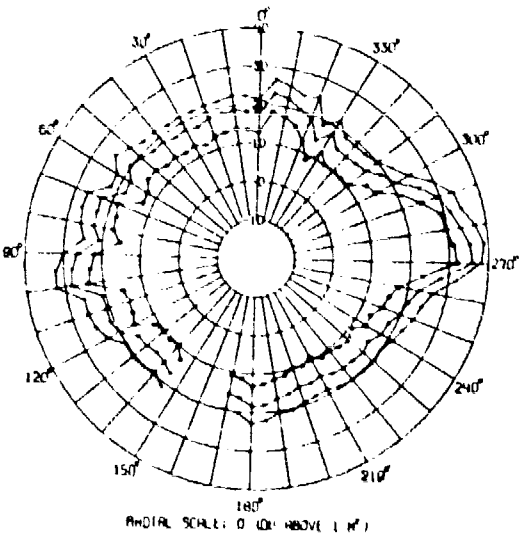

(C) Fig. 31c — Channel 3 XVV RUN 1267 CCW

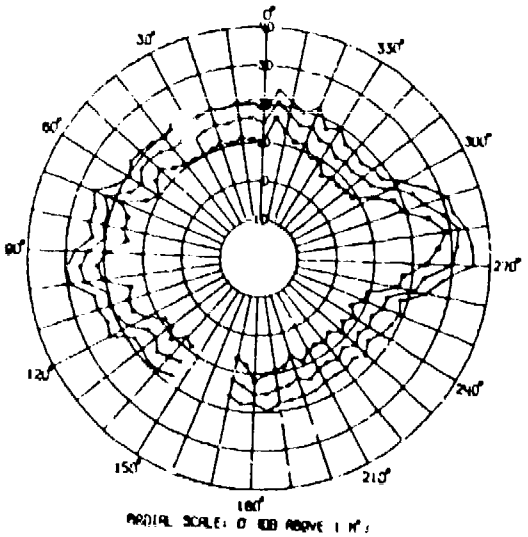

(C) Fig. 31d — Channel 4 CVV RUN 1267 CCW

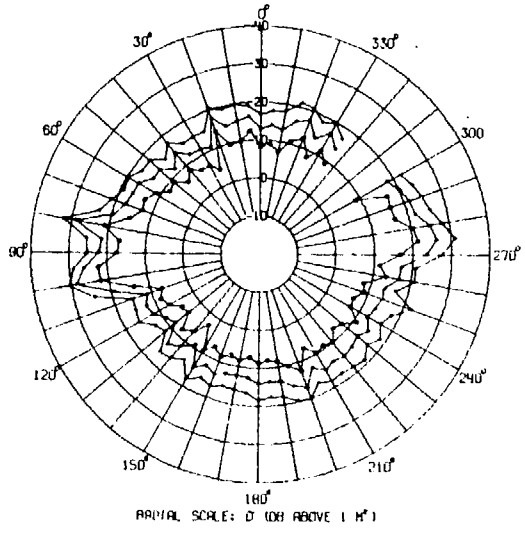

(C) Fig. 32a — Channel 1 LVV RUN 1268 CCW

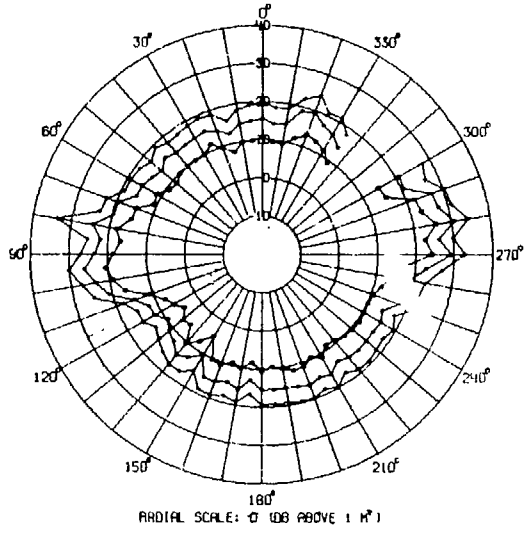

(C) Fig. 32b — Channel 2 SVV RUN 1268 CCW

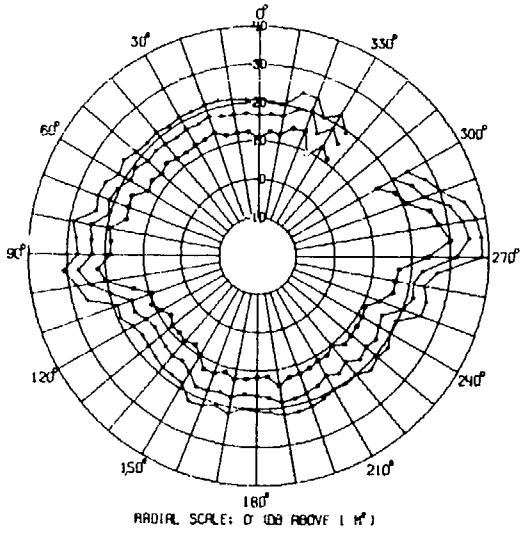

(C) Fig. 32c — Channel 3 XVV RUN 1268 CCW

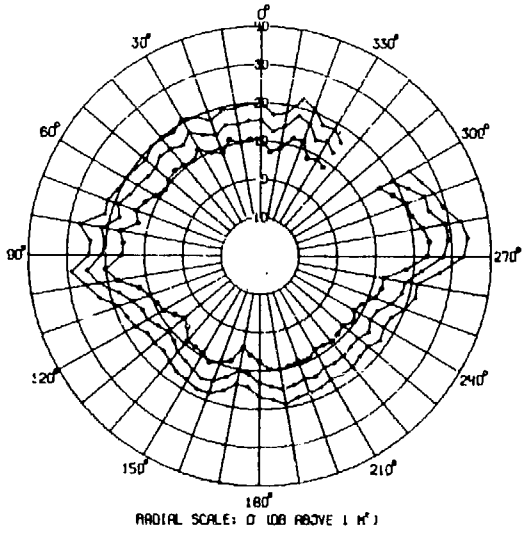

(C) Fig. 32d — Channel 4 CVV RUN 1268 CCW

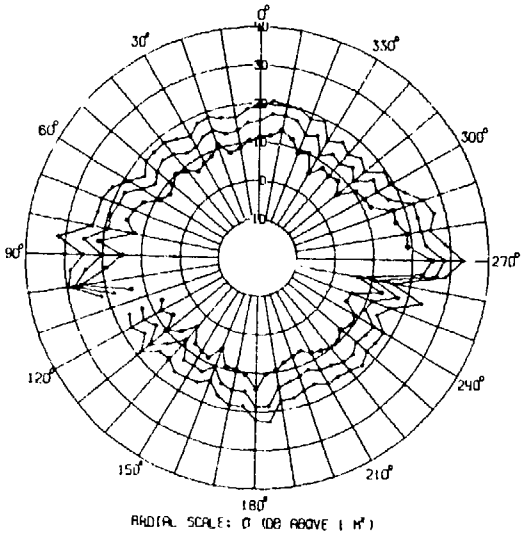

(C) Fig. 33a — Channel 1 LVV RUN 1269 CCW

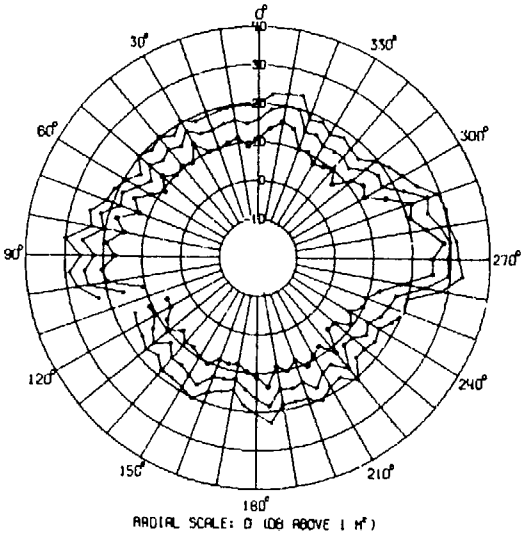

(C) Fig. 33b — Channel 2 SVV RUN 1269 CCW

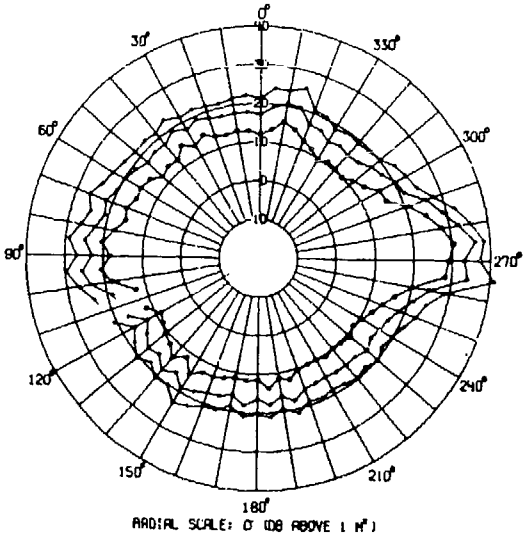

(C) Fig. 33c — Channel 3 XVV RUN 1269 CCW

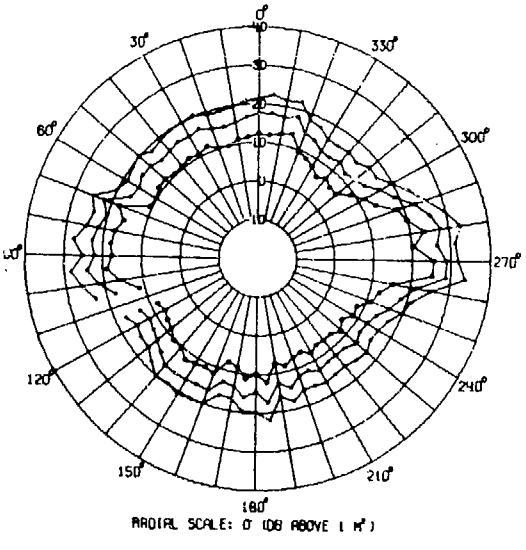

(C) Fig. 33d — Channel 4 CVV RUN 1269 CCW

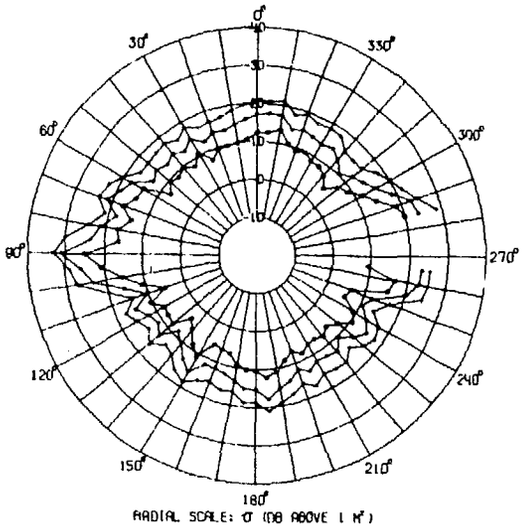

(C) Fig. 34a — Channel 1 LVV RUN 1270 CCW

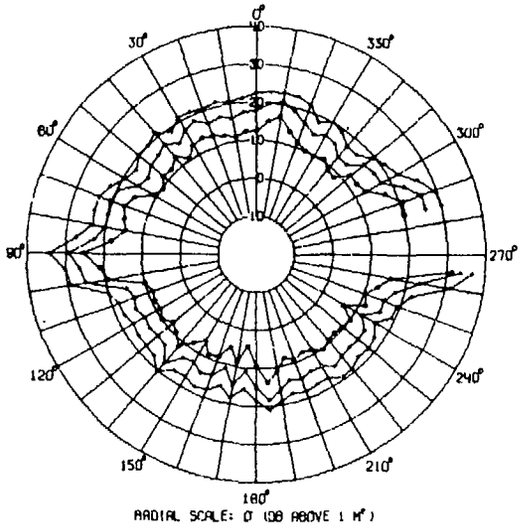

(C) Fig. 34b — Channel 2 SVV RUN 1270 CCW

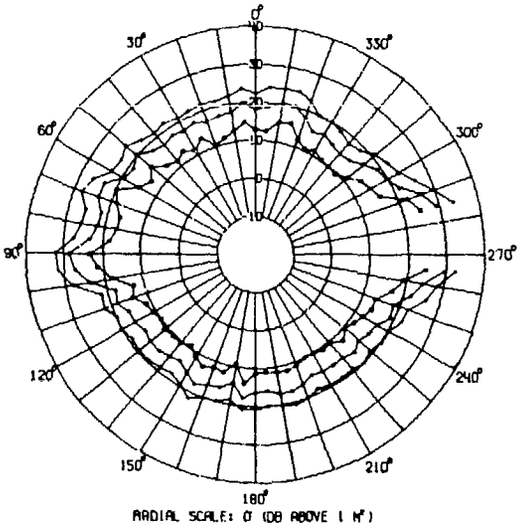

(C) Fig. 34c — Channel 3 XVV RUN 1270 CCW

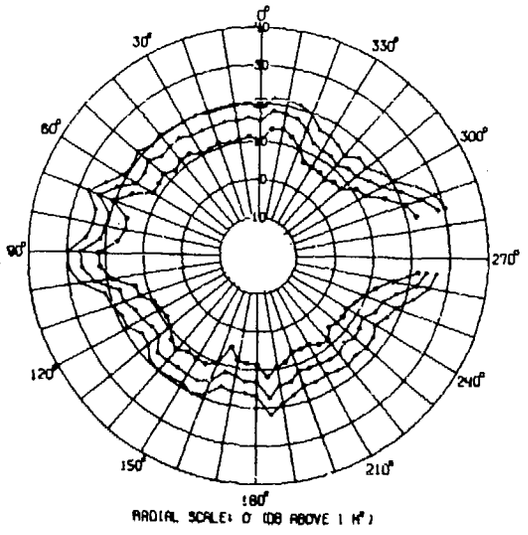

(C) Fig. 34d — Channel 4 CVV RUN 1270 CCW

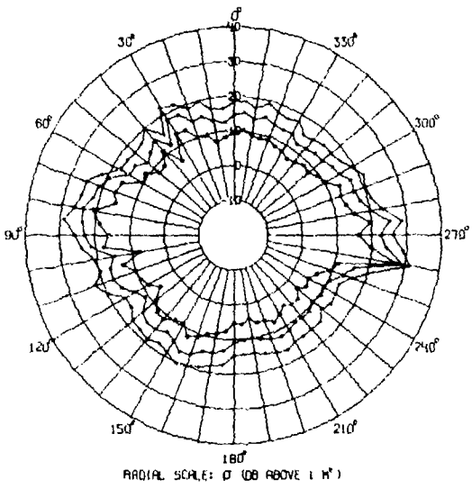

(C) Fig. 35a — Channel 1 LVV RUN 1271 CW

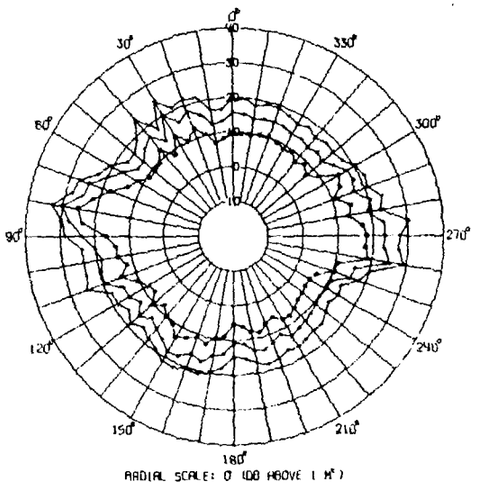

(C) Fig. 35b — Channel 2 SVV RUN 1271 CW

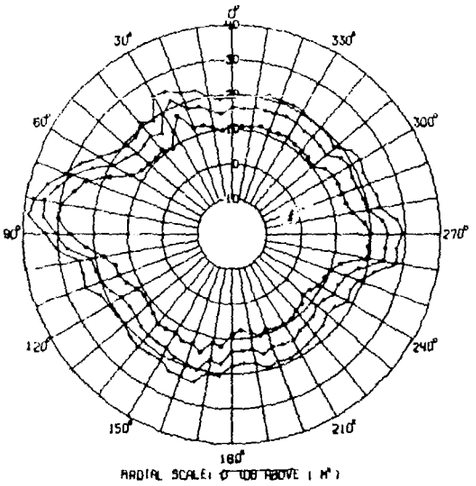

(C) Fig. 35c — Channel 3 XVV RUN 1271 CW

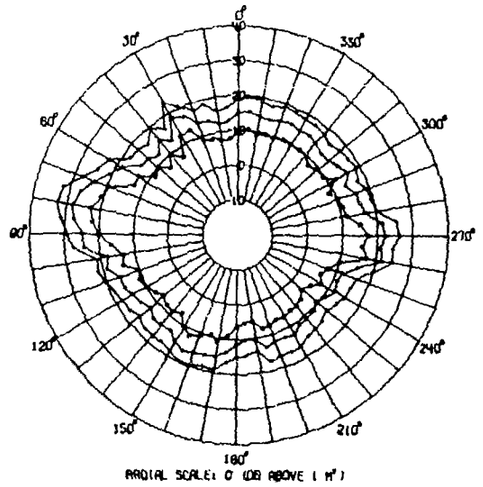

(C) Fig. 35d — Channel 4 CVV RUN 1271 CW

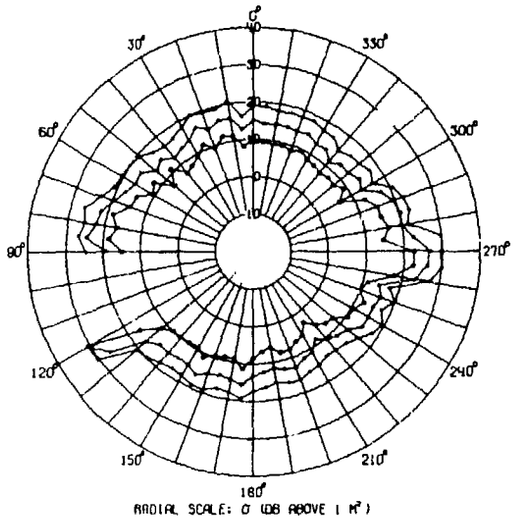

(C) Fig. 36a — Channel 1 LVV RUN 1272 CW

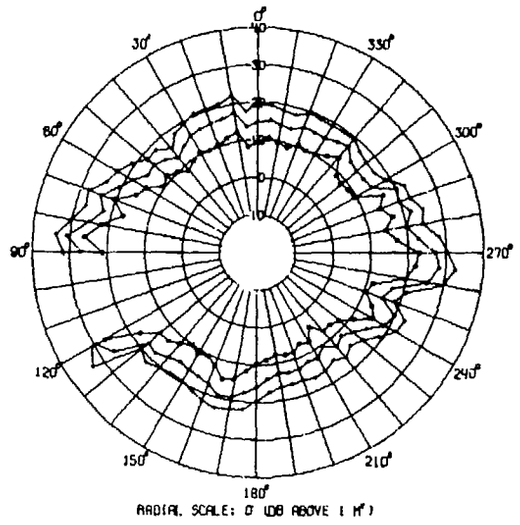

(C) Fig. 36b — Channel 2 SVV RUN 1272 CW

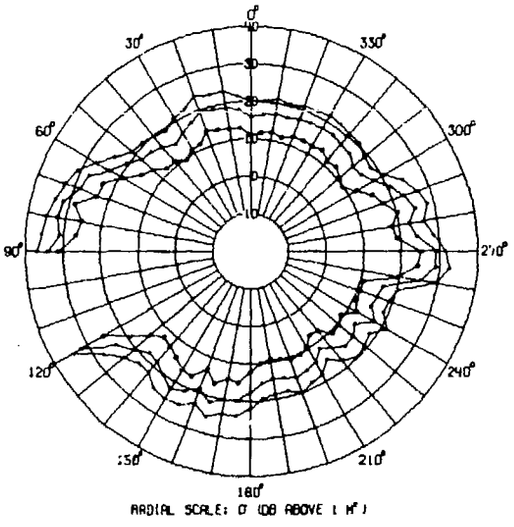

(C) Fig. 36c — Channel 3 XVV RUN 1272 CW

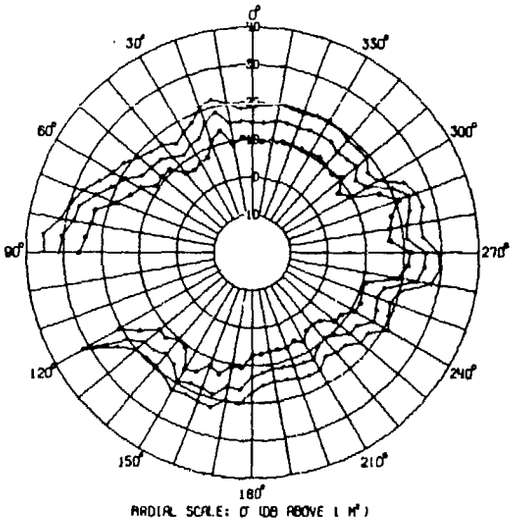

(C) Fig. 36d — Channel 4 CVV RUN 1272 CW

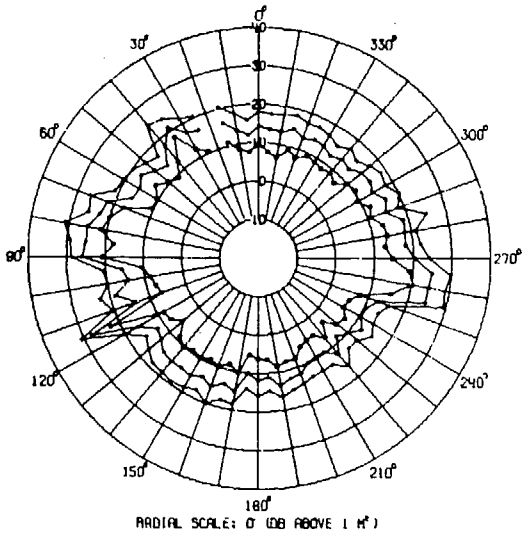

(C) Fig. 37a — Channel 1 LVV RUN 1273 CW

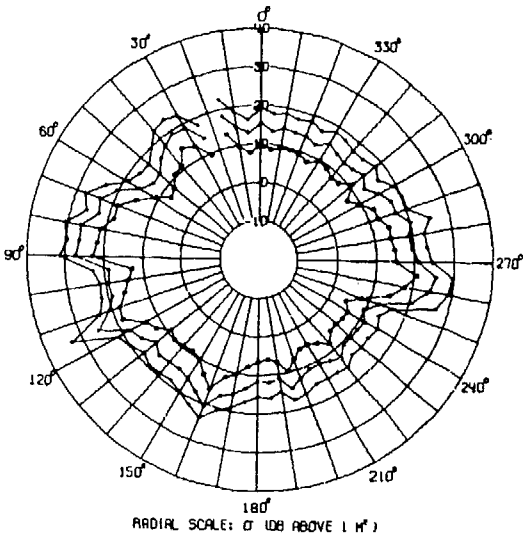

(C) Fig. 37b — Channel 2 SVV RUN 1273 CW

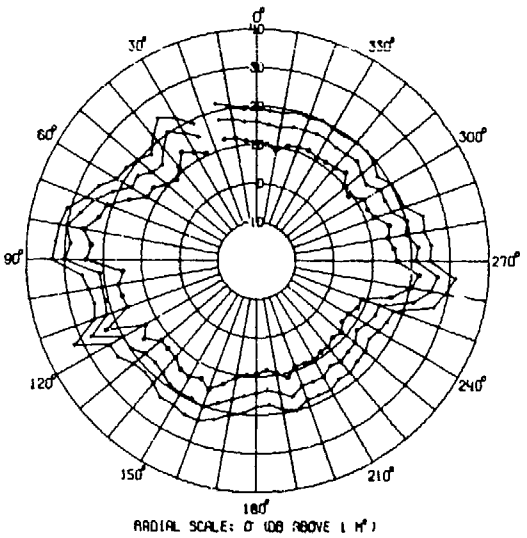

(C) Fig. 37c — Channel 3 XVV RUN 1273 CW

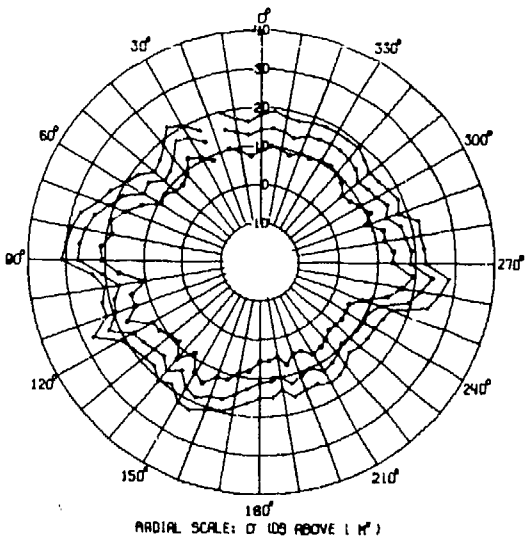

(C) Fig. 37d — Channel 4 CVV RUN 1273 CW

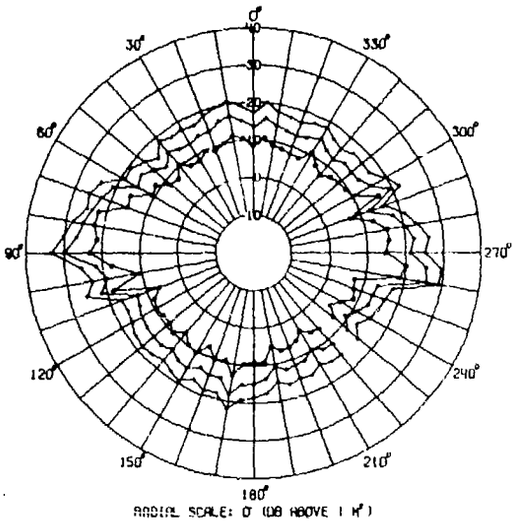

(C) Fig. 38a — Channel 1 LVV RUN 1274 CW

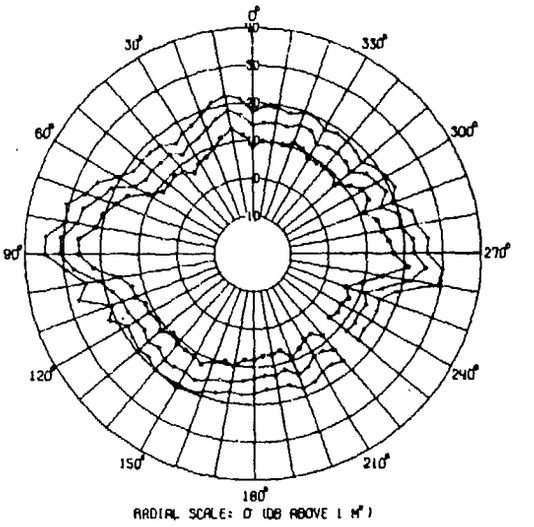

(C) Fig. 38b — Channel 2 SVV RUN 1274 CW

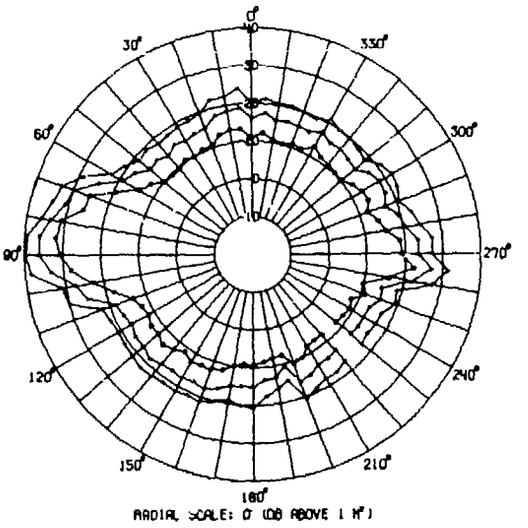

(C) Fig. 38c — Channel 3 XVV RUN 1274 CW

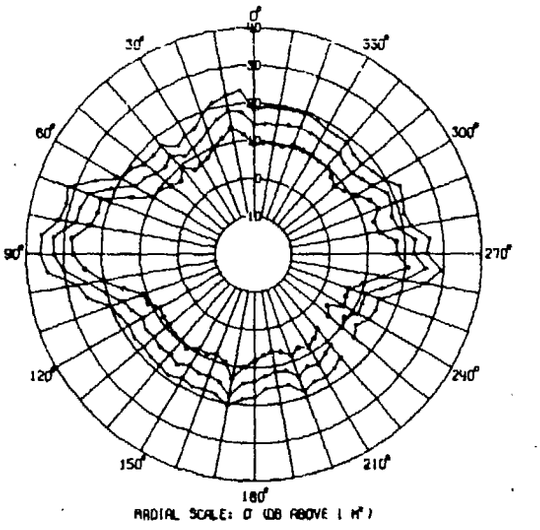

(C) Fig. 38d — Channel 4 CVV RUN 1274 CW

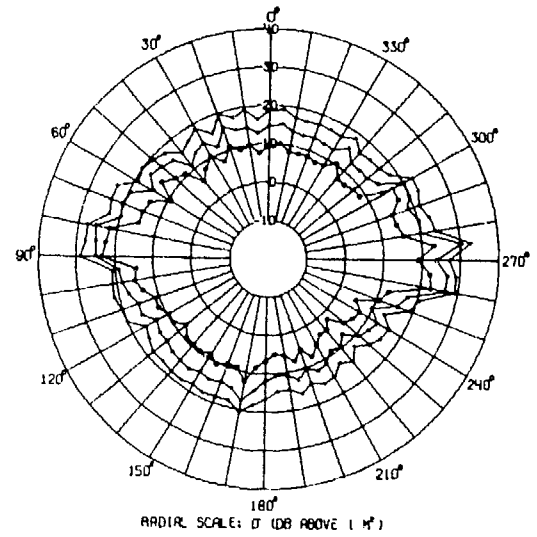

(C) Fig. 39a — Channel 1 LVV RUN 1275 CW

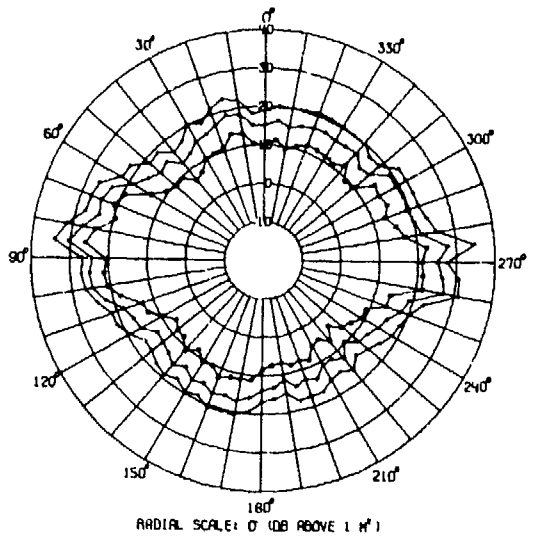

(C) Fig. 39b — Channel 2 SVV RUN 1275 CW

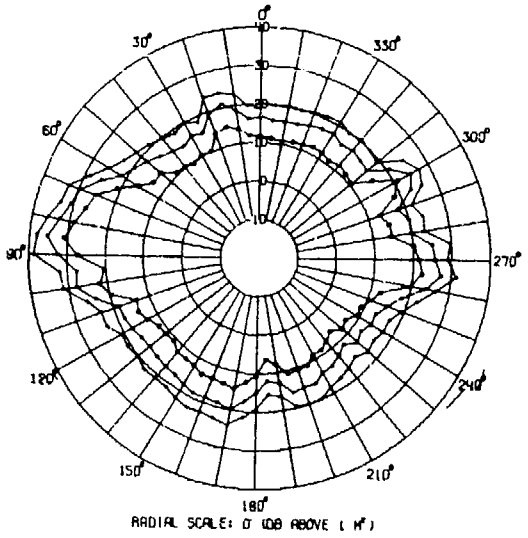

(C) Fig. 39c — Channel 3 XVV RUN 1275 CW

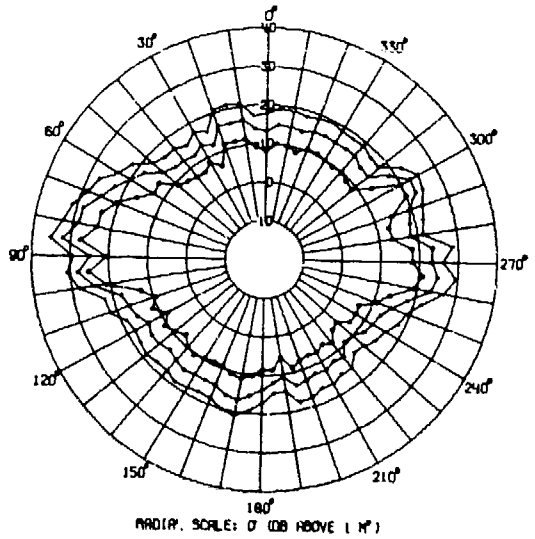

(C) Fig. 39d — Channel 4 CVV RUN 1275 CW

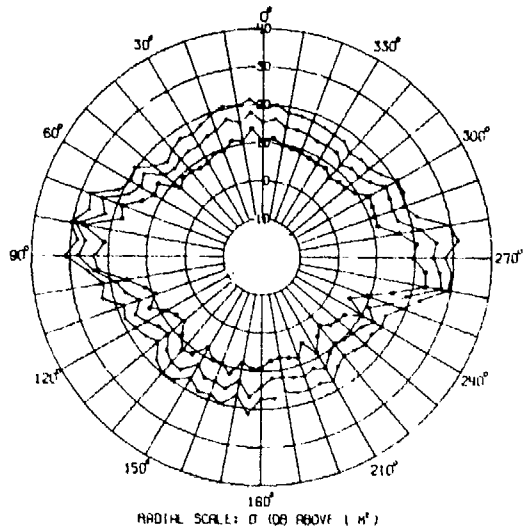

(C) Fig. 40a — Channel 1 LVV RUN 1276 CW

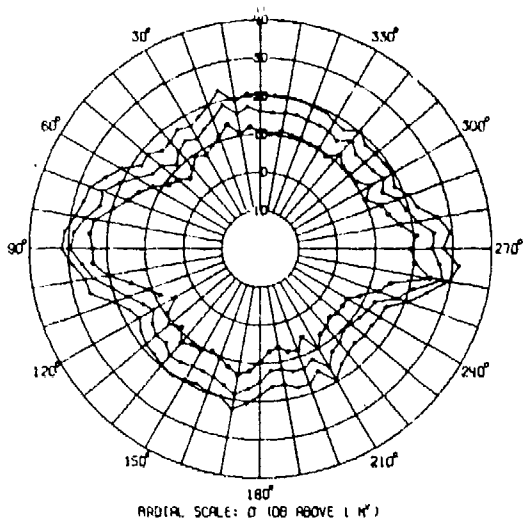

(C) Fig. 40b — Channel 2 SVV RUN 1276 CW

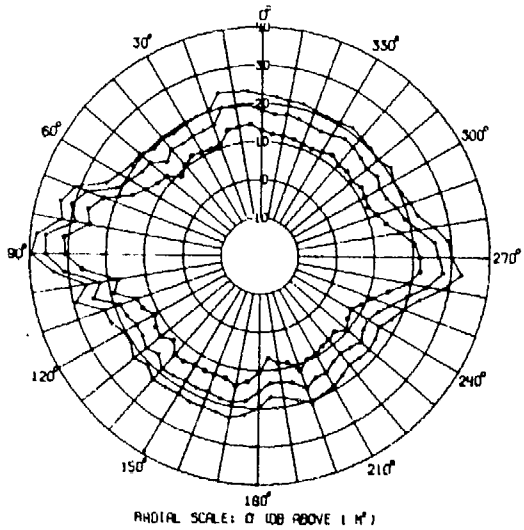

(C) Fig. 40c — Channel 3 XVV RUN 1276 CW

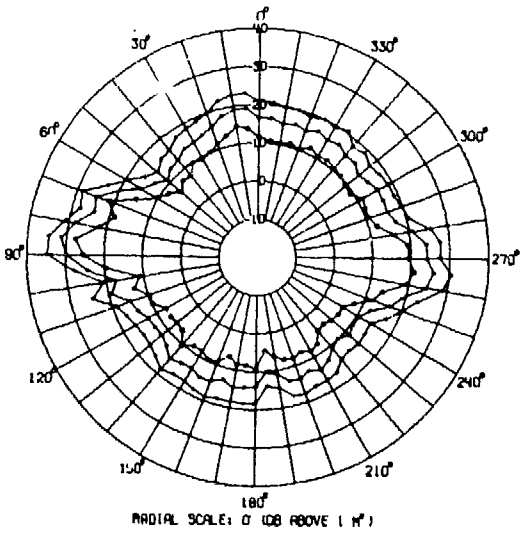

(C) Fig. 40d — Channel 4 CVV RUN 1276 CW

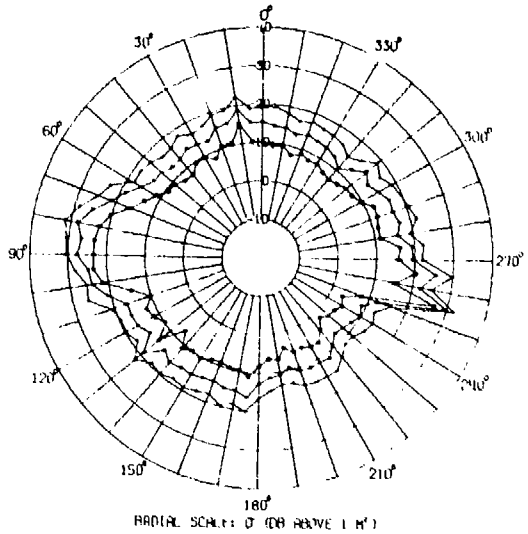

(C) Fig. 41a — Channel 1 LVV RUN 1277 CW

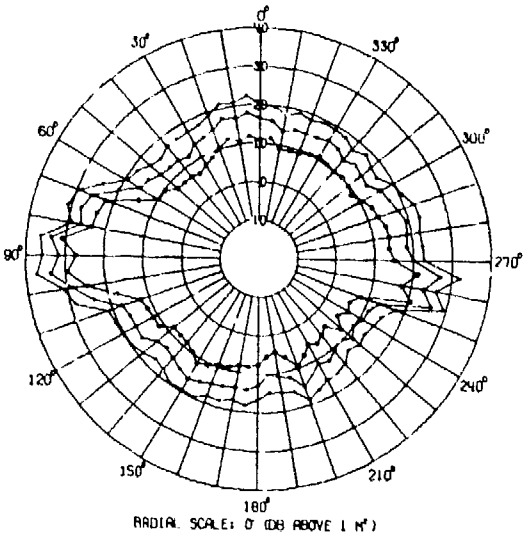

(C) Fig. 41b — Channel 2 SVV RUN 1277 CW

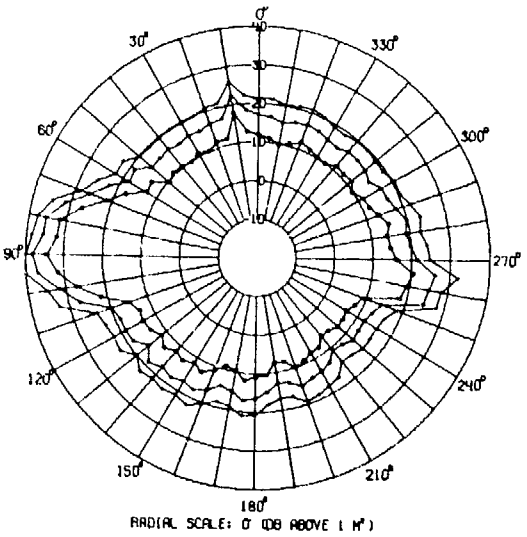

(C) Fig. 41c — Channel 3 XVV RUN 1277 CW

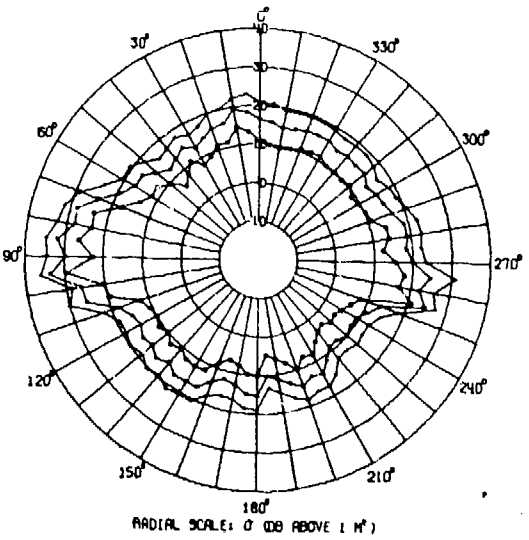

(C) Fig. 41d — Channel 4 CVV RUN 1277 CW

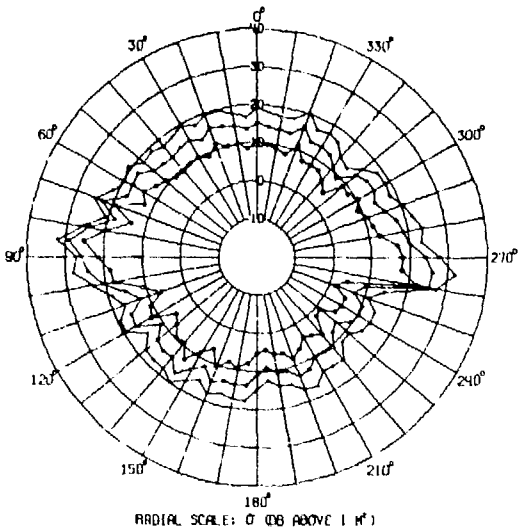

(C) Fig. 42a — Channel 1 LVV RUN 1278 CW

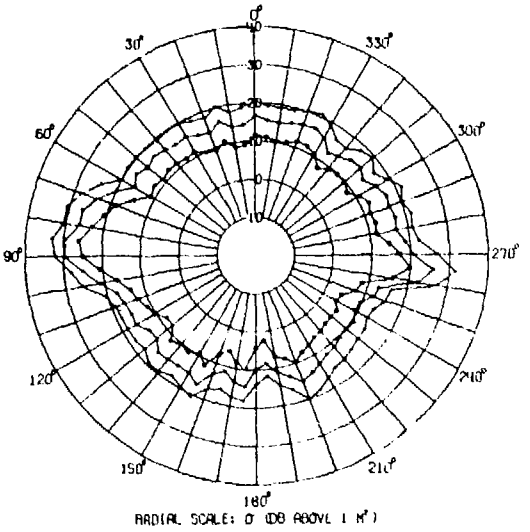

(C) Fig. 42b — Channel 2 SVV RUN 1278 CW

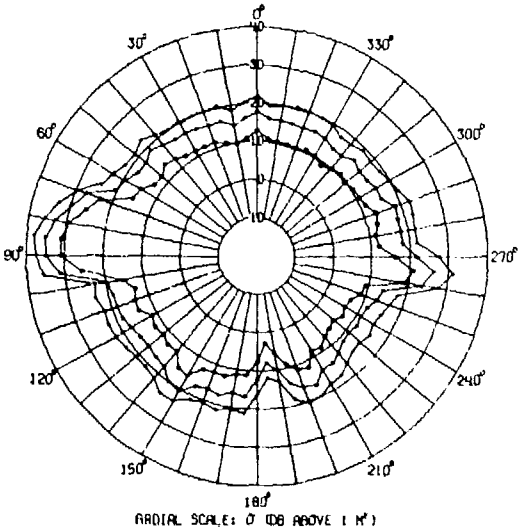

(C) Fig. 42c — Channel 3 XVV RUN 1278 CW

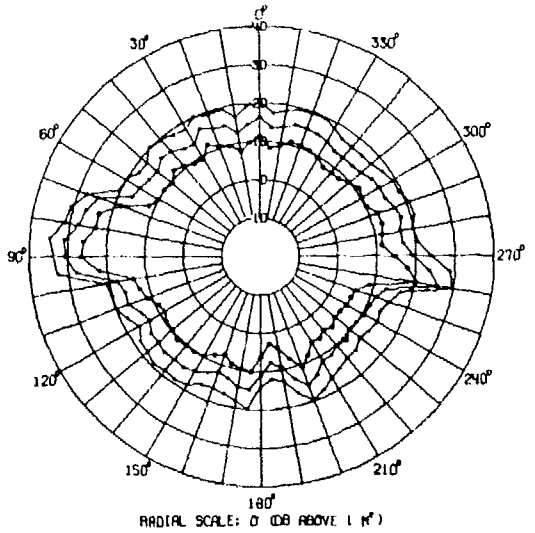

(C) Fig. 42d — Channel 4 CVV RUN 1278 CW

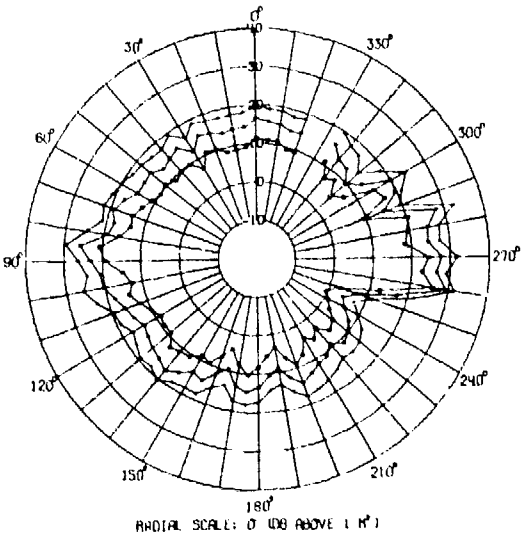

(C) Fig. 43a — Channel 1 LVV RUN 1279 CW

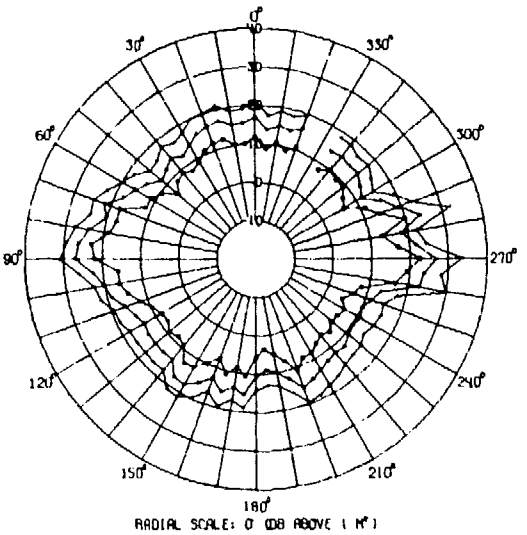

(C) Fig. 43b — Channel 2 SVV RUN 1279 CW

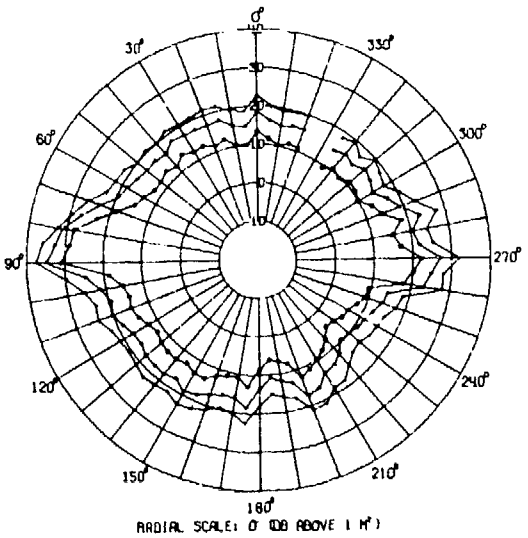

(C) Fig. 43c — Channel 3 XVV RUN 1279 CW

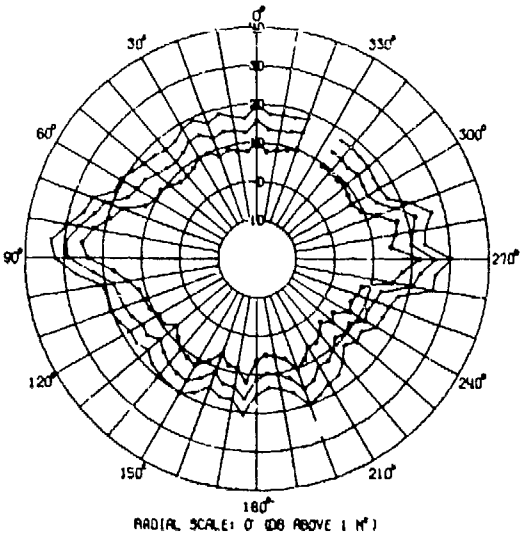

(C) Fig. 43d — Channel 4 CVV RUN 1279 CW

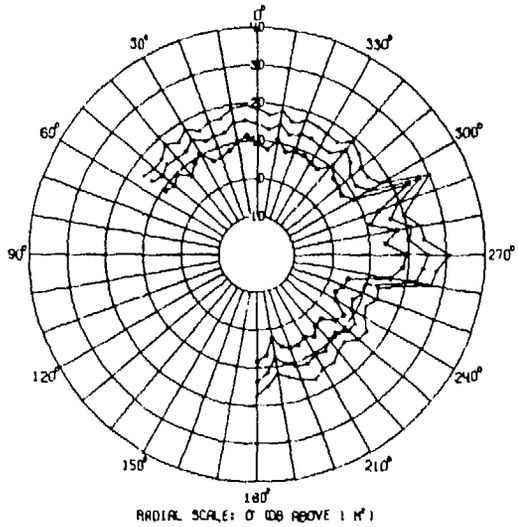

(C) Fig. 44a — Channel 1 LVV RUN 1280 CW

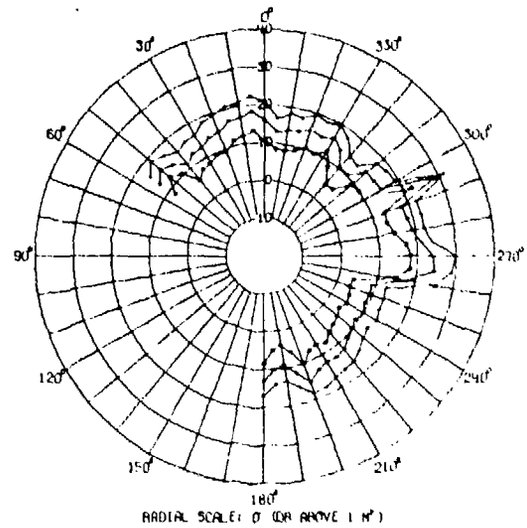

(C) Fig. 44b — Channel 2 SVV RUN 1280 CW

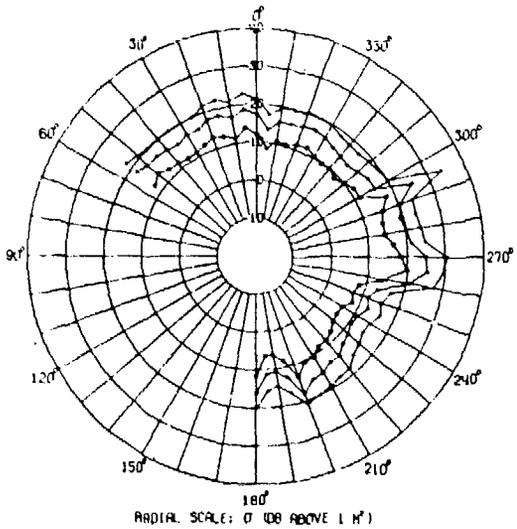

(C) Fig. 44c — Channel 3 XVV RUN 1280 CW

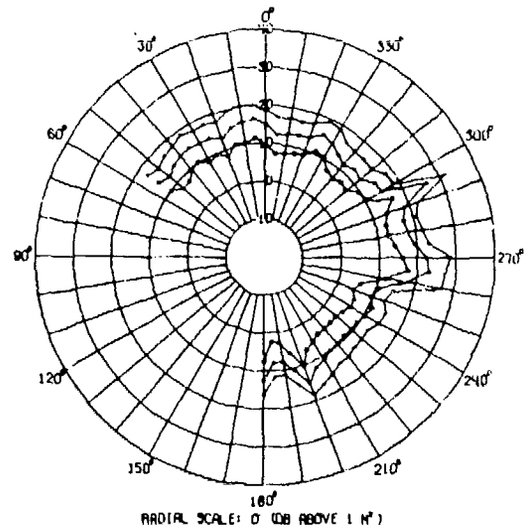

(C) Fig. 44d — Channel 4 CVV RUN 1280 CW

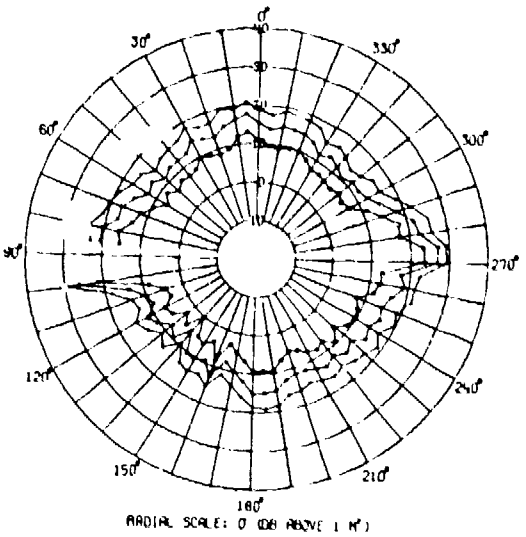

(C) Fig. 45a — Channel 1 LVV RUN 1281 CCW

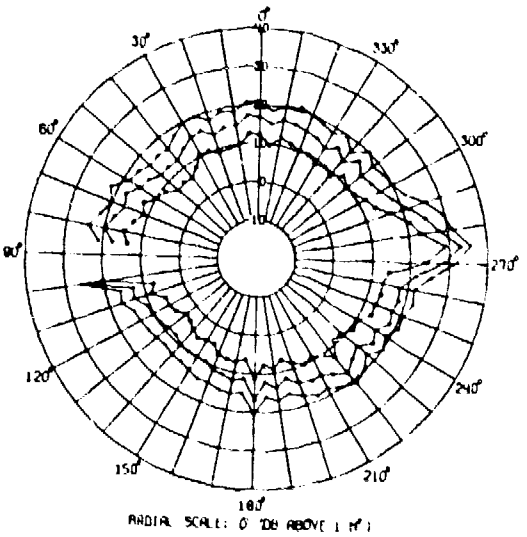

(C) Fig. 45b — Channel 2 SVV RUN 1281 CCW

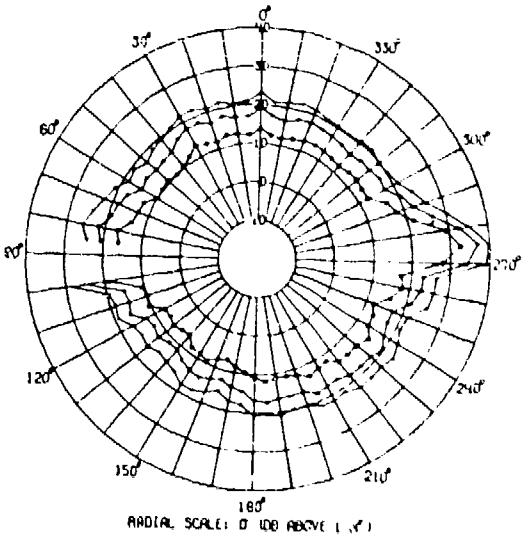

(C) Fig. 45c — Channel 3 XVV RUN 1281 CCW

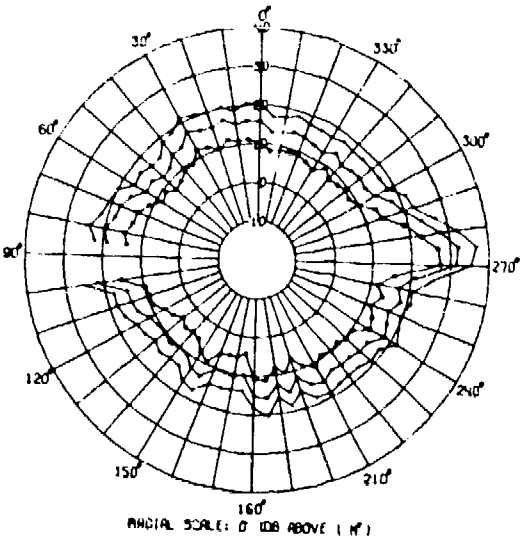

(C) Fig. 45d — Channel 4 CVV RUN 1281 CCW

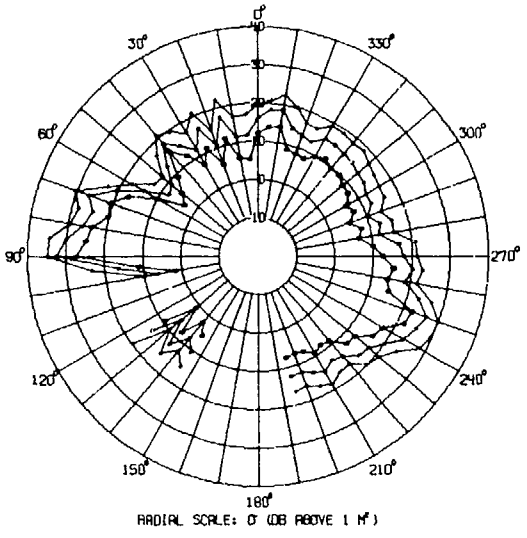

(C) Fig. 46a — Channel 1 LVV RUN 1282 CCW

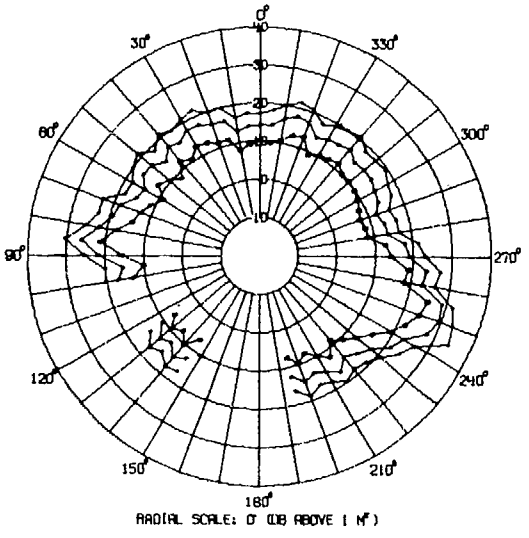

(C) Fig. 46b — Channel 2 SVV RUN 1282 CCW

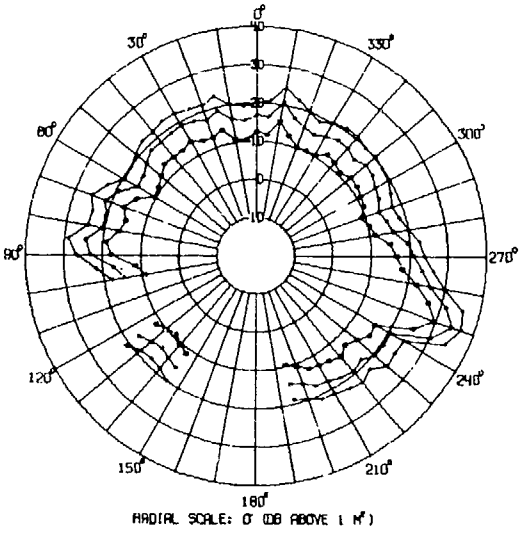

(C) Fig. 46c — Channel 3 XVV RUN 1282 CCW

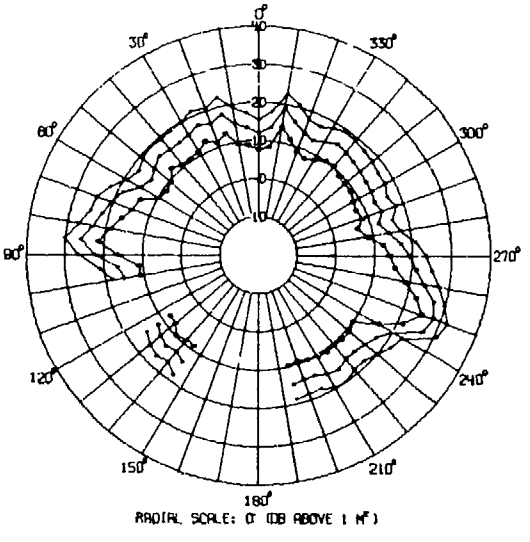

(C) Fig. 46d — Channel 4 CVV RUN 1282 CCW

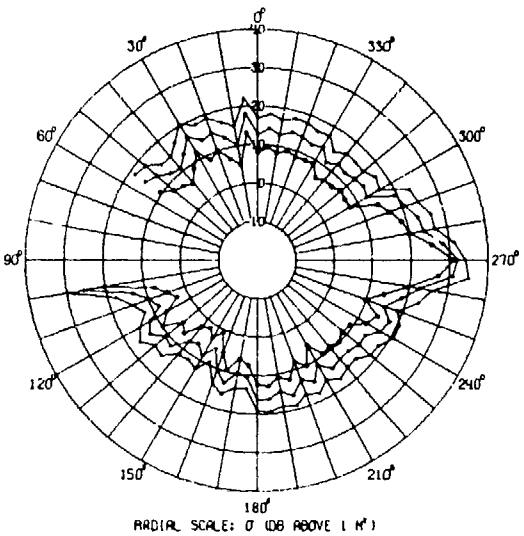

(C) Fig. 47a — Channel 1 LVV RUN 1283 CCW

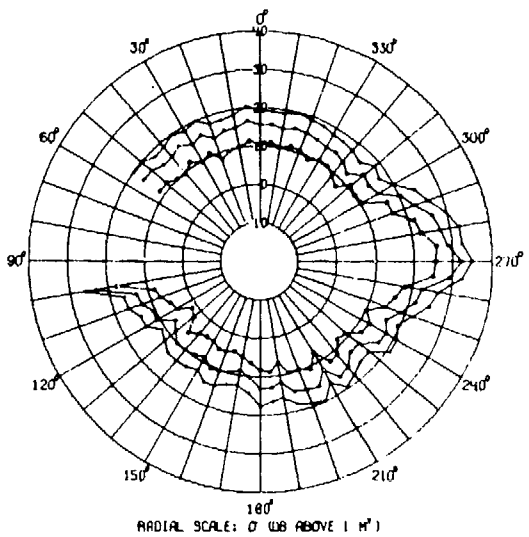

(C) Fig. 47b — Channel 2 SVV RUN 1283 CCW

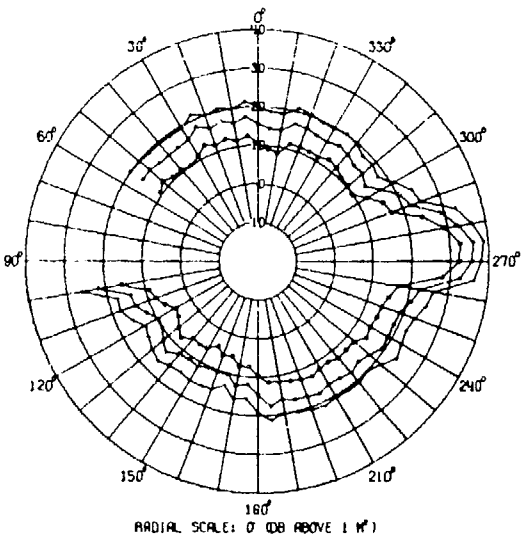

(C) Fig. 47c — Channel 3 XVV RUN 1283 CCW

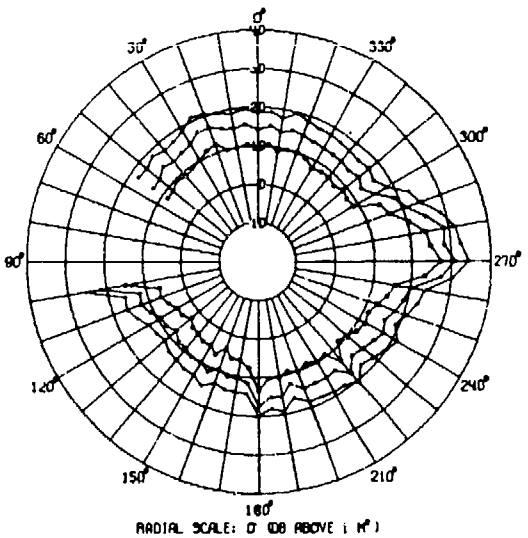

(C) Fig. 47d — Channel 4 CVV RUN 1283 CCW

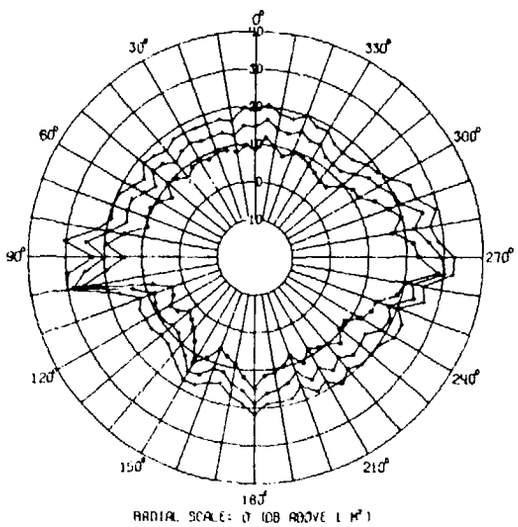

(C) Fig. 48a — Channel 1 LVV RUN 1284 CCW

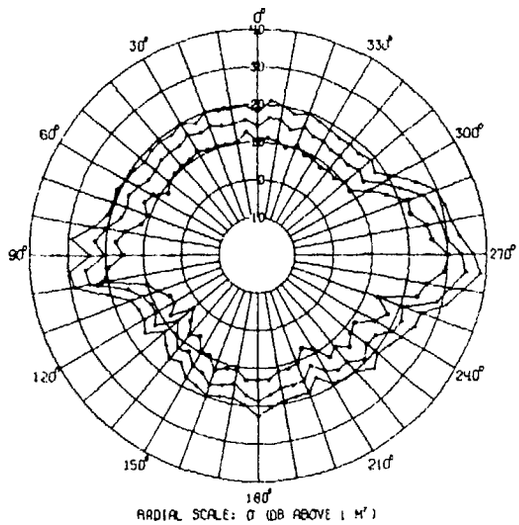

(C) Fig. 48b — Channel 2 SVV RUN 1284 CCW

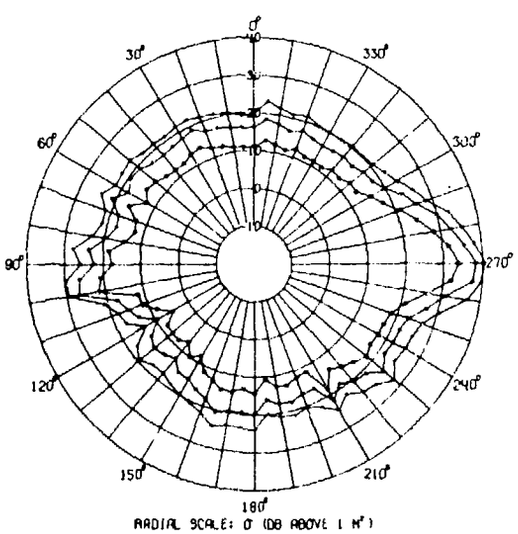

(C) Fig. 48c — Channel 3 XVV RUN 1284 CCW

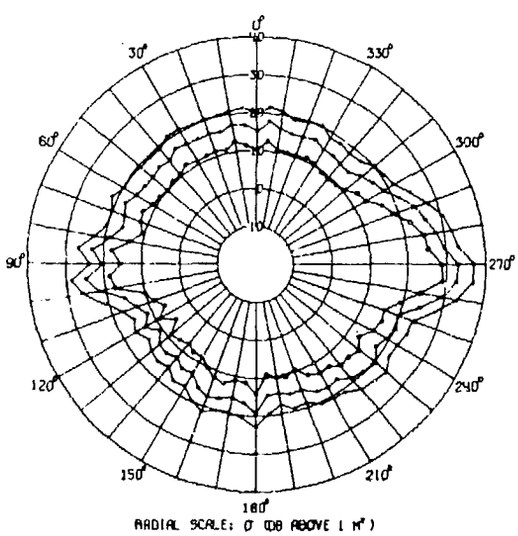

(C) Fig. 48d — Channel 4 CVV RUN 1284 CCW

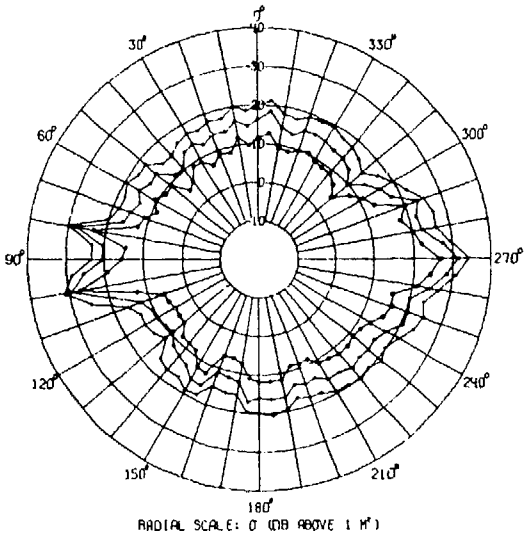

(C) Fig. 49a — Channel 1 LVV RUN 1285 CCW

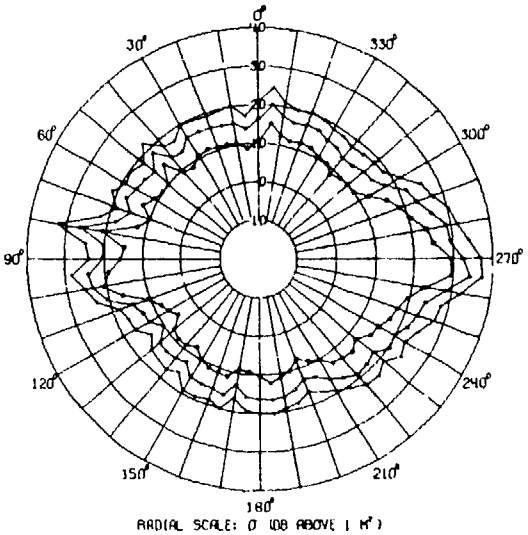

(C) Fig. 49b — Channel 2 SVV RUN 1285 CCW

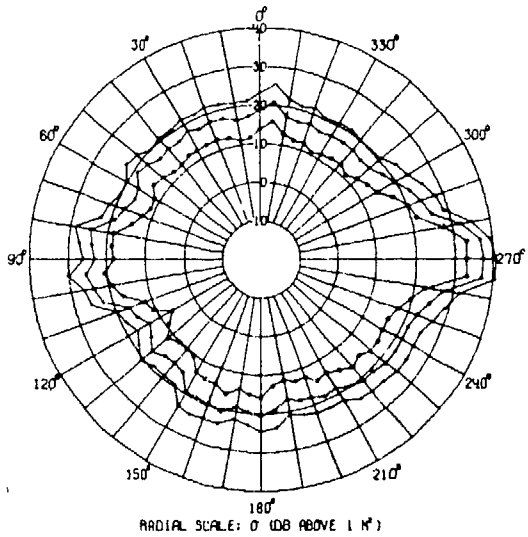

(C) Fig. 49c — Channel 3 XVV RUN 1285 CCW

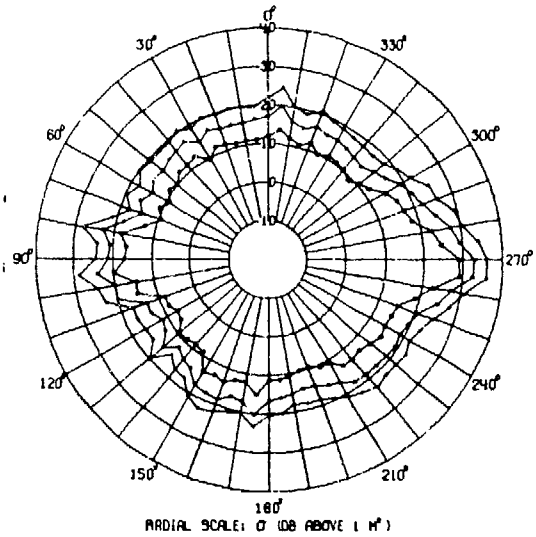

(C) Fig. 49d — Channel 4 CVV RUN 1285 CCW

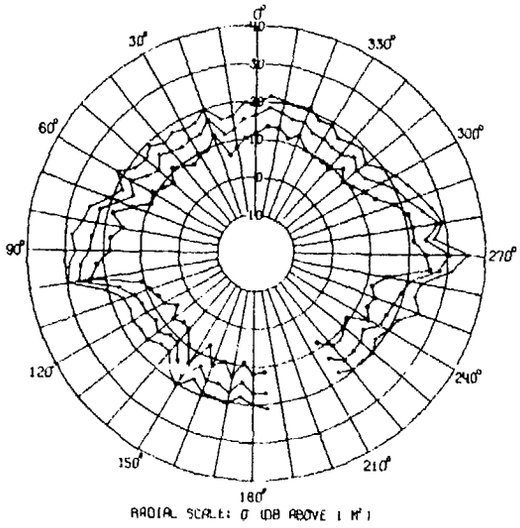

(C) Fig. 50a — Channel 1 LVV RUN 1286 CCW

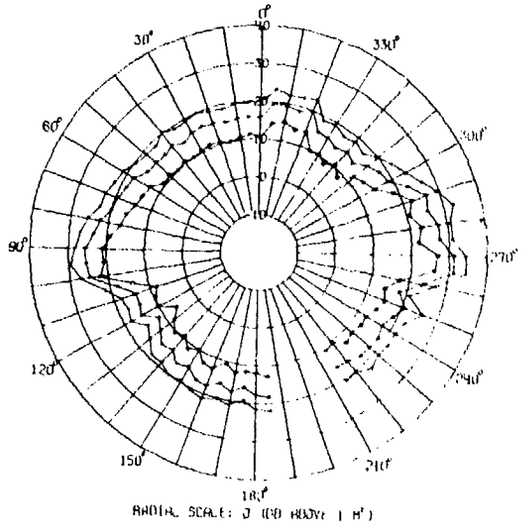

(C) Fig. 50b — Channel 2 SVV RUN 1286 CCW

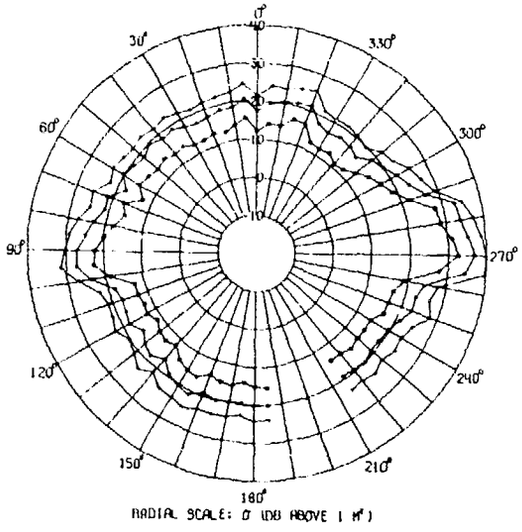

(C) Fig. 50c — Channel 3 XVV RUN 1286 CCW

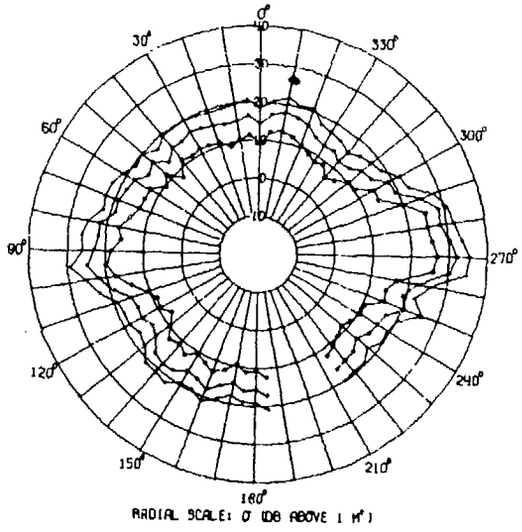

(C) Fig. 50d — Channel 4 CVV RUN 1286 CCW

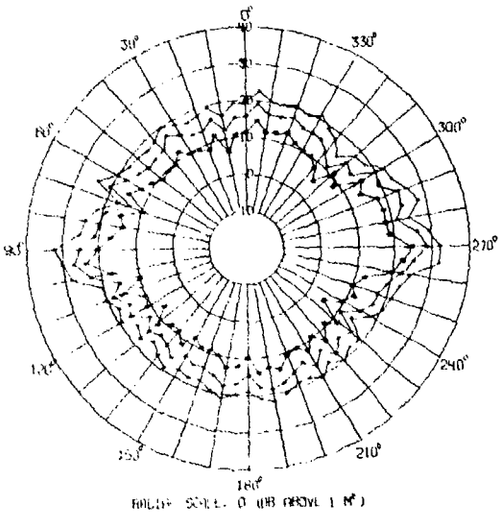

(C) Fig. 51a — Channel 1 LVV RUN 1287 CCW

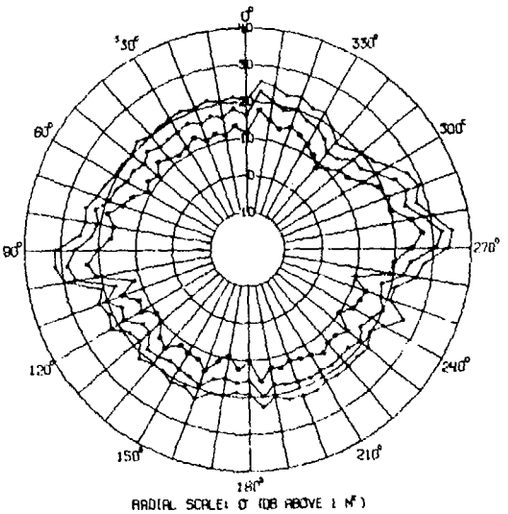

(C) Fig. 51b — Channel 2 SVV RUN 1287 CCW

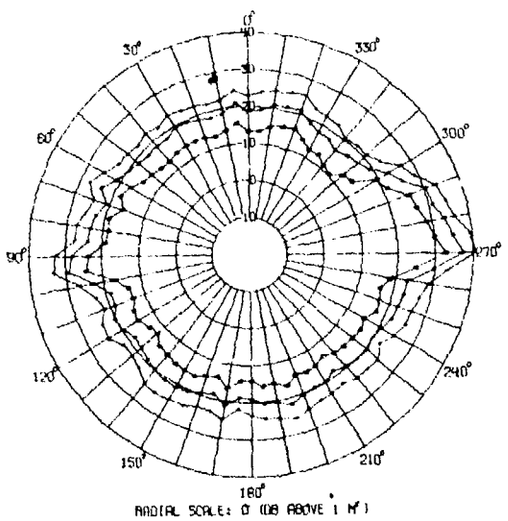

(C) Fig. 51c — Channel 3 XVV RUN 1287 CCW

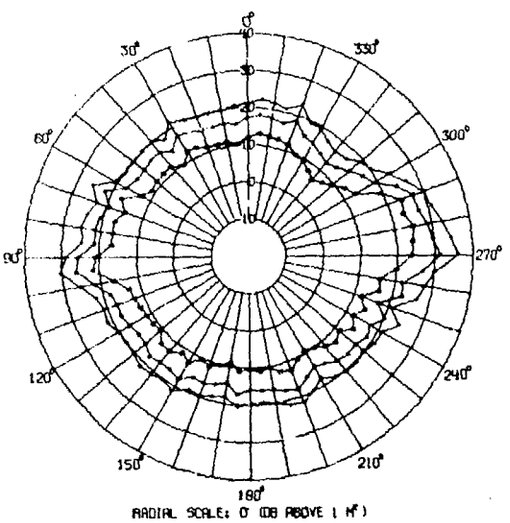

(C) Fig. 51d — Channel 4 CVV RUN 1287 CCW

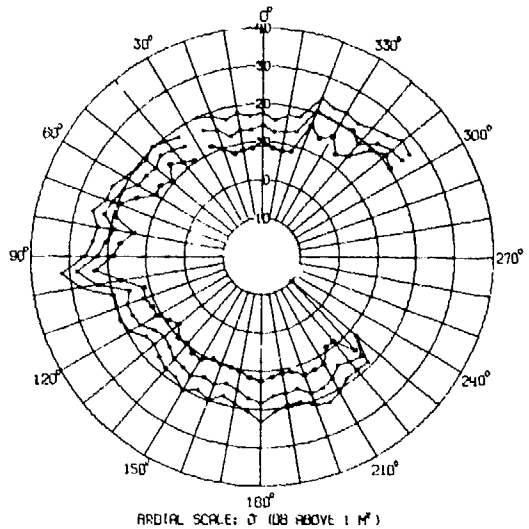

(C) Fig. 52a — Channel 1 LVV RUN 1288 CCW

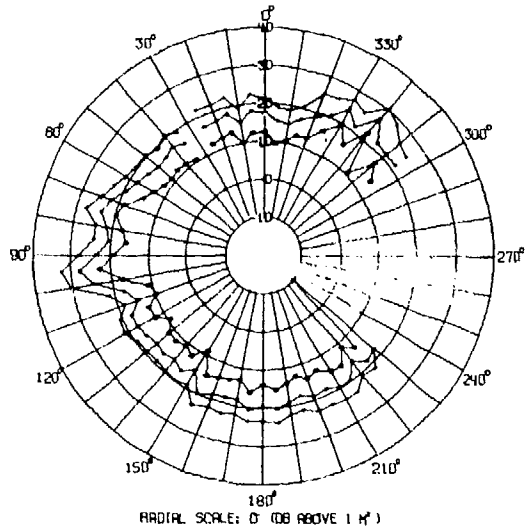

(C) Fig. 52b — Channel 2 SVV RUN 1288 CCW

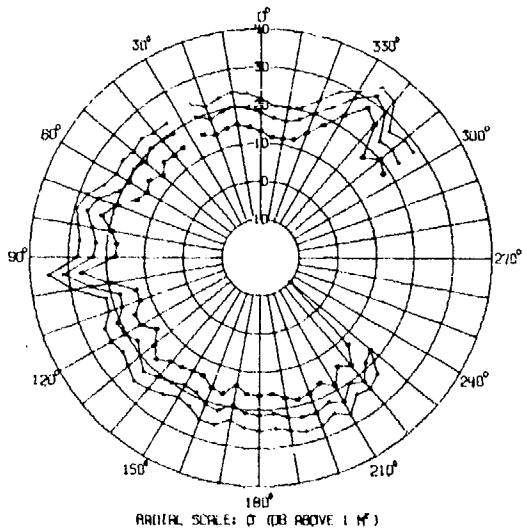

(C) Fig. 52c — Channel 3 XVV RUN 1288 CCW

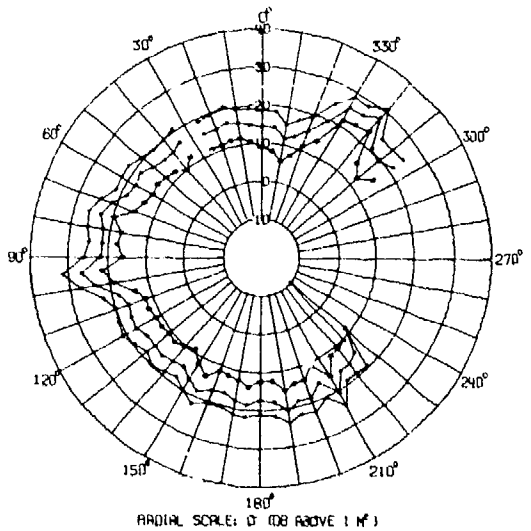

(C) Fig. 52d — Channel 4 CVV RUN 1288 CCW

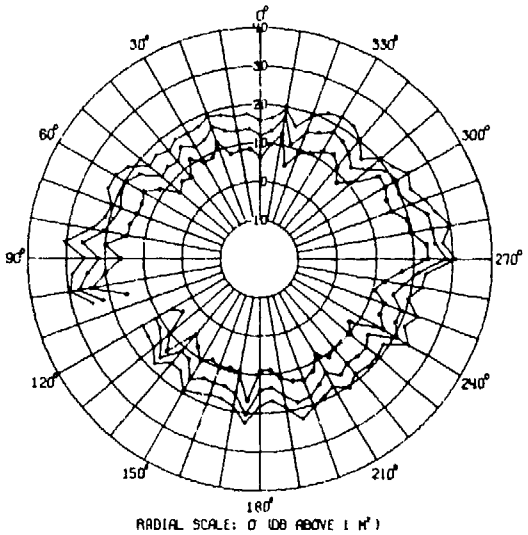

(C) Fig. 53a — Channel 1 LVV RUN 1290 CCW

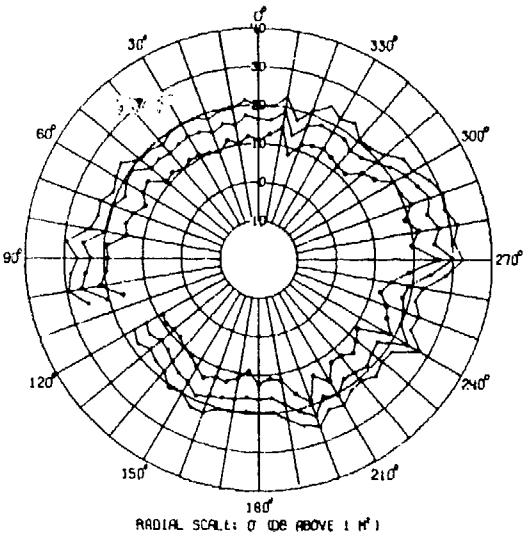

(C) Fig. 53b — Channel 2 SVV RUN 1290 CCW

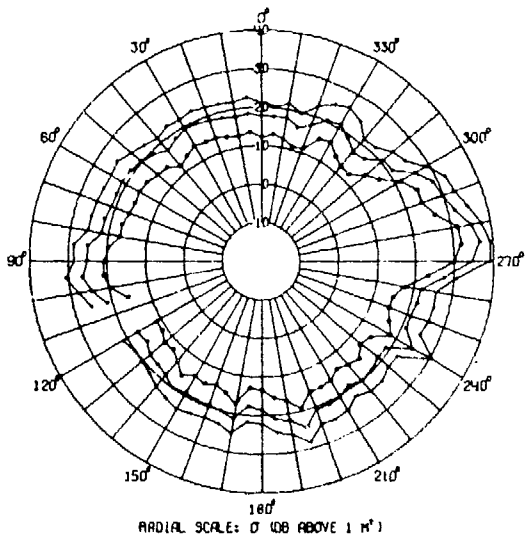

(C) Fig. 53c — Channel 3 XVV RUN 1290 CCW

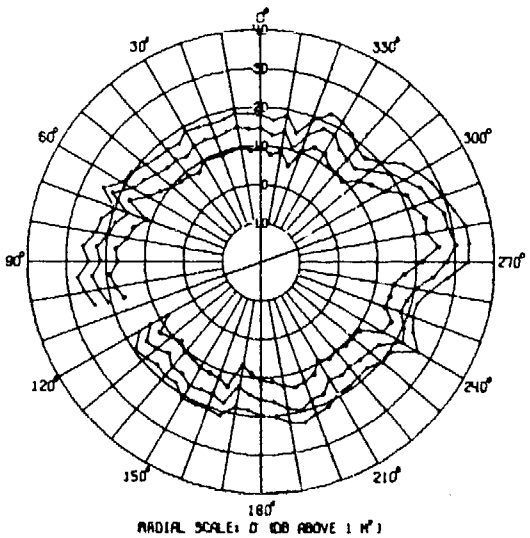

(C) Fig. 53d — Channel 4 CVV RUN 1290 CCW

Appendix A [Unclassified]

RADAR SYSTEM

The measurement system consists of four similar pulse radars operating from a common pedestal. Figure A1 is a view of the on-site equipment, and Table A1 shows some of the basic system characteristics. In operation all transmitters are pulsed simultaneously; the L- and S-band systems use coaxial feeds operating into a single dish, and the C- and X-band systems use separate 122- and 81-cm antennas. To change the polarization of the L-S-band antenna, a physical rotation of the feed through 90 degrees is necessary. The transmitted polarization for C and X bands is controlled remotely by switching the excited port of a dual-mode transducer and by rotating a quarter-wave plate.

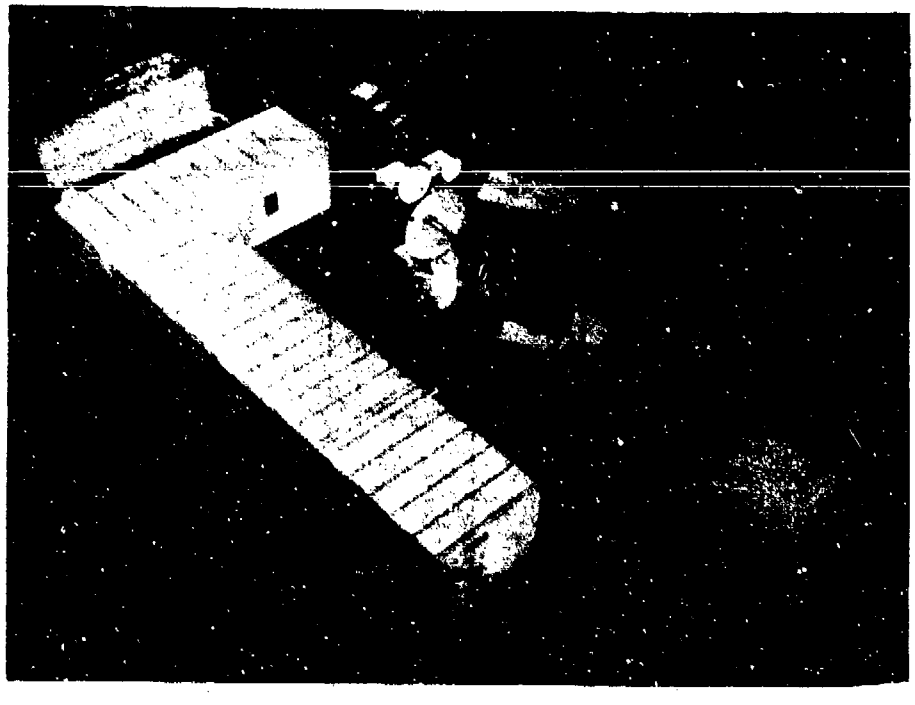

Fig. A1 — The on-site equipment

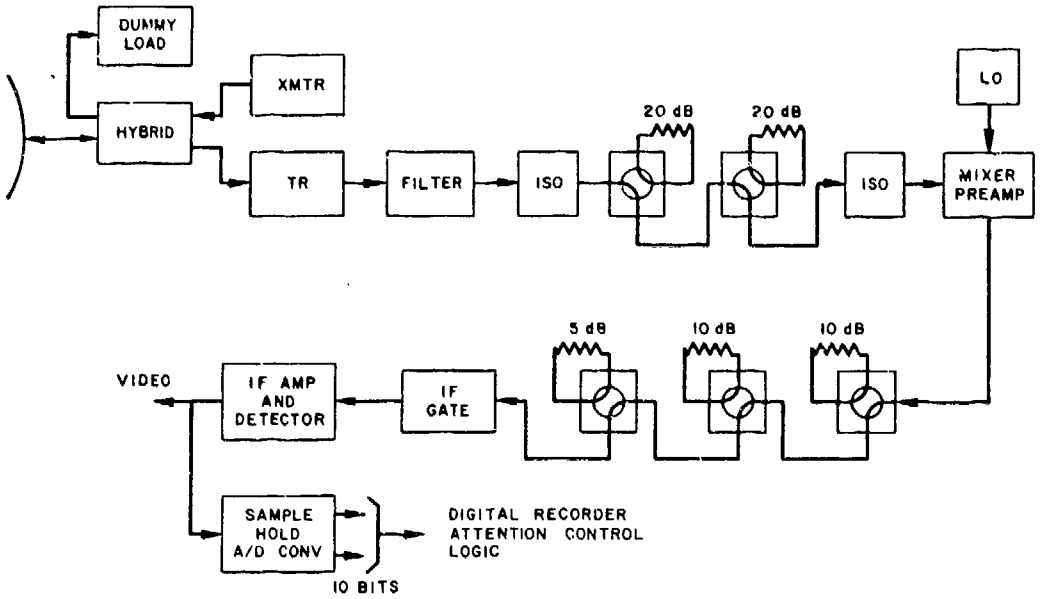

Fig. A2 — The L- or S-band system

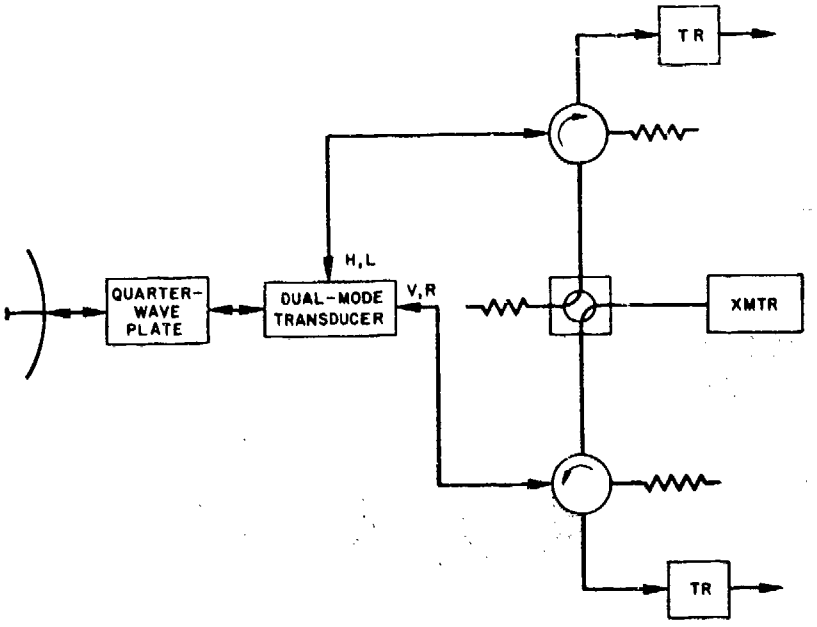

Fig. A3 — The microwave portion of the X-band system

Table A1
Basic System Characteristics

Band	Frequency (MHz)	Peak Radiated Power (kW)	Pulse Width (μs)	Pulse Rate (Hz)	Beamwidth, (EXH plane) (deg)	Transmitted Polarization	Received Polarization
L	1300	250	1	500	7.5 X 6	H, V	Same as transmitted
S	2800	250	1	500	3.5 X 3	H, V	Same as transmitted
C	5500	250	1	500	3 X 3	RC, LC, H, V	Simultaneous reception of parallel and orthogonal components
X	9225	250	1	500	3 X 3	RC, LC, H, V	

Shown in the photograph, mounted between the C- and X-band reflectors, is an X-band monopulse receiver. It employs a four-horn cluster and is polarized at 45 degrees so that, regardless of the transmitted polarization, sufficient signal is available for operation. The monopulse system is used exclusively for initial acquisition of the target.

A basic block diagram for either the L- or S-band system is shown in Fig. A2. The hybrid duplexer consists of a 3-dB coupler arranged so that half the generated power is radiated and half is absorbed in a load. This arrangement permits connection of the receiver to a terminal of the coupler which is isolated from the transmitter by about 30 dB. With this degree of isolation the transmit-receive (TR) tube used for mixer crystal protection deionizes rapidly and thus permits close-in target tracking. With the present system, data can be taken within the interval ≈2 to ≈20 kilometers, although the measurements contained in this report were limited to a ≈10 km maximum range. The receiver system uses no AGC and operates with a linear instantaneous dynamic range of 40 dB; however, much more than this range is needed to handle most targets, especially when the 10:1 range interval is employed. A switched attenuator system is used to extend the range of the receiver. As shown in Fig. A2, a series of fixed attenuators is controlled by the video output level and stepped in 5-dB increments from 0 to 65 dB, providing a total measurement range of 105 dB. Local-oscillator power is supplied by fixed oscillators rather than by a klystron system using AFC. The overall pass band of the receiver is flat within ±1/2 dB over 5 MHz. A block diagram of the microwave portion of the C- of X-band system is shown in Fig. A3. The IF sections are identical for all bands.

System checkout consists of a warmup period followed by an extensive check and adjustment of all functions, including RF and IF attenuator calibration, transmitter and local-oscillator frequencies, data-system calibration, receiver sensitivity, and antenna-mount servo. RF signals during checkout are furnished by a calibrated remote beacon, so that system sensitivities are brought to the same point for each aircraft flight. Final system calibration is accomplished before and after a flight (one fuel load) by tracking a 15-cm balloonborne sphere.

Digital recordings of the pulse-to-pulse backscatter signals are employed to facilitate the reduction process. Detected video from the six receivers is stretched, quantized to

ten bits, and recorded on a 25.4-mm, 16-track recorder. Coordinating data, specifically range, azimuth, elevation, and run number, are recorded on the same tape at a rate which is 1/10 the radar repetition rate. In addition each radar trigger is counted and recorded for use in the tape search system in the laboratory reformatting process. Attenuator values are recorded in the bit locations for video data during the time of a change in value of attenuation.

Additional recordings consist of 16-mm boresight film, a chart recording of the detected stretched video, and a simultaneous voice commentary from all operations' stations.

Appendix B [Unclassified]

DATA REDUCTION

Most data are reduced by a high-speed digital computer. The reduction (Fig. B1) is in four steps, which are linked by input-output data. The first step is the determination of the aspect of the target aircraft. The input data consist of the target position in spherical radar-oriented coordinates sampled twice a second. For straight-line courses aspect data from the aircraft is not required. The position data and target flight constraints are transformed to a new coordinate system erected at the target position.* Once the transformation is complete, the aircraft aspect with respect to the radar line of sight is established in the target-oriented system. The azimuth and elevation aspect as a function of time is then printed via line printer and recorded on magnetic tape for use in later steps in the processing.

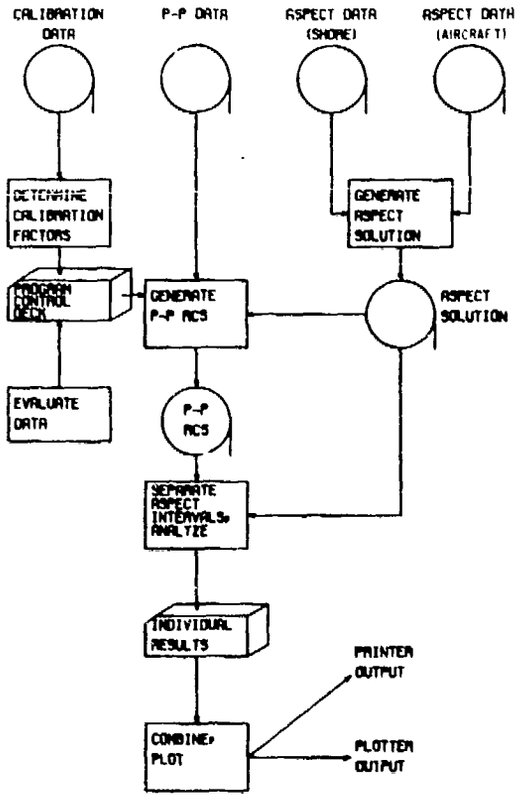

Fig. B1 — Data reduction

*I.D. Olin, "Aircraft Aspect Solution in Dynamic Radar Area Measurement," NRL Report 6194, Feb. 1965.

For circular data runs an additional input of the aircraft heading is used in the computation of the azimuth aspect angle. Normally this angle is determined by correlating data recorded on the aircraft (gyrocompass heading as a function of WWV time) with tracking information recorded at the radar site (range, train, and elevation angles as a function of WWV time). In the case of this report a synthetic onboard recording generated as described in the main text was used. The data recorded at the radar site are recorded not only as a function of WWV time but also as a function of data time, which permits full time synchronization. The aspect analysis consists of trigonometric computation of the angle between the aircraft's fore-and-aft axis and the radar line of sight and results in a single magnetic tape containing raw aspect data and the final solution as a function of data time.

The second step in the processing is the generation of a magnetic tape containing pulse-to-pulse radar cross sections. The data inputs to the computer are a magnetic tape containing voltage amplitudes for four data channels and coded levels for the step attenuators at each of the four frequencies, a magnetic tape containing aspect data, and punched cards containing various calibration factors and information for evaluation of the data. The voltage values are corrected to the 0-dB level by removing step attenuation values present at the time of measurement and calibrated to an absolute cross-section value. Calibration factors are determined by computer processing of four 2-second samples of the return from 15-cm calibration spheres to obtain the final calibration factor. The final result of this part of the analysis is pulse-to-pulse cross section as a function of time on a magnetic tape. This tape now becomes an input to the next step in the processing.

The third step in processing the radar cross section profile is the subdivision of the data satisfying aspect-cell requirements and the determination of the 20, 50, and 80 percentiles of the cross-section distribution. The inputs are the aspect information from the first part of the processing and the cross-section tape from the second part of the processing. The aspect information is examined, and a set of indices is determined to block the data. These indices are used in blocking the cross-section data according to aspect cells and in determining the amplitude distribution function for each aspect cell. From the distribution function the percentiles of interest are determined and held for printing. In addition to being printed, the three percentiles are punched on cards together with the number of amplitude values used in forming the distribution function. These punched cards serve as input to the final step in the processing.

The final step in the processing is the compilation of all results for a single polarization. This is done by a computer routine which accepts punched cards containing percentile values and aspect-cell identification, sorts according to aspect cell, compiles the percentiles from like cells, and plots the final answer. This compilation is an averaging procedure in which each value is weighted according to the number of samples from which it was determined.

DEPARTMENT OF THE NAVY
NAVAL RESEARCH LABORATORY
WASHINGTON D C 20375-5320

IN REPLY REFER TO:

5510
Ser 1221/0647
27 Nov 95

From: Commanding Officer, Naval Research Laboratory
To: Air Intelligence Agency, Air Force Information Warfare Center

Subj: NRL REPORT 8163, RADAR CROSS SECTIONS OF THE AC-130H AT 1300, 2800, 5500, AND 9225 MHZ AD-C013 177

Ref: (a) Your AFIWC/DBES fax of 17 Oct 95

1. Per reference (a), we have reviewed subject report and determined none of the information contained in this report pertaining to this particular aircraft requires any further protection. The distribution statement is changed to "Approved for public release, distribution is unlimited."

2. As for NRL documents created during the 1970s containing information "RELEASABLE TO U. S. GOVERNMENT AGENCIES ONLY" will still require our review since there are some aircraft measurements which should be held close and each report considered individually.

3. If you need further information, contact me at NRL Code 1221, at commercial (202) 767-2240, or DSN 297-2240.

CHARLES ROGERS
By direction

Comp
1/10/00